Title
Advanced Burner Reactor with Breed-and-Burn Thorium Blankets for Improved Economics and Resource Utilization

Author
Zhang, Guanheng

Publication Date
2015

Peer reviewed|Thesis/dissertation

Advanced Burner Reactor with Breed-and-Burn Thorium Blankets for Improved Economics and Resource Utilization

By

Guanheng Zhang

A dissertation submitted in partial satisfaction of the

requirements for the degree of

Doctor of Philosophy

in

Engineering – Nuclear Engineering

in the

Graduate Division

of the

University of California, Berkeley

Committee in charge:

Professor Ehud Greenspan, Chair
Professor Jasmina Vujic
Professor Joonhong Ahn
Professor Massimiliano Fratoni
Professor Chris Dames

Fall 2015

Advanced Burner Reactor with Breed-and-Burn Thorium Blankets for Improved Economics and Resource Utilization

Abstract

Advanced Burner Reactor with Breed-and-Burn Thorium Blankets for Improved Economics and Resource Utilization

by

Guanheng Zhang

Doctor of Philosophy in Engineering – Nuclear Engineering

University of California, Berkeley

Professor Ehud Greenspan, Chair

This study assesses the feasibility of designing Seed and Blanket (S&B) Sodium-cooled Fast Reactor (SFR) to generate a significant fraction of the core power from radial thorium fueled blankets that operate on the Breed-and-Burn (B&B) mode without exceeding the 200 Displacements per Atom (DPA) radiation damage constraint of presently verified cladding materials. The S&B core is designed to have an elongated seed (or "driver") to maximize the fraction of neutrons that radially leak into the subcritical blanket and reduce neutron loss via axial leakage. The blanket in the S&B core makes beneficial use of the leaking neutrons for improved economics and resource utilization. A specific objective of this study is to maximize the fraction of core power that can be generated by the blanket without violating the thermal hydraulic and material constraints. Since the blanket fuel requires no reprocessing along with remote fuel fabrication, a larger fraction of power from the blanket will result in a lower fuel cycle cost per unit of electricity generated. A unique synergism is found between a low conversion ratio (CR) seed and a B&B blanket fueled by thorium. Among several benefits, this synergism enables the very low leakage S&B cores to have small positive coolant voiding reactivity coefficient and large enough negative Doppler coefficient even when using inert matrix fuel for the seed. The benefits of this synergism are maximized when using an annular seed surrounded by an inner and outer thorium blankets. Two high-performance S&B cores were designed to benefit from this unique synergism: (1) the ultra-long cycle core that features a cycle length of ~7 years; (2) the high-transmutation rate core where the seed fuel features a TRU CR of 0.0. Its TRU transmutation rate is comparable to that of the reference Advanced Burner Reactor (ABR) with CR of 0.5 and the thorium blanket can generate close to 60% of the core power; but requires only one sixth of the reprocessing and fabrication capacity per unit of core power.

Nevertheless, these reference cores were designed to set upper bounds on the S&B core performance by using larger height and pressure drop than those of typical SFR design. A study was subsequently undertaken to quantify the tradeoff between S&B core design variables and the core performance. This study concludes that a viable S&B core can be designed without significant deviation from SFR core design practices. For example, the S&B core with 120cm active height will be comparable in volume, HM mass and specific power with the S-PRISM core and could fit within the S-PRISM reactor vessel. 43.1% of this core power will be generated by the once-through thorium blanket; the required capacity for reprocessing and remote fuel fabrication per unit of electricity generated will be approximately one fifth of that for a comparable ABR. The sodium void worth of this 120cm tall S&B core is significantly less positive than that of the reference ABR and the Doppler coefficient is only slightly smaller even though the seed uses a fertile-free fuel. The seed in the high transmutation core requires inert matrix fuel (TRU-40Zr) that has been successfully irradiated by the Fuel Cycle Research & Development program. An additional sensitivity analysis was later conducted to remove the bias introduced by the discrepancy between radiation damage constraints -- 200 DPA applied for S&B cores and fast fluence of $4x10^{23}$ n(>0.1MeV)/cm^2 applied for ABR core design. Although the performance characteristics of the S&B cores are sensitive to the radiation damage constraint applied, the S&B cores offer very significant performance improvements relative to the conventional ABR core design when using identical constraint.

Fuel cycle characteristics of the S&B cores were compared with those of the reference ABR, and a Pressurized Water Reactor (PWR). The fuel cycle cost of the S&B reactor with same LWR TRU transmutation rate as the reference (CR=0.5) ABR is 0.53 cents/kWe-h versus 0.73 cents/kWe-h for the ABR – about 27% lower; it is even lower than that of contemporary PWRs. The longer cycle may enable the S&B cores to operate at a ~10% higher capacity factor and thereby further improve their economic viability. The S&B cores can utilize at least 7% of thorium energy value without a need to develop irradiated thorium reprocessing capability. This is ~12 times the amount of energy that the LWRs generate per unit of natural uranium mined. By softening the blanket spectrum the thorium utilization can increase by a factor of at least three when using thorium hydride rather than metallic fuel; Fully Ceramic Encapsulated (FCM) fueled blanket can achieve the discharge burnup of 481.5 MWd/kg if the FCM fuel keeps its integrity up to such burnup – this is over 80 times the energy extracted by present PWR per unit mass of natural uranium.

If reprocessed, the Trans-Th fuel bred in the S&B core can enable to support new fleets of ^{233}U-Th fuel self-sustaining energy systems that use thermal and epithermal reactors such as Molten Salt Reactors (MSR) and Reduced-moderation Boiling Water Reactors (RBWR). Alternatively, the S&B reactors can be used to close the LWR fuel cycle using a 3-tier system: TRU extracted from Tier-1 LWR is used for fueling the seed of Tier-2 S&B cores while the ^{233}U (Trans-Th) extracted from Tier-2 S&B blanket is used as the fissile feed for Tier-3 LWR. It is estimated that in such a 3-tier energy system 1GWe of

S&B SFRs can support 3.3 GWe of PWRs versus ~1.7 GWe of PWRs that can be supported by 1GWe of CR=0.5 ABR.

In summary, the Seed-and-Blanket core concept studied in this project is found highly promising as it offers:

- Improvement in the economic viability of Sodium-cooled Fast Reactors due to the significant reduction in the fuel cycle cost and possibly increase in the capacity factor that may be enabled by the longer cycles. The improved economics may justify earlier commercialization of SFRs.

- Significantly smaller investment in the construction of the fuel reprocessing and the remote fuel fabrication infrastructure required for a given capacity of SFRs.

- Several new promising fuel cycle options feature substantial increase of the thorium resource utilization without fuel reprocessing

- Supporting a large number of LWRs by a given capacity of SFRs on the S&B configuration. Thus, it enables to close the nuclear fuel cycle faster and with smaller investment.

In conclusion, the S&B reactor concept we proposed is feasible and potential to significantly improve the economic viability of fast reactors and of LWR TRU transmuting system using existing structural materials. It enables significant utilization of thorium resource without reprocessing.

Table of Contents

List of Tables

List of Figures

Acknowledgements

I would like to express my gratitude to all who aid my Ph.D. work at University of California Berkeley. The Department of Nuclear Engineering provides friendly environment where I can study and work with great pleasure.

First of all, I want to thank Professor Ehud Greenspan. As an enthusiastic, intelligent, dedicated, and strict advisor, he guided me to pursue this field as a young researcher. I could not have completed this dissertation without his indispensable advices and continuous inspiration. His trust and understanding through the past four years is greatly helpful to me.

I would like to acknowledge Professor Massimiliano Fratoni, Professor Jasmina Vujic, Professor Joonhong Ahn, Professor Peter Hosemann, and Professor Chris Dames. They are always patient to review my works and help me with the questions.

I highly appreciate the kindly advices from my colleagues in Argonne National Laboratory where I spent a fruitful summer, including Dr. Bo Feng, Dr. Francesco Ganda, Dr. Nicolas Stauff, Dr. Nicholas Brown (BNL), Dr. Edward Hoffman, Dr. Taek Kyum Kim, and Dr. Temitope Taiwo. Special thanks are given to Dr. Florent Heidet who is always willing to provide guidance and help.

I'm grateful for Dr. Anselmo Cisneros, Dr. Staffan Qvist, and Dr. Jeffrey Seifried. Their mentorship helped me start the project. In addition, I would like to thank Dr. Jason Hou, Dr. Xunxiang Hu, Phil Gorman, and my friends for their encouragements.

Finally, I'm so lucky to meet my wife, Hai, in Berkeley. We encourage and respect each other with same faith. It's also the opportunity to express my deepest appreciation to my parents for their sacrifice and trust.

Chapter 1

1. Introduction

The world energy consumption is predicted to increase by 53% between 2008 and 2035 (Figure 1-1) [1]. Nuclear power has reliably contributed almost 20% of electricity generated in the United States over the past two decades. It remains the largest contributor (more than 70%) of non-greenhouse-gas-emitting electric power generation in the United States [2]. In response to the global warming issue, the Obama administration has recently announced to reduce carbon emissions by 32% from 2005 levels between now and 2030 [3]. It is expected that nuclear energy will continuously be a significant low carbon emission electric resource for the United States in the future.

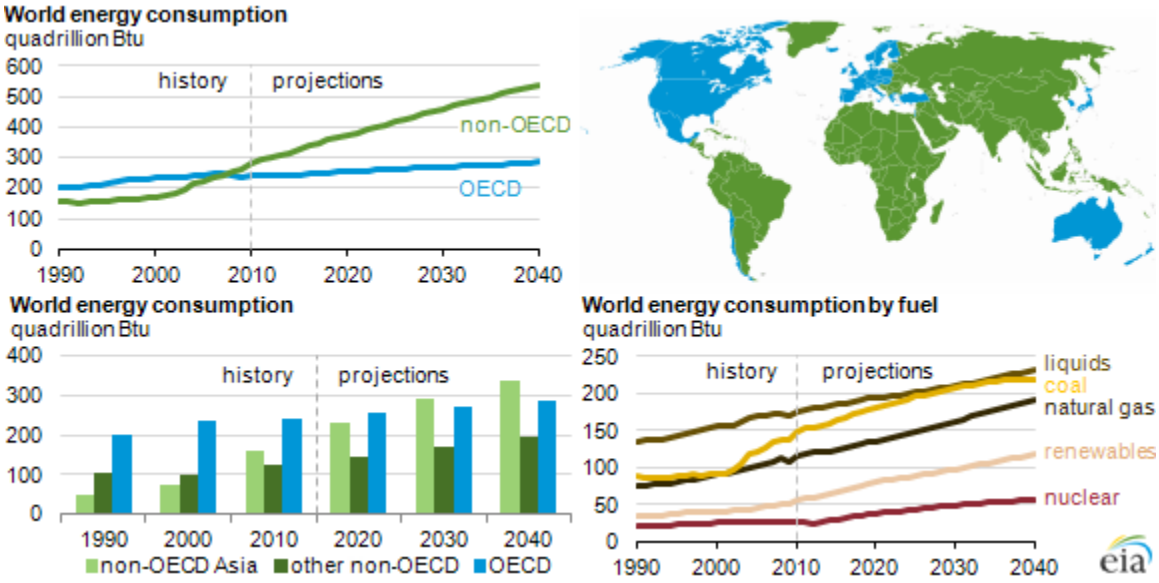

Figure 1-1 World energy consumption [1]

Since the first Light Water Reactor (LWR), Low Intensity Test Reactor, reached criticality on February 4, 1950 at Oak Ridge National Laboratory, LWR reactors have been well commercialized worldwide over the past half-century. Now 31 countries host over 435 commercial nuclear power reactors with a total installed capacity of over 375 GWe [4]. In 2015, the IAEA reports that worldwide there were 67 civil fission-electric power reactors under construction in 15 countries [5]. The AP1000, a Generation III+ nuclear power plant designed by Westinghouse Electric Company, is currently being built

in the United States: two at Vogtle (units 3&4) and two at VC Summer (units 2&3) and planned to be commissioned at 2018 [6]. Nevertheless, contemporary nuclear technology faces with a few challenges and these require to be addressed in the development of Next Generation Nuclear Plants (NGNP):

- Nuclear safety is taken very seriously by those working in nuclear power plants. Two large accidents have had the great impact on global consciousness regarding nuclear power safety – Three Mile Island in 1979 and Chernobyl in 1986. A more recent severe nuclear accident in Fukushima caused by earthquake has resulted in the public concern about the reliability of nuclear technology under seismic disaster. According to United States Nuclear Regulatory Commission [7], the Generation III reactors are designed to have the failure leading to a core melt-down at the probability of one in two million reactor years. This rate is required to be even lower for the Next Generation Nuclear Plants.
- The nuclear waste generated from reactor is radioactive and needs to be stored in the interim spent fuel pool and supervised for decades. It takes up to 100,000 years until the long-lived transuranium elements decay out. Eventually, the nuclear waste will be sent and stored in the geological disposal. However, there are no such sites in United States before the comprehensive environmental evaluation is finished.
- The natural uranium contains fissile isotope – ^{235}U at only 0.72% of total uranium. Current PWR design is fed by enriched uranium with the ^{235}U at the level of 3-5%. It takes eight to ten tons of natural uranium to make one ton of 4.5% enriched uranium. The remaining seven to nine tones of depleted uranium is discarded as the waste. Of the enriched uranium that is loaded into the core, only about 5% is finally converted to the energy; the overall uranium utilization is approximately 0.6% [8]. The next generation nuclear design, like SFR operating on closed fuel cycle, should provide the long-term sustainability for the nuclear energy.
- The enrichment technology required by current nuclear reactors causes the concerns that it is applicable to generate weapon-use materials. Although the Plutonium generated from LWR is believed to be not attractive for the weapon-use or with two many difficulties [9, 10], a recent report from Los Alamos National Laboratory indicates that the present PWRs generate highly attractive plutonium when pre-initiation is not an issue [11]. The next generation nuclear plants should adopt technology with high proliferation resistance.

1.1. Conventional Sodium-cooled Fast Reactor design practice

Sodium-cooled Fast Reactor (shown in Figure 1-2) has been proposed as one of the six Generation IV nuclear reactor designs [12]. The first fast reactor was Clementine, built at Los Alamos in 1946 although it was cooled by liquid mercury [13]. Following this, Experimental Fast Breeder Reactors (EBR-I and EBR-II) were designed and constructed

at Argonne National Laboratory because of the enthusiasm of Enrico Fermi and Walter Zinn [14]; several Liquid Metal-cooled Fast Breeder Reactor in the 250–600 MWe power range began producing electricity during 1970s-1980s [13]. Over half-century R&D (a brief summary is shown on Table 1-1 [15]), the nearly universal acceptance of Sodium-cooled Fast Reactor has been established due to its flexibility to operate either as breeder to achieve the net creation of fissile fuel or as a transmuting reactor to convert the long lived actinides into electricity.

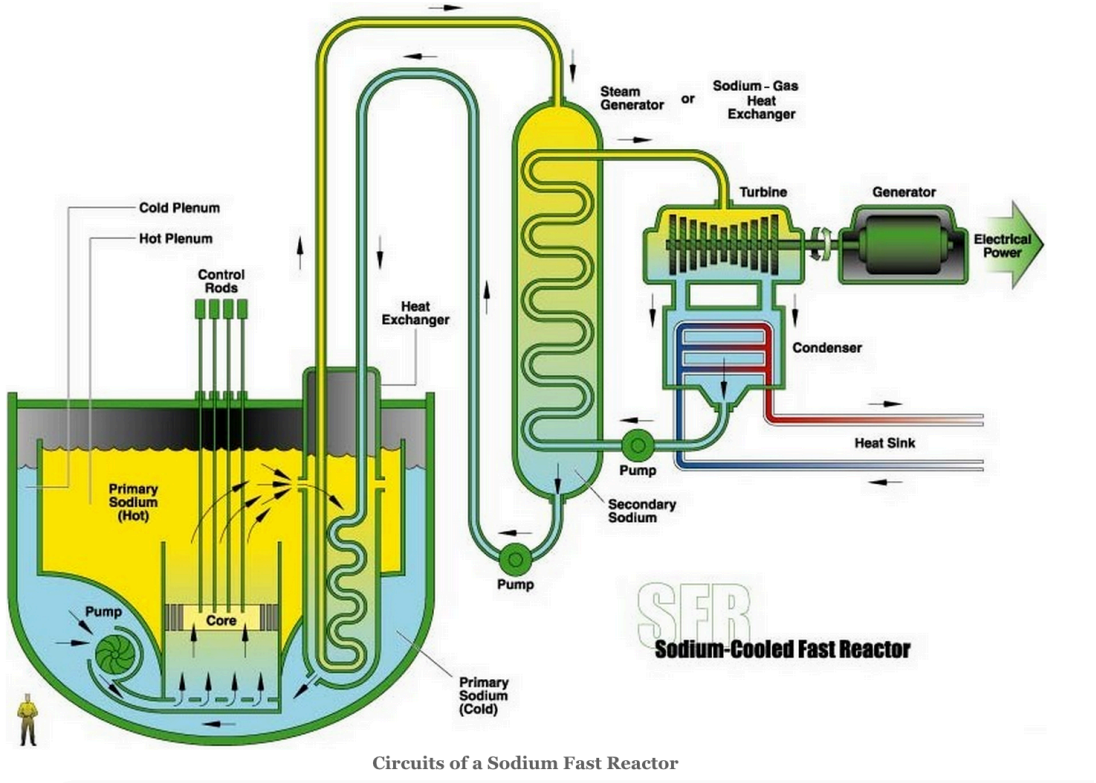

Figure 1-2 Pool type sodium-cooled fast reactor (SFR)

Table 1-1 Experimental Sodium-cooled Fast Reactor in History [15]

Plant	Owner	First criticality	Nominal power (MWt)
Rapsodie (France)	CEA	Jan. 1967	40
KNK-II (Germany)	Kernforschungszentrum Karlsruhe	Oct. 1972	58
FBTR (India)	Department of Atomic Energy, India	Oct. 1985	40
PEC (Italy)	ENEA	-	120
JOYO (Japan)	JNC	Jul. 2003	140

DFR (UK)	UK Atomic Energy Authority	1959	60
BOR-60 (Russian Federation)	Agency for Atomic Energy	1968	55
EBR-II (USA)	U.S. Department of Energy (USDOE) Power Reactor Development Co.	1961	62.5
Fermi (USA)	Detroit Edison Co.	Aug. 1963	200
FFTF (USA)	U.S. Department of Energy	Feb. 1980	400
BR-10 (Russian Federation)	Agency for Atomic Energy	1958	8
CEFR (China)	CIAE	-	65

Instead of light water, sodium is used as coolant since its atomic weight is much heavier than hydrogen. Neutrons lose less energy in collisions with sodium and more than 60% of them have energy above 0.1MeV. The fission reaction of ^{239}Pu induced by fast neutrons generally yields 2.9 neutrons while only 2.4 neutrons come from thermal fission reaction of ^{235}U in PWR [16]. Because of these extra neutrons, fissile contents (^{239}Pu) can be bred (Equation 1-1) and burned in situ without requirement of enrichment technology; ^{233}U yields 2.5 neutrons per fission and therefore can be bred from ^{232}Th with external neutron source.

$$^{232}Th(n,\gamma)^{233}Th \xrightarrow[22.2m]{\beta^-} {}^{233}Pa \xrightarrow[27.4d]{\beta^-} {}^{233}U$$
$$^{238}U(n,\gamma)^{239}U \xrightarrow[23.5m]{\beta^-} {}^{239}Np \xrightarrow[2.35d]{\beta^-} {}^{239}Pu$$

(Equation 1-1)

In addition, closed fuel cycle is often applied for Sodium-cooled Fast Reactor from which the discharge fuel is reprocessed by pyro-metallurgical process or advanced aqueous process (demonstrated by Integral Fast Reactor [17]). Theoretically all of the heavy metals are recovered from the spent fuel and converted to electricity; only fission products are the nuclear waste generated from nuclear power plants and decay out within few hundred years. According to a fuel cycle report from US DOE [18], the Sodium-cooled Fast Reactor is identified as one of the most promising nuclear technologies with metrics of nuclear waste, resource utilization and environmental impact.

1.2. Breed-and-Burn reactor concept and challenges

Breed-and-Blanket (B&B) reactors were proposed in the past [19-27] as an alternative mode of operation of fast breeder reactors (A brief history is shown in Figure 1-3). The principle of B&B reactors is that it is fed with depleted uranium (or natural uranium, or recovered uranium), breeds plutonium, and then fissions a significant fraction of the bred plutonium in situ. Since B&B reactors require no fuel reprocessing and the non-

radioactive feed fuel is easy to fabricate, it is expected that B&B reactors can improve the economics of fast reactors and the resource utilization of contemporary nuclear power plants [28]. Their development is presently being pursued by Terra-Power [29-31] with two design variants: in a traveling wave reactor, nuclear reactor deflagration wave propagates through the fertile material after a small amount of fissile fuel provides the ignition; in a standing wave reactor, the wave is stationary but the fuel is relocated. Terra-Power currently focuses on the standing wave option. Since 2008, the team led by Professor Greenspan focused on the practical designs of the B&B concept including the core performances [32-37] and the safety features of the large fast breeder reactors [38].

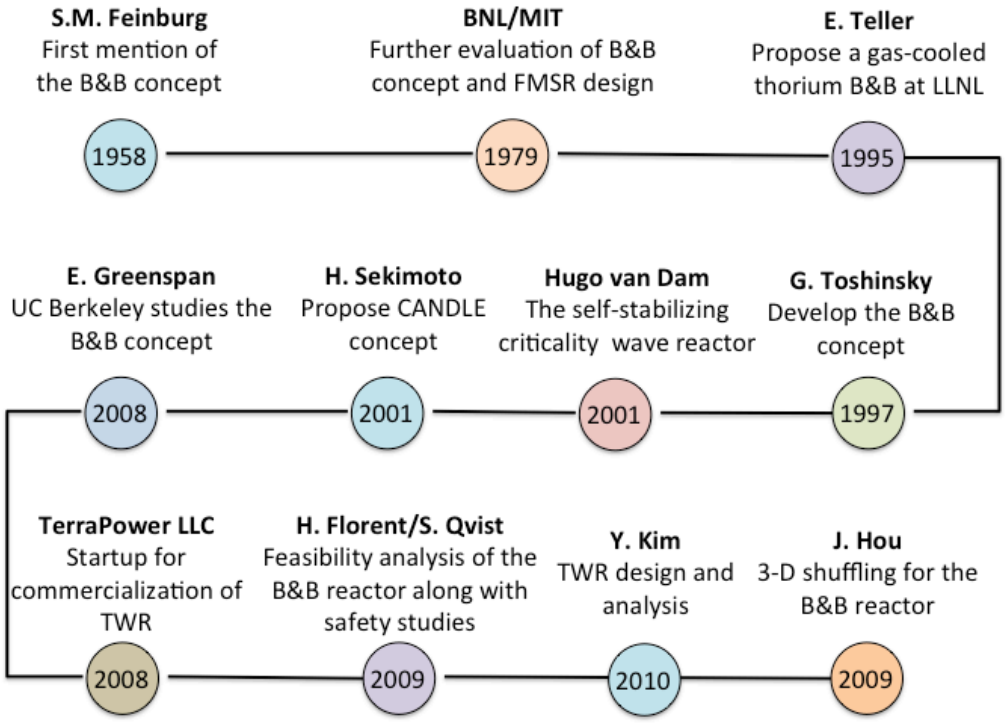

Figure 1-3 A history review of the B&B concept

Nevertheless, in order to sustain the B&B mode of operation, it is necessary to fission, on average, at least about 20% of the depleted uranium fed [34-37]. This corresponds to a peak discharge burnup of up to at least 30% Fissions per Initial Metal Atom (FIMA). The corresponding peak radiation damage to the cladding material at this burnup exceeds 500 Displacements Per Atom (DPA) [32, 33]. A 3-D shuffling fuel cycle scheme has been developed recently such that the peak radiation damage to sustain the B&B reactor is reduced to 350 DPA [39]. The maximum radiation damage that cladding and structural

materials had been exposed to so far is approximately 200 DPA in Fast Flux Test Facility (FFTF) [40]. Hence, an extensive R&D effort is required to develop and certify cladding materials that can retain the fuel integrity up to approximately 500 DPA. Such a program will have to include irradiation experiments in fast spectrum together with post-irradiation analysis and may take long time and large resources.

1.3. Incentives for Seed-and-Blanket reactor concept

Typical Sodium-cooled Fast Reactor (SFR) cores, such as the Advanced Recycling Reactor (ARR) and the Advanced Burner Reactor [41-43], are designed to have a pancake shape with an axial neutron leakage probability on the order of 20%. This value is even larger in some transmuting reactors that feature large TRU loading. The large neutron leakage provides passive safety by reducing the positive coolant temperature reactivity coefficient and increasing the negative temperature reactivity feedback due to core radial expansion and fuel axial expansion. Besides the safety reason, there is no constructive use of these leaking neutrons except in certain breeding cores that use axial depleted uranium blankets.

It was recently proposed [8] to design the SFR core to consist of an elongated seed (or "driver") that is radially surrounded by a fertile-fueled subcritical blanket and use the excess neutrons that leak in the radial direction to drive the blanket in the B&B mode without exceeding 200 DPA. The seed fuel is to be of a prolate ("cigar") shape from which the majority of the neutron leakage is in the radial direction (Figure 1-4). When coolant starts voiding, neutrons are prompted to leak from high reactivity seed fuel to low reactivity subcritical blanket for passive safety.

The driver fuel (or the "seed") will be similar to that of a conventional SFR core; it can use TRU from LWR UNF and have a low conversion ratio as an ABR, or to be TRU self-sustaining as an ARR. The blanket can be fueled with depleted uranium, thorium or other types of low fissile content fuel such as limited-reprocessed LWR UNF, thorium hydride fuel or FCM fuel and operate on once-through fuel cycle. The fuel of both seed and blanket is discharged without exceeding the 200 DPA radiation damage constraint of current cladding materials.

The proposed Seed-and-Blanket concept could facilitate the development and introduction of the B&B reactor technology by designing the B&B blanket to be subcritical. The seed will provide enough excess neutrons at the early burnup of the fertile fuel. The attainable discharge burnup of the blanket fuel will progressively increase as the cladding and fuel are licensable to higher DPA and burnup, respectively. Until reaching the burnup of 30% FIMA and 500 DPA, the S&B design will be converted to sustain the B&B model of operation in a critical stationary-wave core.

As the blanket fuel is inexpensive and not recycled, it is expected that the overall fuel cycle cost of such S&B reactors will be lower than that of standard SFRs and that the cost benefit will be proportional to the S&B core power fraction generated by the blanket. The new concept will improve the SFR economic viability and accelerate the commercialization of fast reactor technology.

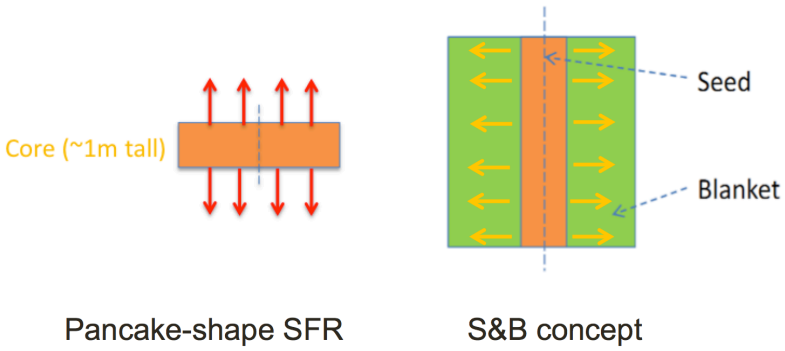

Figure 1-4 Pancake-shape SFR vs. S&B concept proposed by UCB

1.4. Objective and plan of this study

The overall objective of this work is to assess the feasibility of the S&B core design concept. Most of the work focused on LWR TRU burning seeds and thorium blankets; significant effort was devoted to understanding the physics of Seed-and-Blanket interaction that enables a unique synergism between a low TRU conversion ratio seed and a thorium B&B blanket. Specific objectives are: (1) to identify the most promising seed and blanket design concept in terms of geometry and fuel composition; (2) to find the S&B core design that offers the maximum fraction of core power generation by the blanket; (3) to find the S&B core design that requires the minimum fuel reprocessing capacity per unit of electricity generated; (4) to establish tradeoff between the S&B core performance and several design parameters (like core height, pressure drop); (5) to quantify the S&B core performance benefits as the result from an increase in the DPA level that cladding materials will be allowed to withstand; (6) to find innovative approaches for maximizing the thorium utilization without exceeding 200DPA; (7) to identify new promising fuel cycle options that could be enabled by the S&B core concept; (8) to compare fuel cycle related characteristics of the S&B cores against those of conventional SFR core design and present PWR.

The chapters of this dissertation are organized as follow:

- Chapter 2 discusses the methodology including neutronics simulation, radiation damage calculation, and thermal hydraulic analysis. The fuel cycle scheme, design variables and study constraints are also explained.
- Chapter 3 presents the preliminary results from a simplified S&B core. The tradeoff study is performed as a function of the TRU conversion ratio of the seed. The performance of subcritical blankets fueled by depleted uranium and thorium are compared as well.
- Chapter 4 focuses on a more promising design in which an annular driver fuel is surrounded by an external and an internal blanket. The synergism between the seed and the blanket are identified and explained.
- Chapter 5 evaluates the performance of heterogeneous compact core in which blanket assemblies are interspersed between the driver fuel assemblies. The primary purpose of this task is to quantify the benefits from introducing the B&B blanket rather than as a conventional blanket in a compact core in which a large fraction of the neutrons are lost via axial leakage.
- Chapter 6 describes a sensitivity study in which the S&B core performance is traded off against the active core height, the coolant pressure drop and the DPA value that the cladding will be able to withstand.
- Chapter 7 summaries the fuel cycle analysis for the S&B core in terms of the fuel cycle cost, nuclear High Level Waste (HLW) characteristics, fuel utilization, and proliferation resistance. The present PWR and typical SFR are considered as the reference.
- Chapter 8 shows several new fuel cycle options enabled by the S&B concept including use of innovative fuel in the subcritical blanket and multi-stage power systems.
- Chapter 9 provides the study conclusions together with future directions.

Chapter 2

2. Methodology

2.1. Reference fast reactors

2.1.1. Super - Power Reactor Innovative Small Module

The Super-Power Reactor Innovative Small Module (S-PRISM) was developed by GE in the 1990s [44]. The reference commercial S-PRISM plant is composed of six reactor modules for an overall net electrical power of 2286 MWe. The S-PRISM is a more advanced fast reactor module based on the DOE sponsored program to design Advanced Liquid Metal Reactor (ALMR) in 1995. The thermal power of each individual module is 1000 MWt and two identical modules share the 825 MWe turbine-generator unit. In October 2011, it was reported by The Independent [45] that the UK Nuclear Decommissioning Authority (NDA) and senior advisors within the Department of Energy and Climate Change (DECC) had asked for technical and financial details of the PRISM, partly as the way to reduce the large plutonium inventory in the UK. An independent institute [46] has recently offered the recommendations about fast reactor technology and describes how PRISM could reduce the plutonium stockpile worldwide.

As Generation IV reactor, S-PRISM is expected for improved economics and passive safety [44]:

- Compact pool-type reactor modules for factory fabrication and affordable full-scale prototype test.
- Nuclear safety related envelope limited to the nuclear steam supply system.
- Passive response to major Anticipated Transient without Scram (ATWS), like overpower, loss of coolant, and loss of flow.
- Passive heat removal and containment cooling systems
- High flexibility as fuel self-sustaining core or TRU transmuting core.

S-PRISM was designed with the capacity to operate with either oxide or metallic fuel to interest a wide range of potential owners, national infrastructures and commercialization approaches. While oxide fuel has been widely used for current industry, the early metal fuel experience indicates that fueling the fast reactors with metallic fuel may have significant safety and performance improvements. In addition, the pyro-processing of the metallic fuel is expected to be significantly less costly than of oxide fuel [14]. The S&B cores studied in this project are primarily charged by metallic fuel.

2.1.2. Advanced Burner Reactor

The Advanced Burner Reactor (ABR) was pursued by US DOE's Argonne National Laboratory (ANL) as an integral part of the Global Nuclear Energy Partnership (GNEP) [47]. The GNEP developed and demonstrated the ABRs that consume transuranic elements generated from current LWR fleet. Instead of a geological repository and waiting for 100,000 years when long lived actinides decay out, an ABR core is able to destroy or "burn" the radioactive, toxic, and heat-producing High Level Waste (HLW) in the Used Nuclear Fuel (UNF). Due to the unique feature of fast spectrum, these transuranic elements are transmuted into short-lived isotopes through nuclear fissions. It is expected to significantly reduce the volume of HLW which is an urgent need for the current nuclear industry and improve the fuel utilization by closing the fuel cycle. The ABR design also incorporates several safety features and operational methods; a key objective of the ABR program was to obtain design certification from the U.S. Nuclear Regulatory Commission. Future commercial SFR would operate in accordance with this license [47].

A 2006 technical report [43] by ANL summarized several preliminary ABR designs charged with either metallic or oxide fuel based on the S-PRISM design in [44]. The ABR cores were designed to accommodate a wide range of TRU conversion ratios from 1.0 to as low as 0.0. The reactor physics and safety considerations shown by a more recent paper [41] indicates that it enables designing sodium-cooled advanced TRU burner reactors to have a conversion ratio as low as ~0.2 for cycle length of ~7 months or as low as ~0.6 for cycle length of ~12 months. A metallic fuel ABR design that features a conversion ratio of ~0.7 is recommended whose fuel had undergone successful irradiation and, therefore, is licensable in the near-term [48]. The reference ABR for this studies has TRU conversion ratio of 0.5 in [43] which is a challenging design based on present fuel irradiation experiment; nevertheless, it is considered as the representative of fast reactors for TRU transmutation by US DOE's Fuel Cycle Evaluation and Screening campaign [18].

The main issue with the low conversion ratio ABR designs is the increased number of primary control assemblies to avoid the excessive reactivity of individual control assembly. To resolve this issue, the cycle length of the ABR design has to be cut and this deteriorates the economics as the capacity factor of the ABR design is reduced substantially.

2.2. Seed-and-Blanket cores examined

The S&B core is composed of the ABR as the seed fuel based on [43] and a more recent paper [41]. By incorporating the subcritical blanket from which a significant power is

generated, the S&B will partially improve the performance of the ABR cores and resolve the issue of short cycle length. The S&B core has same diameter as the S-PRISM [44] to fit within the reactor vessel.

Figure 2-1 shows the S&B core configuration considered for this study. The radial dimensions of fuel, reflector, and shielding assemblies are those of the metallic fuel version of the S-PRISM core developed by General Electric [44]. The active core height is 250 cm – the typical of B&B reactor cores [33, 35] but about two and a half times that of compact cores, like the ANL designed Advanced Burner Reactor (ABR) [41, 43] and S-PRISM. The seed diameter is initially set at 102.5 cm in order to have about 20% of its fission neutrons leak into the blanket [49]. All other geometry (Table 2-1) and composition specifications are derived from S-PRISM [44] including the core nominal power — 1000 MWt. The seed fuel is the ternary metallic alloy U-TRU-10wt%Zr that has a theoretical density of 15.7 g/cm^3. A smear density of 75% is assumed to accommodate the fuel swelling during burnup. The blanket fuel is natural thorium in metallic form that has a theoretical density of 11.7 g/cm^3 and a smear density of 85%. The low-swelling ferritic martensitic steel HT9 is selected as the structural and cladding material at density of 7.874 g/cm^3. A uniform sodium density of 0.849 g/cm^3 is set throughout; it corresponds to an average coolant temperature of 700 K. The assembly pitch, inter-duct gap and duct thickness are the same as in S-PRISM — 16.142 cm, 0.432 cm, and 0.394 cm, respectively. The pitch-to-diameter ratio is determined by thermal hydraulic calculations such that large enough coolant path is preserved to deliver the peak assembly power. Grid spacers are applied with a spacing of 25 times the fuel outer diameter. Fuel rod outer diameter and P/D are design variables. The ratio of cladding thickness and fuel diameter is kept constant at 0.075, as for the S-PRISM driver fuel.

Table 2-1 Dimensions and Composition of the Components for the S&B Design [44]

Property	Value	Material (volume %)
Axial Dimension (cm)		
Upper Reflector	60.0	50% HT9 – 50% Na
Upper End Plug	2.5	22% HT9 – 78% Na
Upper Plenum	191.1	design variables[1]
Lower End Plug	111.7	22% HT9 – 78% Na
Grid Plate	5.2	50% HT9 – 50% Na
Lower Shielding	30.0	47% B_4C - 21% HT9 - 32% Na

[1] Same volume fractions for cladding and coolant are applied as those for active core region.

Radial Dimension[2] (cm)		
Active Core OD[3]	270.3	design variables[4]
Reflector OD	326.2	50% HT9 – 50% Na
Shielding OD	354.1	47% B_4C - 21% HT9 - 32% Na
Assembly Geometry (cm)		
Assembly Pitch	16.124	-
Duct Gap	0.432	-
Duct Wall Thickness	0.394	-

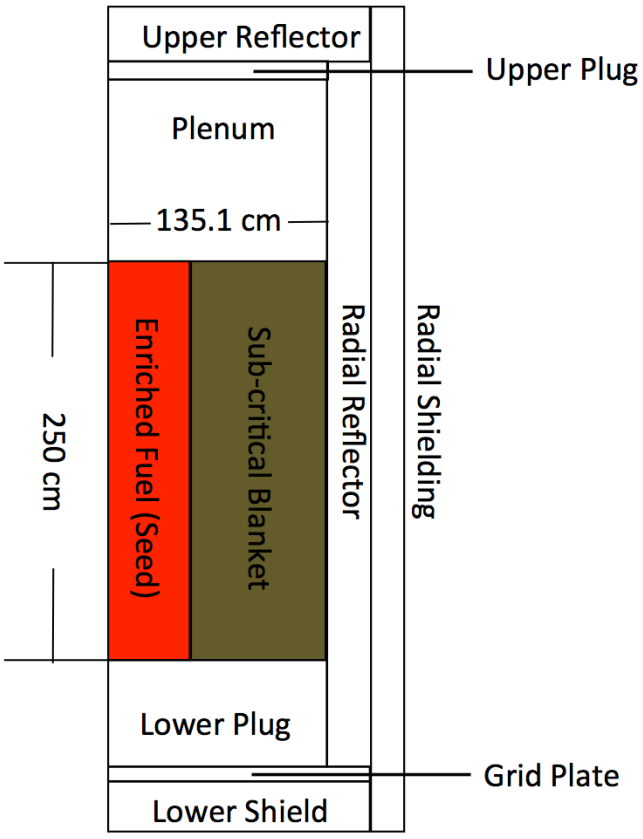

Figure 2-1 Layout of the S&B core

[2] Approximate value for R-Z model
[3] Outer Diameter (OD)
[4] The fractions of fuel/cladding/coolant depend on the P/D ratio of fuel assemblies

Figure 2-2 shows the fuel management scheme of the S&B core. The seed fuel is managed as in a conventional ABR [41, 43]: at the end of each cycle, a fraction of the seed fuel is discharged and sent to reprocessing; no shuffling is applied to the fuel assemblies that remain in the core. The neutronic analysis assumed that heavy metals are fully recovered and recycled into fresh seed fuel; the fuel cycle analysis in Chapter 7 discards 1.2% heavy metal in the waste stream due to the reprocessing and fabrication losses. Depleted uranium and TRU from LWR UNF (burnup of 50 MWd/kg followed by 10-year cooling time [41]) as make-up fuel is added to the recovered heavy metal. Table 2-2 provides the composition of the TRU used in the make-up mix. The blanket region of the core operates in a multi-batch once-through breed and burn mode. Natural thorium is loaded in the outermost blanket batch. At End of Equilibrium Cycle (EOEC) each blanket batch is shuffled inward and the innermost blanket batch is discharged and stored.

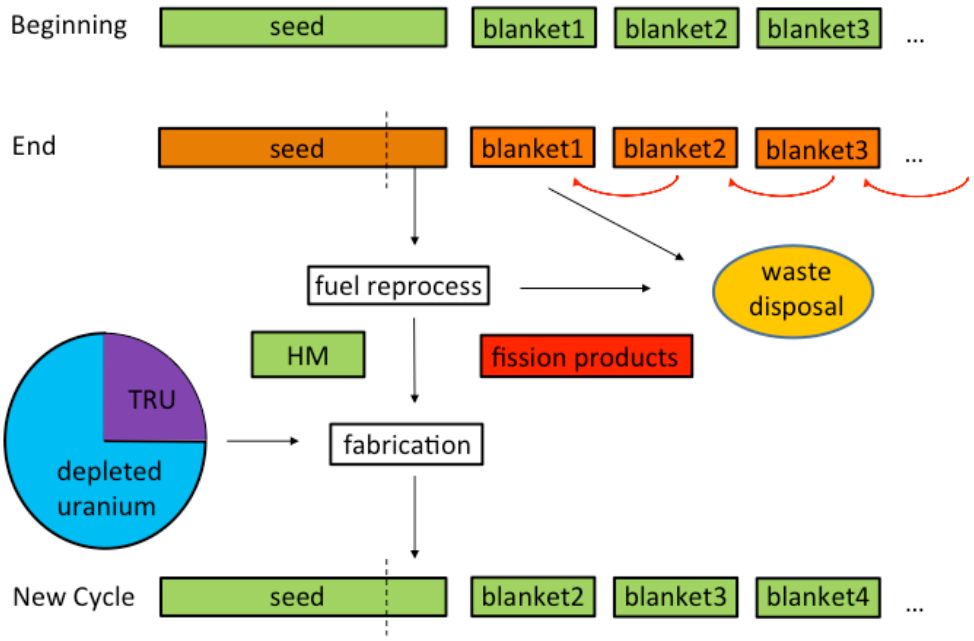

Figure 2-2 Fuel management scheme

Table 2-2 Composition of TRU Extracted from LWR's UNF at Discharge Burnup of 50 MWd/kg and 10-years Cooling [41]

Isotope	Weight Percent

^{237}Np	4.7%
^{238}Pu	2.2%
^{239}Pu	47.3%
^{240}Pu	22.8%
^{241}Pu	8.4%
^{242}Pu	6.8%
^{241}Am	5.6%
^{243}Am	1.6%
^{244}Cm	0.5%

2.3. Design variables

Besides the zone dimensions and composition (Table 2-1) consistently used for this study, the S&B core design variables investigated are summarized in Table 2-3. Figure 2-3 shows the overview of the multi-physic study where the design options are selected based on the specific objective of the S&B design. The core design involves several interactive modules. For example, in order to achieve large TRU transmutation rate, neutronic analysis suggests more TRU contents loaded in the core while fuel irradiation data require a higher Zr fraction for such high TRU content fuel [50]. The major design variables include the number and location of seed and of blanket fuel assemblies, the seed and blanket batch numbers, fuel shuffling scheme, cycle length, TRU-to-HM ratio in the makeup fuel of the seed, diameter of fuel pins and pitch-to-diameter ratio. The design variables of the core configuration and the fuel cycle are determined through the neutronic analysis. The thermal hydraulic analysis is conducted to assure that the design constraints are met.

Table 2-3 Summary of the Design Variables for the S&B Study

Core Configuration	
	Number of seed/blanket fuel assemblies
	Number of seed/blanket batches
	Inner/outer diameter of annular seed
	Active core height
	Fuel type charged into the blanket
Fuel Cycle	
	Cycle length
	TRU wt% in feed fuel of seed
	Fraction of seed fuel recycled
Thermal Hydraulics	
	P/D ratios for assemblies in seed/blanket

Outer cladding diameter D
Coolant mass flow rate

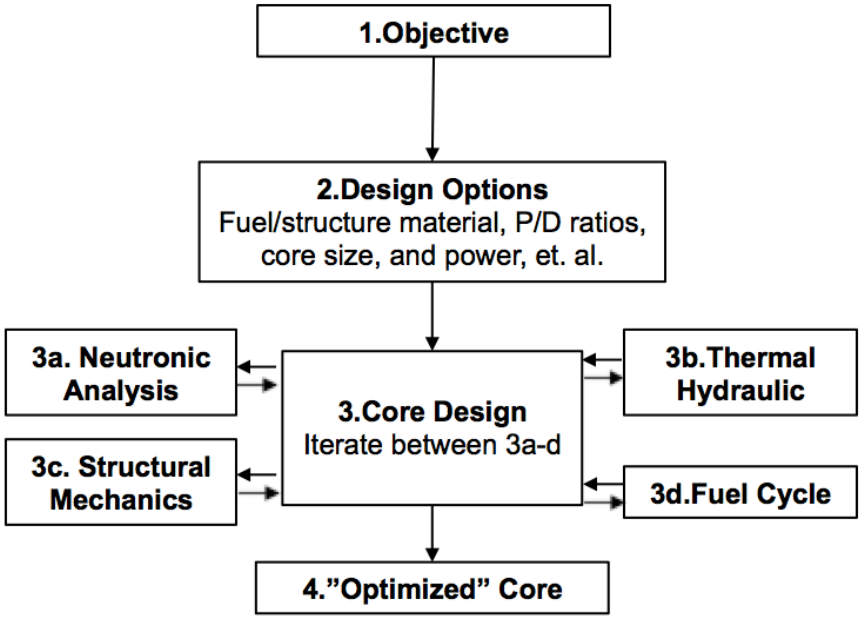

Figure 2-3 Overview of the multiphysics core design

2.4. Design constraints

The following engineering design constraints (Table 2-4) are applied throughout the analysis:

- The coolant pressure drop across the core, including the pressure drop at the core inlet and outlet along with the 1.9 m long fission gas plenum, is constrained to 0.9 MPa [15, 51, 52];
- The coolant temperature rise across the active core is fixed at 155 °C with inlet temperature of 355 °C [41, 43]; it is assumed that the coolant flow rate of each fuel assembly will be adjusted by coolant inlet orifice according to the assembly power as a function of the assembly location;
- The maximum sodium coolant velocity is set at 12 m/s [52];
- The inner cladding temperature is required to be lower than 650 °C — the melting temperature of the HT-9 and plutonium at eutectic point, and the fuel centerline temperature is conservatively constrained to 800 °C [53];

- The peak radiation damage on cladding for both seed and blanket is limited by 200 DPA that is the presently acceptable based on the irradiation data obtained in the FFTF [40]. In order to achieve 200 DPA for both seed and blanket at discharge point, a DPA value no more than 210 is still at the margin of acceptability;
- There is no hard limit for burnup reactivity swing, but it is desirable to limit the burnup reactivity swing over one cycle to ~3.5% Δk/k; the small burnup reactivity swing avoids too large reactivity worth assigned to each control assembly and reduce the number of control assemblies for higher fuel loading.

Table 2-4 Major Design Constraints

Design Constraints	Value
Min. k_{eff} over cycle	1.000
Burnup reactivity swing per cycle (Δk/k)	3.5%
Coolant temperature rise (°C)	155
Maximum coolant velocity (m/sec)	12
Maximum cladding temp (°C)	650
Maximum fuel temp (°C)	800
Core pressure drop (MPa)	0.9
Peak radiation damage at discharge (DPA)	200

Nevertheless, two of the reported constraints are different from the practices applied to the design of the ABR cores that the S&B cores in this study are widely compared against. (1) The 0.9 MPa assumed for the pressure drop through the core. It is at least twice the value commonly used for the SFR cores and the sensitivity of S&B core performance to the pressure drop constraint is reported in Section 6.3. (2) The 200 DPA radiation constraint supported by literature related to the analysis of structural material samples irradiated in the FFTF. An investigation concludes that the 200 DPA from typical S&B core corresponds to the fast fluence of $5.0\sim5.6\times10^{23}$ n(>0.1MeV)/cm^2 – significantly higher than the fast fluence constraint of 4×10^{23} n(>0.1MeV)/cm^2 in use by ANL and other SFR designers. Although the DPA calculation in this study is verified in Section 2.7 and takes into account the specific energy dependence of neutron spectrum that may significantly vary across S&B cores, the comparisons of the performance characteristics between the S&B versus the ABR cores are biased in favor of the S&B cores. The sensitivity of the S&B core performance to the radiation damage constraint was investigated in the later part of this project and is presented in Section 6.5. It quantifies the bias introduced by the inconsistent use of the radiation damage constraint.

2.5. Neutronic analysis

As the neutron mean free path in fast reactors is larger than the lattice pitch, it is common to represent each burnup node for neutronic analysis as homogenized [54]; the fuel, cladding-structural material, and coolant are mixed preserving their volume fractions. The results from the core that is represented by a simplified "R-Z" model are found to be in acceptable agreement with those obtained using a detailed heterogeneous core model [33, 54]. The core is radially divided into three equal-volume concentric burnup zones for the seed and one burnup zone for each blanket batch; each radial zone is further divided into six axial burnup nodes. The two computational codes used for the neutronic analysis are described below.

2.5.1. Monte-Carlo based codes: MCNP/ORIGEN2.2

An advanced Monte Carlo depletion simulator, called MocDown, is used for this study. Like MOCUP[55], MONTEBURNS[56], IMOCUP[57], PyMOCUP[58], and MCODE[59], neutron transport by MCNP [60] and transmutation by ORIGEN2.2 [61] were coupled by Dr. Jeffrey Seifried at University of California Berkeley [62] for the depletion of nuclear reactor cores. MocDown, written in object-oriented Python 3, is able to search for the composition of equilibrium fuel cycle in an efficient manner. To provide a robust and user-friendly experience, MocDown facilitates the following features [62]:

- The depletion matrix (region-wise fuel composition, region-wise flux magnitude, one-group cross-sections) is prepared from a single MCNP tally that is dynamically generated. Based on a user-defined threshold for abundance and contribution to nuclear reaction, MocDown automatically selects which actinides and fission products to track for neutronic and burnup calculations. During depletion, any isotopes whose atom fraction, weight fraction, absorption rate fraction, and fission rate fraction do not exceed the cutoff fraction (0.001% is applied for this study) are not tracked and included in the transport calculation. Unlike most other Monte Carlo depletion simulators, it is not required for a priori specification of the isotopes to be tracked.

- The execution of ORIGEN2.2 is concurrently threaded by using the Python 3 libraries. The depletion of 20 regions is executed on parallel.

- Regular expression parsing is applied for robust extraction of the depletion matrix such that the restrictions on the format of neutron transport codes are removed. In addition, the transport module in MocDown can utilize different versions of MCNP, including MCNP5, MCNPX, and MCNP6.

- The number of source neutrons per second (S) is generated by (Equation 2-1) after considering the decay heat (P_d) and photon heating. In the equation, P_{th} is specified by user for the target thermal power; E is the total energy deposited in the core per source neutron and is estimated directly with MCNP using a single F6 tally: neutron/photon track-length estimated energy deposition tally [60]; the studies of the S&B cores conducted neutron transport calculation only and thus recoverable energy (Q) from both fission and neutron capture reactions are taken into account for E; P_d is calculated based on isotopic inventory and corresponding decay rate.

$$S = \frac{P_{th} - P_d}{E}$$

(Equation 2-1)

In this study, MCNP6 [60] is used with the ENDF/B-VII.0 cross section library [63] for the neutronic calculations with 1200 neutron histories per cycle and 200 active cycles to obtain a target statistical error in k_{eff} of ~100 pcm. ORIGEN2.2 [61] is applied for the burnup calculations using effective one-group cross sections generated by MCNP6. The zone-dependent neutron flux calculated by MCNP is normalized by the zone power before being used in ORIGEN 2.2. Burnup-dependent compositions calculated by ORIGEN2.2 are sent back to MCNP6 after each burnup step. MCNP6 and ORIGEN2.2 are coupled via a two-tiered solver (Figure 2-4) that automates an efficient iterative search for equilibrium composition of multi-batch cores depending on a prescribed fuel management scheme [62]. The outer loop performs full-fidelity cycle (with updated transmutation constants from transport calculation) until the multiplication factors between two cycles fall within a prescribed tolerance. Following each fuel cycle on the outer loop, the accelerated module initiates the inner loop that the fuel depletion and recycling is conducted continuously until the fuel composition between two successive fuel cycle falls below a prescribed tolerance. In the inner loop, the transmutation constants are preserved such that no transport calculation is performed and the computation time is significantly reduced with the use of this acceleration strategy.

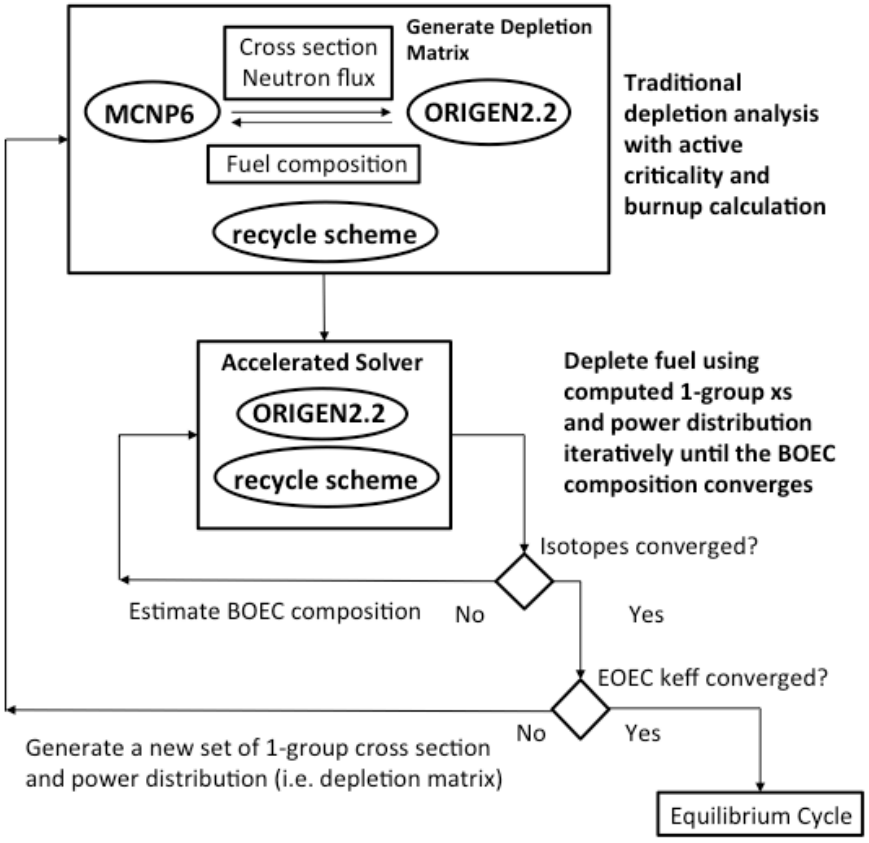

Figure 2-4 Computation scheme of MocDown for equilibrium cycle search

2.5.2. Deterministic codes: MCC-3/DIF3D/REBUS

A code package for fast reactor analysis, called Argonne Reactor Computation (ARC), was developed by Argonne National Laboratory based on the deterministic method. The codes are more computationally efficient compared with the Monte Carlo simulator. The package is composed of several modules, including Multigroup Cross-section generation Code (MCC-3) for the multi-group cross-section preparation, DIF3D for the whole core neutronic calculation, REBUS for the depletion calculation and the searching for the equilibrium cycle, and PERSENT for the calculation of safety coefficients. An overall computational flow is shown in Figure 2-5 and the detail functions of each module are described below.

The multi-group cross-section libraries for fast reactor analysis are prepared by MCC-3 [64]. The code solves the consistent P1 multigroup transport equation using basic neutron

data from ENDF/B data files. A 1-D cylindrical problem is solved in ultrafine group (ANL 2082-group) level. The point-wise ultrafine group cross sections are sent to a 2-D transport module, call TWODANT, for the whole core criticality calculations. The region-dependent neutron spectra generated by TWODANT – accounting for neutron leakage out of the core, are used by MCC-3 for the region-dependent broad-group cross-sections generation (ANL 33-group). The multigroup cross-sections are written in the ISOTXS format. Lumped fission product cross sections are generated by weighting the cross-sections of 137 fission products with their fission yields. Since MCC-3 only accommodates the assumptions for fast spectra (up-scattering is not considered and no thermal scattering law is implemented [64]), ARC is limited to fast reactor analysis. Instead, MocDown uses continuous cross-sections and is therefore applicable for the analysis of several special S&B cores that feature relatively softer neutron spectra in their blanket.

The whole core criticality analysis is performed by the advanced nodal diffusion code DIF3D [65]. Using homogenized assembly group constants prepared by MCC-3, DIF3D solves the broad-group (ANL 33-group) diffusion equation for three-dimensional Cartesian or hexagonal geometries. The depletion calculation together with the equilibrium search is performed by REBUS-3 [66] for the fast reactor fuel cycle. REBUS-3 conducts the transmutation calculation by using the flux on region-dependent basis. The decay chain spans the range from ^{232}Th to ^{246}Cm and all other minor actinides are stored in two dump vectors. Both the non-equilibrium cycle problem and equilibrium cycle problem that determines the equilibrium composition of a reactor pertaining to a fixed fuel management scheme can be solved by REBUS-3. Two basic types of the equilibrium cycle searches can be made: (1) search for the enrichment of the charged fuel and (2) search for the reactor cycle length. This study applies the enrichment option where the TRU contents (both external TRU and recycled TRU) in the charged fuel are automatically searched such that k_{eff} at End of Equilibrium Cycle (EOEC) is above 1.000 with the margin of 100pcm. REBUS allows the users to simulate a specified fuel cycle scheme or reprocessing activity, like the isotopic dependent removal fractions.

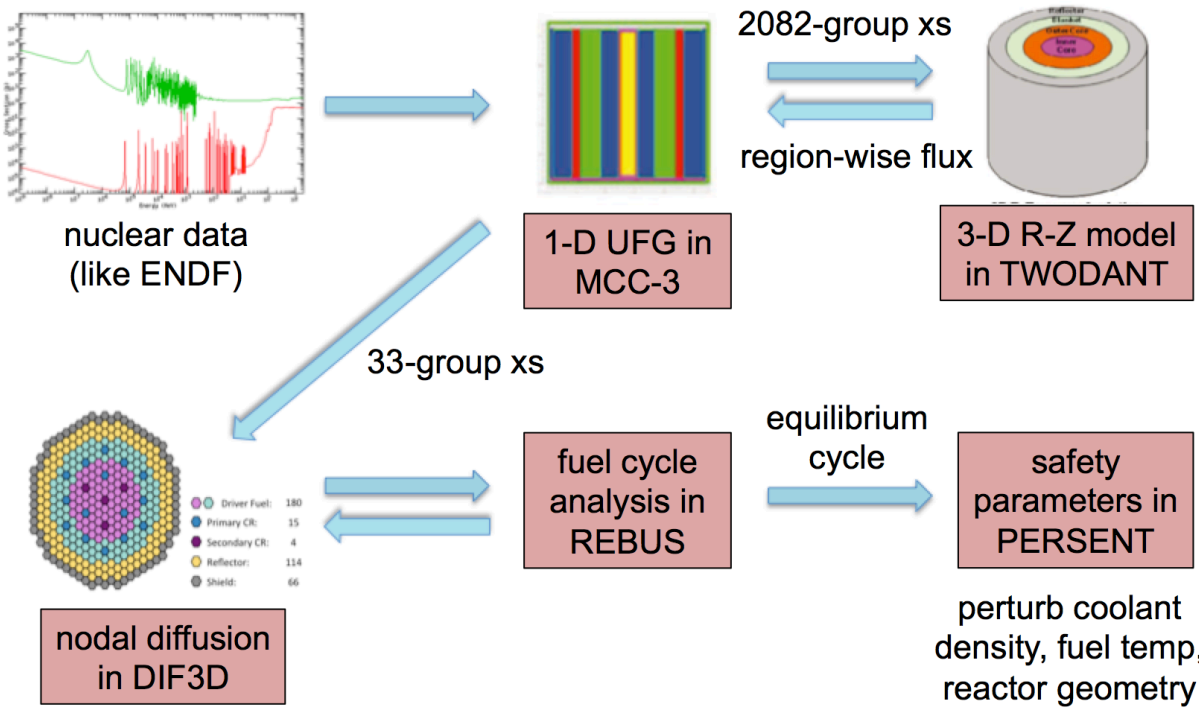

Figure 2-5 Overview of the computational flow for MCC-3/DIF3D/REBUS/PERSENT [54]

2.6. Benchmarking between MocDown and REBUS

The model used for benchmarking the two code systems is the S&B core in which the thorium blanket is driven by cylindrical seed that features a TRU CR of 0.5 (described in [67]). The driver fuel volume is equivalent to 37 assemblies at the center of the core while the blanket volume is equivalent to 234 assemblies surrounding the seed zone. The active core has 3 seed batches and 26 blanket batches; each batch has 6 equal volume axial burnup zones. The active core height is 250cm. The model used roughly represents the configuration of S&B core defined in (Table 2-1) including seed/blanket fuel, zones, reflector, shielding, plenum, and grid plate.

Different core compositions are assumed for the depletion analysis and for the equilibrium cycle analysis. For the depletion analysis the seed fuel is made of U-30TRU-10Zr with the TRU from a typical LWR SNF; ^{232}Th with 5% ^{233}U is charged uniformly to the blanket. For the equilibrium core analysis the makeup fuel is TRU from a typical LWR UNF along with depleted uranium for the seed; fresh thorium is fed to the blanket.

2.6.1. Criticality

MocDown and ARC are used to calculate the core k_{eff} at beginning of life described above. Multi-group (ANL33) cross-sections are condensed by MCC3-TWODANT from ENDF7 point-wise format. Multi-regions with leakage sources are modeled in MCC-3 (step 1). Macro cross-sections generated for each region are used for the transport calculation in TWODANT (step 2). Same as MocDown, the fuel, cladding, and coolant are homogenized in TWODANT and MCC-3 based on the volume fraction. In step 3, MCC-3 is applied along with major actinides and lumped fission products to generate group constants using the actual region-wise spectra from the previous step.

Following the cross-section preparation, a R-Z model is used in DIF3D with same configurations as used in MocDown. The k_{eff} values calculated at beginning of life are summarized in Table 2-5. The results from Monte-Carlo code and ARC are generally within good agreement.

Table 2-5 k_{eff} at 0 MWd/kg for Criticality Benchmark

k_{eff} at BOL	Value	Difference (Δk)
MCNP (Reference)	1.25761	±41 (uncertainty)
TWODANT	1.25978	217
DIF3D	1.25627	-134

2.6.2. Depletion calculation

REBUS tracks nineteen actinides (^{234}U, ^{235}U, ^{236}U, ^{238}U, ^{237}Np, ^{236}Pu, ^{238}Pu, ^{239}Pu, ^{240}Pu, ^{241}Pu, ^{242}Pu, ^{241}Am, ^{242}Am, ^{243}Am, ^{242}Cm, ^{243}Cm, ^{244}Cm, ^{245}Cm, ^{246}Cm) for uranium-based transmutation and additional three actinides (^{232}Th, ^{233}Pa, ^{233}U) for thorium-based cycle. Other than these active actinides, minor actinides with low importance for the isotope series are dumped into two non-active actinide vectors that involve no nuclear reactions. Seven lumped fission products are used in REBUS covering the atomic weight from 232 to 241. MocDown tracks the active isotopes above the cutoff fraction (Section 2.5.1); the fission products are explicitly tracked from the ORIGEN2.2 depletion calculation. The depletions with a cycle length of 6000 days and a thermal power of 1000 MWt were conducted by MocDown and REBUS for benchmark purpose.

The evolution of k_{eff} over 6000 Effective Full Power Days (EFPD) is shown in Figure 2-6. At the end of cycle the average core burnup is 97.6GWd/MT while the average burnup of the seed and blanket are 332.2 GWd/MT and 69.5 GWd/MT, respectively. The

maximum difference of 319pcm occurs at end of cycle; it is ignorable relative to the burnup reactivity swing of 33470pcm.

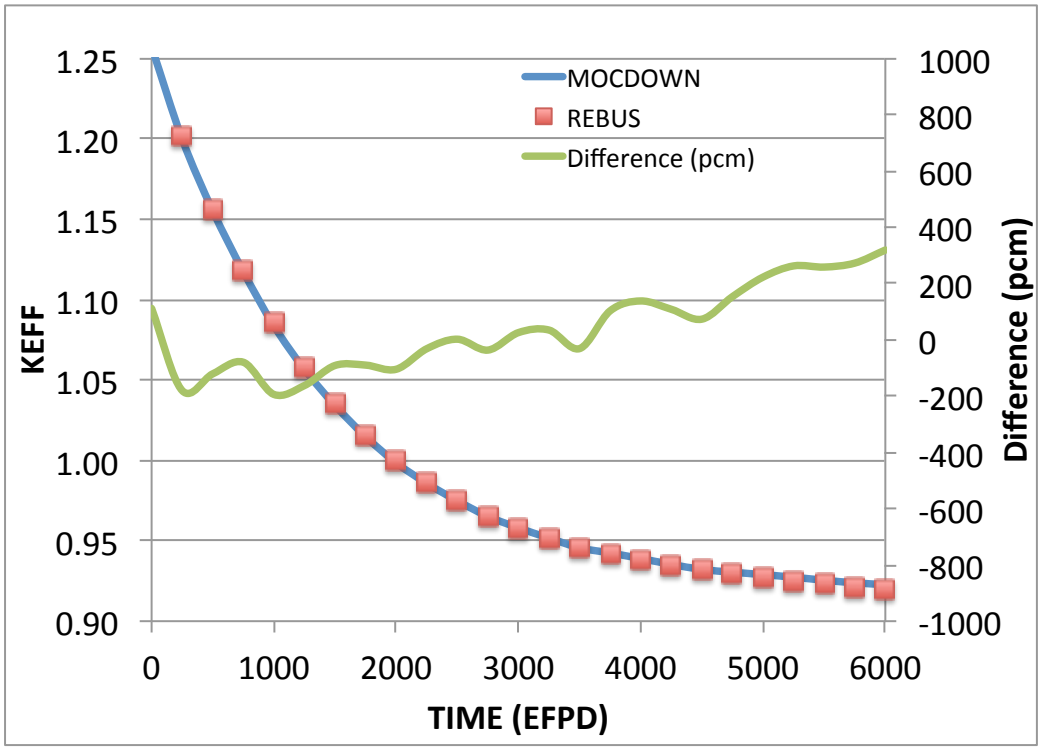

Figure 2-6 Benchmark calculation of the keff evolution with burnup

The performance characteristics of the depletion benchmark are summarized in Table 2-6. The cell average flux is compared in Figure 2-7 at seed burnup of 0 MWd/kg and 220 MWd/kg. The axial middle layer of the core is selected to represent the maximum cell average flux. The middle layer flux distributions from MocDown and REBUS are in good agreement for the fresh fuel (Figure 2-7a). At 220 MWd/kg, MocDown reports a lower flux – 3% for the seed and 6-10% for the blanket (Figure 2-7b) throughout the core. The difference is attributed to the slight difference between deliverable fission energy used by the two codes; the energy per fission used by MocDown is ~5% higher than that used by REBUS (Table 2-6).

Table 2-6 Performance Characteristics Comparison for the Depletion Benchmark

	MocDown	REBUS
keff		

	at BOL	1.257±0.00041	1.25627
	at EOL	0.923±0.00027	0.91949
Power from blanket			
	at BOL	28.1%	28.2%
	at EOL	81.8%	82.8%
Cycle length (EFPD)		6000	
Ave. discharge burnup, %FIMA (S/B)		35.7/6.7	35.3/7.2
Ave. MeV per fission		211.4	200.6
Max. cell average fast fluence, n/cm^2 (S/B)		1.25E+24/9.11E+23	1.30E+24/9.45E+23
Peak fast fluence, n/cm^2 (S/B)		-/-	1.36E+24/1.00E+24

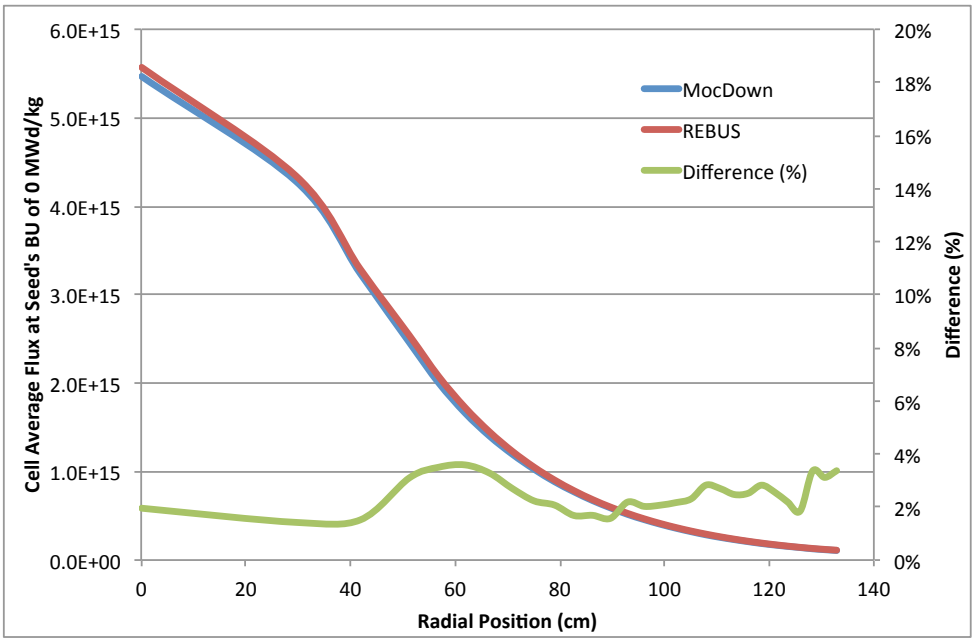

(a)

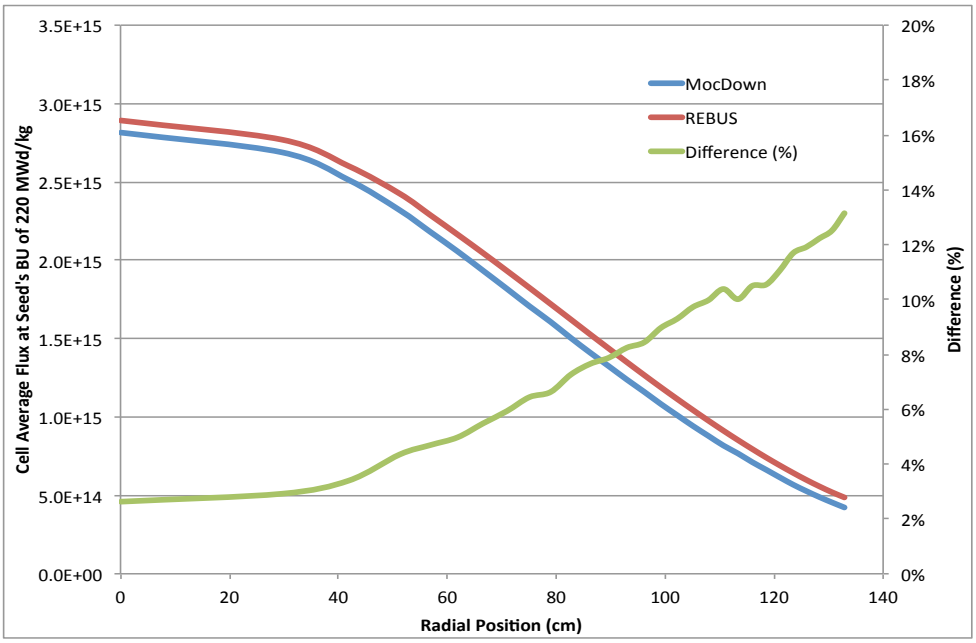

(b)

Figure 2-7 Comparison of the flux distribution at the seed's burnup of 0 MWd/kg (a) and 220 MWd/kg (b)

2.6.3. Equilibrium cycle

MocDown and REBUS were applied to search for the equilibrium cycle assuming the same fuel management scheme. REBUS has two modes to search for the equilibrium cycle: enrichment and burnup modes. For the enrichment mode, there are two classes: class 1 is the "fissile" fuel while class 2 is the "fertile" fuel. For the seed fuel of this benchmark class 1 is recycled TRU plus LWR's TRU while class 2 is depleted uranium. REBUS searches the enrichment that ensures criticality throughout the cycle. Since the blanket fuel is shuffled from an outer batch inwards, the fuel composition discharged in the previous batch is the composition of the fuel loaded into the next (inner) batch. To simulate this scenario, half of the fuel in the blanket batch, including the thorium and all trans-thorium isotopes, is defined as class 1 and the other half (including the thorium and all trans-thorium isotopes) as class 2 so that the enrichment searching won't change the blanket fuel composition. Cooling of the fuel between shuffling is ignored for this benchmark.

Whereas MocDown is based on Monte-Carlo simulation and uses multi-cycle to search for the equilibrium composition, REBUS is a deterministic code and uses an enrichment

search method. REBUS is computationally more efficient - typically REBUS can converge to the equilibrium cycle in 20 minutes compared with hours it takes MocDown.

A comparison of the equilibrium cycle characteristics arrived at by the two codes is included in Table 2-7. The equilibrium cycles identified by the two codes are generally in good agreement. REBUS predicts a somewhat higher leakage probability from the seed to the blanket and, hence, a larger fraction of core power generated by the blanket and, therefore, a higher blanket but lower seed discharge burnup, and a corresponding difference in the cell-average neutron flux magnitude for the middle of equilibrium cycle (MOEC) in Figure 2-8; the smaller seed discharge burnup predicted by REBUS makes the core burnup reactivity swing smaller; the seed TRU enrichment level somewhat lower and the TRU conversion ratio correspondingly higher. REBUS predicts a slightly higher cell-average fluence for the blanket and slightly lower value for the seed due to the larger (lower) blanket (seed) power it predicts (Table 2-7).

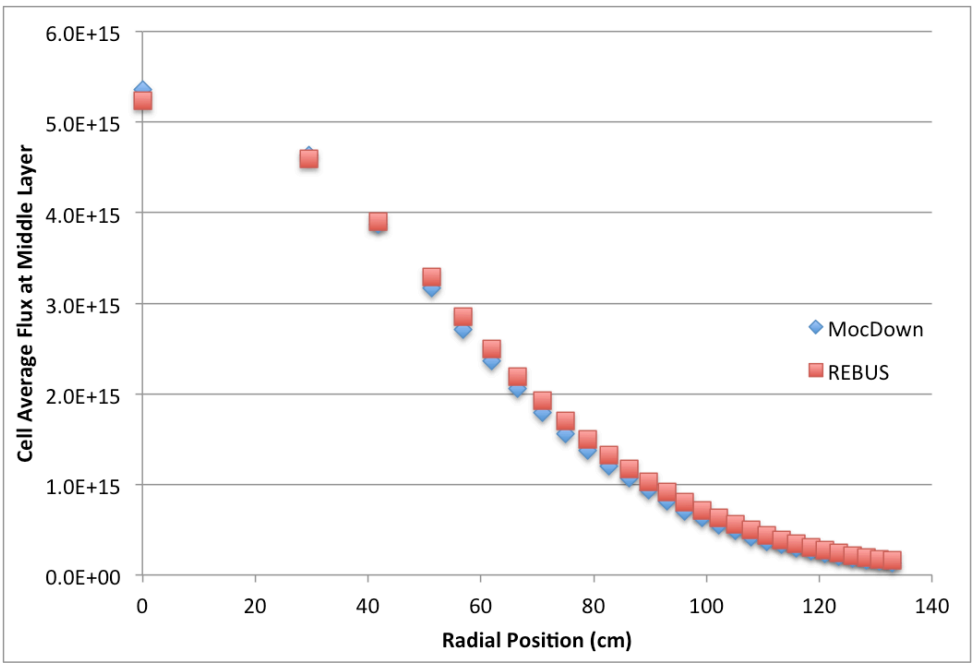

Figure 2-8 Flux distribution in the axial middle layer at the MOEC

REBUS has the ability to track the peak fast fluence through the fuel residence time and this value is higher than the maximum cell-average fluence by 8-13%. The peak fast fluence is overestimated for the fuel in the blanket because the blanket fuel is shuffled. Fuel shuffling can be executed in a way that minimizes the peak-to-average zone fluence.

The peak-to-cell average fast fluence in an annular seed – used for all the optimal S&B cores, is significantly smaller than in the central seed assumed for this benchmark.

Table 2-7 Performance Characteristics Comparison for the Equilibrium Cycle

	MocDown	REBUS
k_{eff}		
at BOEC	1.041±0.001	1.03872
at EOEC	1.007±0.001	1.00651
Leakage from seed to blanket at BOEC	25.1%	25.7%
Power from blanket		
at BOEC	40.6%	42.7%
at EOEC	45.1%	46.4%
TRU/HM at BOEC	30.4wt%	29.2wt%
TRU conversion ratio at BOEC	0.51	0.54
Cycle length (EFPD)	405	
Ave. discharge BU, %FIMA (S/B)	16.1/7.7	14.1/8.9
Ave. MeV per fission (S/B)	215.3	205.6
Max. cell average fast fluence, n/cm^2 (S/B)	5.02E+23/5.55E+23	4.83E+23/6.10E+23
Peak fast fluence, n/cm^2 (S/B)	-/-	5.24E+23/6.89E+23
DPA, (S/B)	194/196	-/-

2.7. Radiation damage induced by high-energy neutrons

2.7.1. Basic theory

The high-energy neutrons move through the lattice of cladding materials and encounter lattice atoms. When sufficient energy is transferred to lattice atom, the atom is displaced from its original site and a collision sequence is initialized [68].

The radiation damage rate is quantified by

$$R_d = N\int_{\bar{E}}^{\bar{E}} \phi(E_i)\sigma_D(E_i)dE_i$$

(Equation 2-2)

where

N = the lattice atom density

$\Phi(E_i)$ = the energy-dependent particle flux

$\sigma_D(E_i)$ = the energy-dependent displacement cross section

The displacement cross-section is a probability for the displacement of lattice atoms by incident particles:

$$\sigma_D(E_i) = \int_{\bar{T}}^{\tilde{T}} \sigma(E_i, T) v(T) dT$$

(Equation 2-3)

where

$\sigma(E_i, T)$ = the probability that a particle of energy E_i will impart a recoil energy T to a struck lattice atom

v(T) = the number of displaced atoms resulting from such a collision

The Kinchin and Pease (K&P) Model is widely used for the atom displacement when a moving particle strikes a stationary atom. The detail of K&P model is discussed in [68] and the number of displaced atoms resulting from a collision is given

$$v_{K\&P}(T) = \begin{cases} 0 & for\ T < E_d \\ 1 & for\ E_d < T < 2E_d \\ \dfrac{T}{2E_d} & for\ 2E_d < T < E_c \\ \dfrac{E_c}{2E_d} & for\ E_c < T \end{cases}$$

where

E_d = the minimum energy that must be transferred in order to produce a displacement

E_c = the energy when collisions with electrons compete for energy loss against collision with lattice atoms.

Lindhard further developed a detailed theory for energy partitioning that was used to compute the fraction of the neutron energy that is dissipated in the nuclear system through elastic collisions with nuclear atom and energy losses with electrons. Instead of a sharp cutoff between nuclear collisions and electronic collision (in K&P model), Lindhard model considers the electronic collisions below E_c and nuclear collisions above E_c. This work was further developed by Norgett, Robinson, and Torrens (NRT) as a displacement model that is still applied as a standard in the nuclear industry to compute atomic displacement rate [69]:

$$\nu_{NRT} = \frac{0.8T}{2E_d}$$

(Equation 2-4)

The probability of the particle interaction $\sigma(E_i, T)$ takes into account the elastic scattering (low energy range), inelastic scattering (high energy range), (n,2n) and (n, γ) reactions [68]. The isotopic dependent displacement cross-sections are stored in the ENDF/B library.

2.7.2. DPA calculation

The accumulated DPA value is calculated using the equation below. The region-wise effective (spectrum weighted) one group DPA cross-sections, σ_d, are generated by an FM4 tally of MCNP in unit of barns-MeV; the efficiency η is assumed to be 80%; the displacement energy for Fe and Cr is suggested to be 40eV [70]; the same value is recommended [70] for steels. Since the average neutron energy increases significantly from the periphery to the center of the S&B core and the DPA cross section increases steeply with energy in the range above 0.1 MeV (Figure 2-9), this method consistently takes into account the specific shape of the neutron spectrum in estimating the accumulated radiation damage that the structural materials are exposed to throughout their residence in the core.

$$DPA = \eta \frac{\sigma_d}{2E_d} \int dt\phi$$

(Equation 2-5)

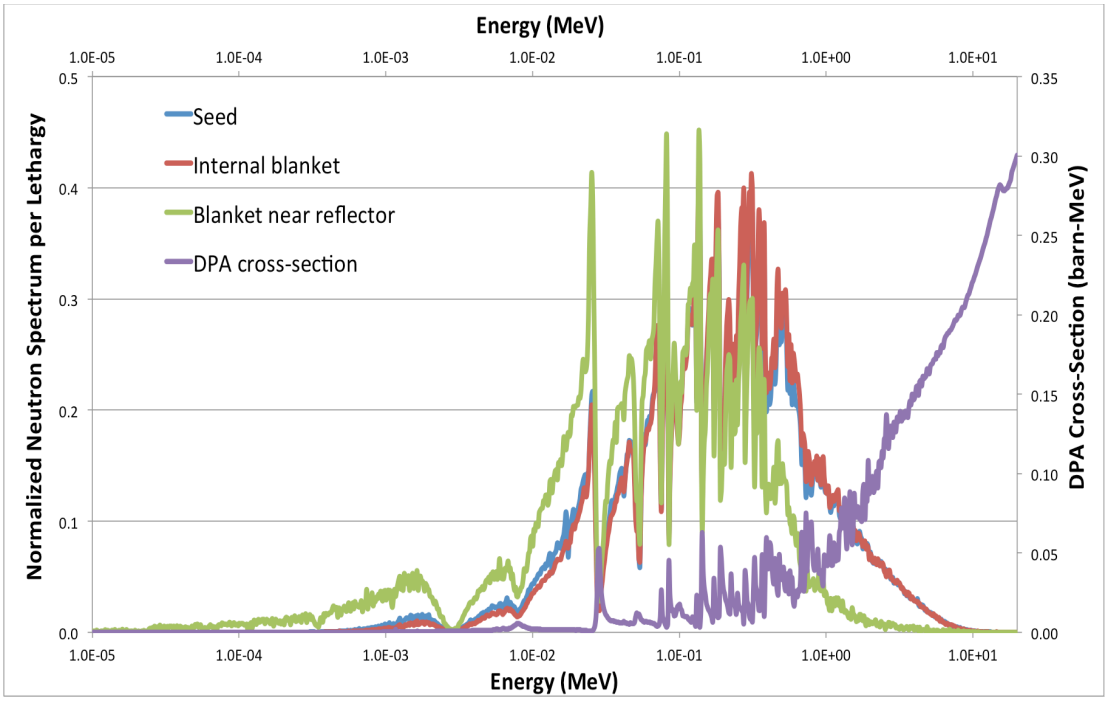

Figure 2-9 Comparison of neutron spectra in the S&B core and the energy dependent DPA cross section

Figure 2-10 shows the radiation damage accumulated in the fuel while in different batches of the benchmark problem as calculated by MocDown (Section 2.6.3). Figure 2-11 shows the relative contribution of different energy neutrons to the radiation damage using a couple of measures. One measure is the fraction of the batch-dependent radiation damage contributed by neutrons pertaining to one of three energy groups. For example, whereas in the innermost blanket zone neutrons of energy below 0.1 MeV contribute approximately 8% of the radiation damage, in the outermost blanket batch their contribution is 20%. The other measure is the batch-dependent total DPA to fast (E>0.1 MeV) neutron fluence ratio. It varies from 29 for the outermost batch to 38 (dpa per 10^{23} n/cm^2) for the innermost blanket batch. As a non-negligible fraction of the radiation damage on the blanket fuel cladding is induced by relatively low energy neutrons, especially near the periphery of the core where the neutron spectrum is softer, using DPA to measure the radiation damage appears to simulate the system physics more consistently than using the fast neutron fluence. However, it is necessary to accurately determine the value of the displacement energy so that the calculated DPA value will be consistent with the existing experimental data.

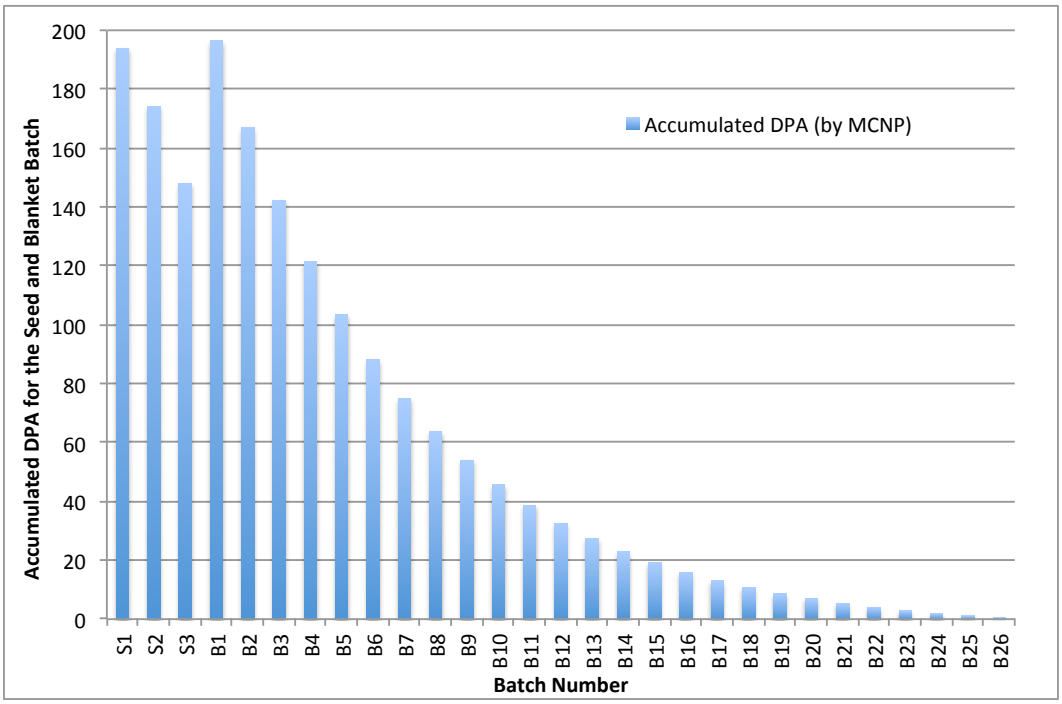

Figure 2-10 Accumulated DPA in the batch-wise axial central zone

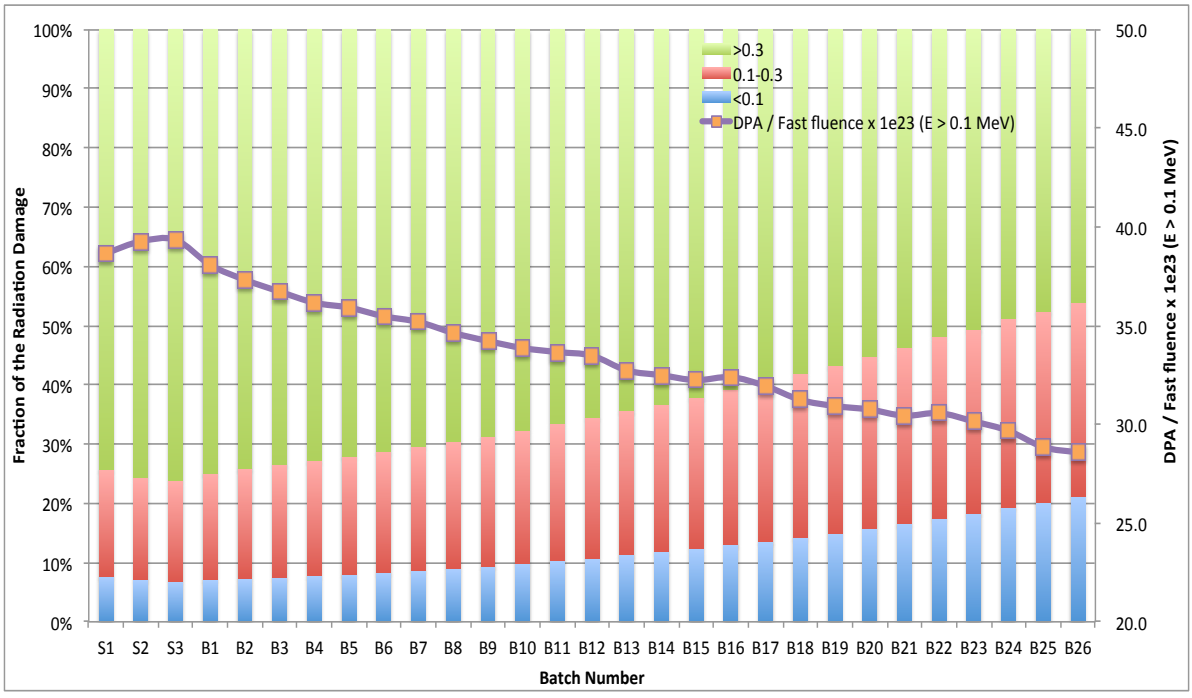

Figure 2-11 Relative three-group DPA cross-section and DPA/Fast-fluence ratios in the batch-wise axial central zone

The radiation damage constraints of 200 DPA and 3.9×10^{23} n(E>0.1MeV)/cm^2-sec have been deduced, to the best of our knowledge, from fuel irradiated in the core of the FFTF [40]. In order to verify the method used to calculate DPA value mentioned above, MCNP was applied to a 0-D model of the FFTF core to get a typical neutron spectrum and deduce the DPA-to-fast fluence ratio for this core. The fuel, cladding, and coolant are mixed together based on the volume fractions from the IAEA database [15]; they are summarized in Table 2-8. There is no information on the plutonium isotopic vector loaded into the FFTF core except that the fissile plutonium fraction of the FFTF is 88% of the plutonium [15]. Therefore, the plutonium composition in a depleted uranium blanket discharged at ~70 MWd/kg is used for the plutonium vector; its fissile plutonium fraction is 88.2%. An inner core enrichment of 22.4% is used for the 0-D FFTF simulation.

The MCNP calculated spectrum of the FFTF is shown in Figure 2-12. Since the FFTF uses oxide fuel, its spectrum is softer compared with that of the innermost blanket batch of the S&B benchmark (in Figure 2-9). The fast neutron fractions (neutrons energy >1MeV) and (neutron energy >0.1 MeV) are, respectively, 10.6% and 60.0%; the corresponding values reported in [71] are 12.0% and 62.0%. It is concluded that the spectrum obtained by the 0-D FFTF model can reasonably represent the experimental spectrum of the FFTF.

Table 2-8 Information for FFTF Simulation [15]

	Parameters
Driver fuel	PuO_2-UO_2
TD for the fuel (g/cc)	11.1
Smear density (%)	85.5%
Enrichment Pu/(Pu+U)	0.2243
Fissile Pu/Pu	88%
Volume Fraction	
fuel	0.31
coolant	0.39
steel	0.26
void	0.04
Cladding material	316 (20% CW)

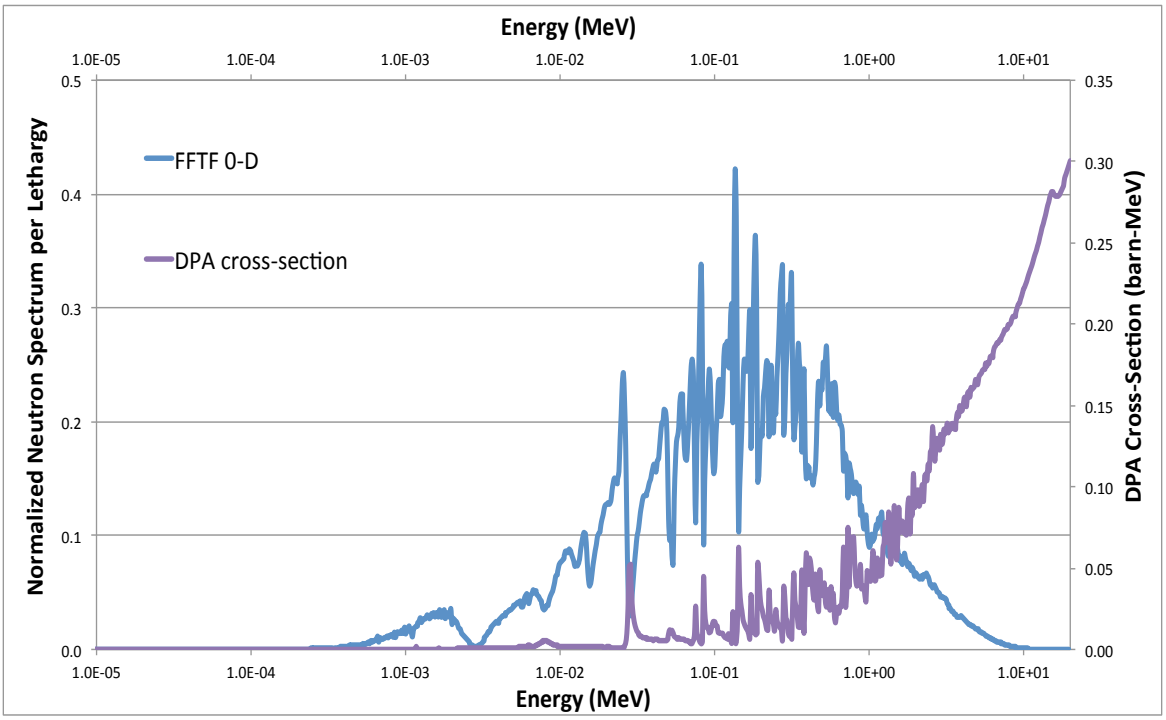

Figure 2-12 Neutron spectrum of the FFTF and DPA cross-section

The 1-g DPA cross-section generated for the FFTF by MCNP is 0.0239 barns-MeV and the fast neutron fraction is 60.0%. In case that 40eV is used for the displacement energy, the DPA corresponding to fast fluence of $4x10^{23}$ n(>0.1 MeV)/cm^2 is 159. The conversion factor is 4.0 DPA per 10^{22} n(E>0.1MeV)/cm^2, which is close to the range between 4.1 and 4.5 DPA per 10^{22} n(E>0.1MeV)/cm^2 estimated for the Material Open Test Assemblies (MOTA) in the FFTF core [72]. Table 2-9 reproduced from reference [71], gives another ratio between DPA and fast fluence for a number of fast neutron facilities including the FFTF for which it is 34.8 DPA per 10^{23} n(E>0.1MeV)/cm^2. This is close but somewhat smaller than the ratio of 39.8 DPA per 10^{23} n(E>0.1MeV)/cm^2 calculated for the 0-D FFTF model. The assumptions used to arrive these values on Table 2-9 are not clear and need to be further explored.

Nevertheless, the conversion factor obtained for the FFTF by MCNP – 4.0 DPA per 10^{22} n(E>0.1MeV)/cm^2 – is definitely lower than the factor widely accepted by the fast reactor community – 5 DPA per 10^{22} n(E>0.1MeV)/m^2 [40, 41, 43, 44, 73, 74]. In order to match this conversion factor, the displacement energy has to be reduced to 32eV, which is close to the value (28eV) recommended by ANL [75]. The radiation damage constrained directly by the fast fluence of $4x10^{23}$ n(E>0.1MeV)/cm^2 is also widely used by the fast reactor community. To be conservative, the core performance characteristics will be

evaluated under these new constraints in Section 6.5; it is found that the fast fluence along with the achievable discharge burnup allowed for 200 DPA decrease when smaller displacement energy is applied for the radiation damage calculation. The core performance change correspondingly with more details shown in Table 6-5.

Table 2-9 DPA to Fast Fluence Ratio for Typical Fast Neutron Facilities in Russia and US [71, 76-78]

	SM-2 AZ	BOR-60	EBR-II	FFTF
Thermal power, MWt	100	55	62.5	295
Fast neutron flux (>0.1 MeV), n/cm^2-sec	1.00E+15	1.80E+15	2.30E+15	3.10E+15
Fraction of neutron (>1 MeV)	17.1%	24.8%	21.8%	12.0%
Fraction of neutron (>0.1 MeV)	28.6%	89.1%	83.6%	62.0%
DPA/yr (Fe)	27	24	33	34
DPA/Fast_fluence ratio, $x10^{23}$	85.6	42.3	45.5	34.8

2.8. Thermal hydraulic analysis

The thermal hydraulic analysis for this project is based on a loosely coupled approach. A thermal hydraulic module, called Assembly Design and OPTimization (ADOPT) [51], is a comprehensive computer code that automates the process of designing and analyzing the thermal hydraulic aspects of fast reactor fuel assemblies. According to the assembly specification (like fuel diameter D and Pitch-to-Diameter ratio P/D), inlet/outlet coolant temperature, and pressure drop constraint, the maximum power deliverable by the fuel assembly is calculated and this value is required to safely accommodate the peak assembly power inferred from the neutronic analysis. This section briefly summarizes the functions of thermal hydraulic analysis based on references [13, 51].

2.8.1. Coolant velocity

The coolant velocity is defined from the equation below. As the inlet and outlet temperatures together with the cross-section area of coolant channel are fixed, the maximum power deliverable by the assembly is obtained without violating the coolant velocity constraint of 12m/s (Section 2.4) as below:

$$v = \frac{\dot{Q}}{\rho c_p A \Delta T_{axial}}$$

(Equation 2-6)

where

$\dot{Q}$= the peak assembly power (W); it is inferred from the total core power and peak radial to average assembly power ratio,

ρ = the coolant density (kg/m^3)

c_p= coolant specific heat capacity (J/kg-K)

A = the coolant flow area per assembly (m^2)

ΔT_{axial}= the difference between inlet and outlet coolant temperature (K).

2.8.2. Coolant pressure drop

The pressure drop Δp in the flow across the core is composed of form Δp_{form}, friction $\Delta p_{friction}$ and elevation (ignorable) pressure losses [13]. The form pressure losses are given by the equation

$$\Delta p_{form} = K \frac{\rho v^2}{2}$$

(Equation 2-7)

where

K is the form factor determined experimentally for the particular design.

The friction pressure losses through bare fuel bundle are given by [13]

$$\Delta p_{friction} = f \frac{L}{D_h} \frac{\rho v^2}{2}$$

(Equation 2-8)

where

L = the length of flow path in the active core and fission gas plenum

D_h = the hydraulic diameter (m)

After an extensive review of friction factor (f) correlations, the correlations used in ADOPT [51] were those developed by Cheng and Todreas [79].

2.8.3. Fuel/cladding/coolant peak temperature

Radial fuel temperature distribution in steady state is obtained for a cylindrical rod with an internal heat source. It is assumed that the heat source – $\dot{q}$ is uniform in the fuel and there is no neutronic spatial self-shielding within the fuel pin considering the mean free path of the fast neutrons. The heat transfer in the axial direction is ignorable for a thin axial slice:

$$\frac{1}{r}\frac{d}{dr}(rk_{fuel}\frac{dT}{dr})+\dot{q}=0$$

(Equation 2-9)

The two boundary conditions are

(1) $\frac{dT}{dr}=0$ at $r = 0$;

(2) $T=T_s$ at r = R_f,

Where

R_f = outer diameter of fuel pellet (m)

k_{fuel} = thermal conductivity of the fuel (W/m-K)

$\dot{q}$ = uniform volumetric heat source in the fuel (W/m^3)

T_s = temperature at the outer surface of the fuel.

By integrating through the radial direction, the centerline fuel temperature T_{cl} is

$$\int_{T_s}^{T_{cl}} k_{fuel}\,dT=\frac{\dot{q}}{4}R_f^2$$

(Equation 2-10)

The Linear Heat Generation Rate q' (W/m) and volumetric heat source $\dot{q}$ (W/m^3) are related by

$$q' = \dot{q}\pi R_f^2 = 4\pi \int_{T_s}^{T_{cl}} k_{fuel}\, dT$$

(Equation 2-11)

The thermal conductivity of metallic fuel k_{fuel} (W/m-K) depends on the average fuel temperature and the analytical expression is given in the code package as

$$k_{fuel} = 22 + 0.023\ T_{ave} \quad for\ metallic\ uranium$$

$$k_{fuel} = 34 + 0.0133\ T_{ave} \quad for\ metallic\ thorium$$

(Equation 2-12)

The fuel centerline temperature is based on the boundary condition of the fuel rod T_s. The fuel-cladding gap provides great resistance to heat flow and the temperature drop across the gap, $T_s - T_{ci}$, is defined by the equation below. A gap conductance, h_g, strongly depends on the bonding material and the correlations are implemented in ADOPT package [51].

$$T_s - T_{ci} = \frac{q'}{h_g 2\pi R_f}$$

(Equation 2-13)

The temperature difference between the inside and outside cladding surfaces, $T_{ci} - T_{co}$, is obtained from Fourier's law. Since the thermal conductivity of the cladding, $k_{cladding}$, can normally be assumed constant, integrating across the cladding gives

$$T_{ci} - T_{co} = \frac{q'}{2\pi k_{cladding}} \ln\left(\frac{R_{co}}{R_{ci}}\right)$$

(Equation 2-14)

where

R_{ci} = inner radius of cladding (cm)

R_{co} = outer radius of cladding (cm)

Energy is transferred from the cladding surface by convection to the coolant based on following equation:

$$h(T_{co} - T_b(z))2\pi R_{co}dz = q'dz = \dot{m}c_p dT_b(z)$$

(Equation 2-15)

where

$\dot{m}$ = the coolant mass flow rate (kg/sec)

h = heat convection coefficient (W/m^2-K)

$T_b(z)$ = the bulk temperature of coolant at axial position z.

The coolant temperature rise in a single flow channel is obtained by integrating the linear heat generation rate q' through the fuel pin. The average temperature rise from the inlet is

$$\Delta\overline{T}_b = \overline{T}_b(z) - T_{inlet} = \frac{1}{\dot{m}c_p}\int q'(z)dz$$

(Equation 2-16)

Finally the centerline fuel temperature T_{cl}, which is constrained by melting temperature, is obtained as follow

$$T_{cl}(z) = T_{inlet} + \frac{1}{\dot{m}c_p}\int q'(z)dz + \frac{q'(z)}{2\pi R_f}[\frac{R_f}{2\overline{k}_{fuel}} + \frac{1}{h_g} + \frac{R_f}{k_{cladding}}\ln(\frac{R_{co}}{R_{ci}}) + \frac{R_f}{hR_{co}}]$$

(Equation 2-17)

2.9. Optimization strategy

The core design optimization variables are cycle length, the number of seed and blanket batches, number of seed fuel assemblies, fuel pin diameter, and pitch-to-diameter ratio.

The optimization process is schematically shown in Figure 2-13. The cycle length is determined by the core criticality with consideration of preferred burnup reactivity swing (less than 3.5% Δk/k). The number of batches in the seed and blanket are determined such that the peak radiation damages for both seed and blanket fuel are below the DPA limit at discharge point. While keeping the core critical, the number of driver fuel assemblies is reduced by adding more thorium fuel assemblies to the blanket to maximize the power generated in the blanket. The radial power peaking factor and fuel composition inferred from the neutronic calculations are sent to ADOPT [51] for thermal hydraulic calculations. The intra-assembly parameters, like the number of fuel pins per assembly (of fixed outer dimensions) and the fuel pin outer diameter, are optimized by the ADOPT [51] code to meet thermal-hydraulic and structural design constraints. ADOPT uses P/D from the neutronic calculation to evaluate the maximum assembly power that could be delivered without violating the peak fuel and cladding temperature as well as permissible coolant speed and pressure drop. The core optimization strategy searches for the largest seed assembly P/D ratio and the TRU enrichment that gives the desired Conversion Ratio (CR) with sufficient excess reactivity to enable a cycle length that will result in ~200 DPA for both seed and blanket at discharge point. The blanket, instead, is designed to have the smallest P/D ratio required for safely accommodating the peak blanket assembly power. A comparative study was conducted to understand the effects of the blanket heavy metal loading on the core performance (Table 2-10); Case 1 is the reference based on the benchmark study on Section 2.6.3 while the heavy metal loading in the blanket of Case 2 is reduced by half and all other parameters in Case 2 are same as Case 1. As less fuel is loaded in the blanket, the leakage probability from the seed to the blanket decreases along with the fraction of core power generated by the blanket. The less fuel in the blanket also results in the larger blanket discharge burnup and radiation damage value. The maximized heavy metal loading in the blanket makes all other core performance characteristics more preferable and therefore is pursued as an important optimization strategy through this study.

Table 2-10 Effects of Blanket Heavy Metal Loading on the Core Performance

		Case 1	Case 2
k_{eff}			
	at BOEC	1.041±0.001	1.040±0.001
	at EOEC	1.007±0.001	0.997±0.001
Leakage from seed to blanket at BOEC		25.1%	24.8%
Power from blanket			
	at BOEC	40.6%	39.5%
	at EOEC	45.1%	43.4%
TRU/HM at BOEC		30.4wt%	30.7wt%

TRU conversion ratio at BOEC	0.51		0.51
Cycle length (EFPD)		405	
Ave. discharge BU, %FIMA (S/B)	16.1/7.7		16.4/16.9
HM at BOEC, tons (S/B)	5.7/53.5		5.7/26.1
DPA, (S/B)	194/196		193/241

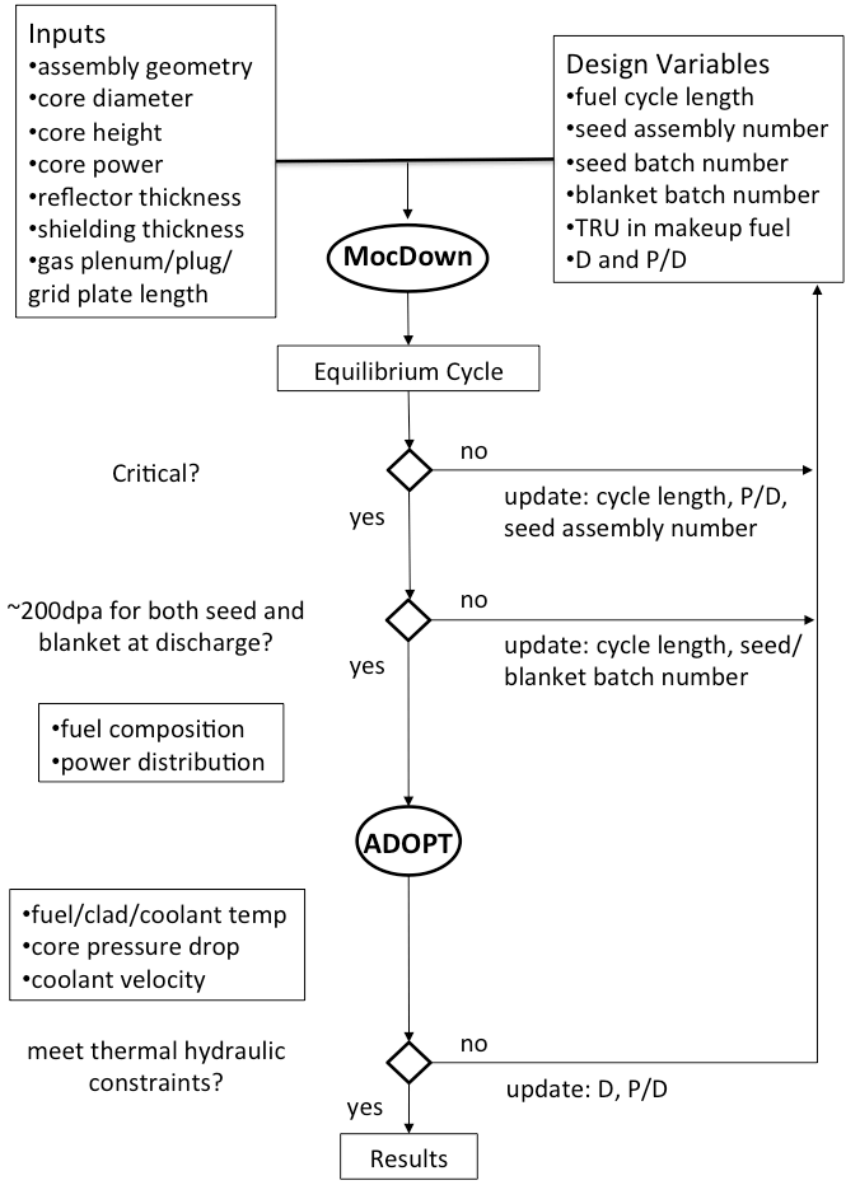

Figure 2-13 Computation flow chart and optimization of design variables

Chapter 3

3. Preliminary Study of SFR with Subcritical B&B Blanket

This chapter summarizes the preliminary studies of an SFR with subcritical B&B blanket. A wide range of TRU Conversion Ratio (CR) was investigated to understand their effect on the core performance, especially the fraction of power generated by the blanket. Two types of fuel -- uranium based vs. thorium based -- are charged to the blanket. Due to the different physics, these two types of fuel exhibit different full core performance. All the cores discussed in this paper are at the equilibrium composition as calculated by MocDown.

3.1. Tradeoff study of TRU driver with wide range of TRU CR

A tradeoff study was performed to quantify the maximum fraction of core power that can be generated from the thorium-fueled blanket and its dependence on the seed (driver) CR. The TRU CR is defined as the ratio of the neutron capture rate by ^{238}U in the seed to the fission rate of all the TRU isotopes in the seed and is calculated at BOEC. Since the effective microscopic cross-sections in SFR change moderately with most core design variations, the CR depends primarily on the TRU-to-^{238}U atom ratio so that the required BOEC TRU loading in the seed can be readily estimated. The approximate average enrichments (TRU-to-HM ratio) at BOEC required for CR of 1.00, 0.75, 0.50, 0.25 and 0.00 are, respectively, 14%, 21%, 33%, 56% and 100% [43]. The present tradeoff study was performed for a fuel self-sustaining seed – CR of 1.0 and for a TRU transmuting seed – CR of 0.5. The resulting core performance is summarized in Table 3-1. Due to the depletion of TRU in the seed and buildup of fissile contents in the blanket, the power shifts from seed to the blanket over the cycle; therefore, the peak assembly power occurs at BOEC in the seed and at EOEC in the blanket.

It is observed that the power fraction that can be generated by the thorium blanket that is driven by the low CR seed is significantly higher than by the high CR seed. This is due to the fact that the low CR seed requires higher TRU enrichment and features a higher k_∞ and can therefore maintain the core criticality using a smaller number of seed fuel assemblies with a larger P/D ratio. This leads to a higher neutron leakage probability from the seed into the blanket and proportionately higher fraction of power generated by the blanket. The fuel assemblies with larger P/D ratio have larger coolant cross-section area and can therefore safely accommodate higher assembly power for given coolant velocity and pressure drop constraints. It is also found that the CR 0.5 seed discharges its fuel at higher average burnup for the same peak radiation damage of ~200 DPA. The

higher burnup per DPA is mainly attributed to the smaller flux amplitude required by the high TRU content seed to achieve a given fission rate. Due to the high burnup, the reprocessing capacity required for recycling the seed fuel per unit of electricity generated by S&B core – 1295.0 kg per GWt-EFPY, is significantly smaller than that required for the CR 1.0 core – 2392.5 kg per GWt-EFPY. These are about 50% of those required for the ANL's reference SFR designs in Section 2.1.2 [43] of identical CR—2767.2 kg per GWt-EFPY for the CR 0.5 ABR and 5000.0 kg per GWt-EFPY for the CR 1.0 ARR. The smaller reprocessing capacity of the S&B cores is also due to the fraction of power generated from the once-through blanket.

Table 3-1 Comparison of Performance Characteristics of 1000 MWt S&B Cores Driven by Self-sustaining Seed and TRU Transmutation Seed with Thorium Blanket

Property	CR 0.5		CR 1.0	
	Seed	Blanket	Seed	Blanket
Fuel form	U-TRU-10Zr	Th	U-TRU-10Zr	Th
Target TRU CR of seed	0.5		1.0	
Number of batches	4	26	3	14
P/D ratio	1.368	1.187	1.210	1.115
Fuel volume fraction	22.29%	37.62%	28.49%	42.63%
Permissible assembly power (MWt)	16.8	9	10	5.6
Peak-to-permissible power ratio	0.97	0.98	0.86	0.88
Seed diameter (cm)	102.5		158.4	
Core power (MWt)	1000		1000	
Cycle length (EFPD)	405		940	
k_{eff} at BOEC	1.041±0.001		1.004±0.001	
k_{eff} at EOEC	1.007±0.001		1.009±0.001	
Burnup reactivity swing (%Δk/k)	-3.26		+0.46	
Burnup reactivity swing rate (%Δk/k /EFPY)	-2.94		+0.18	
Radial leakage probability from seed	25.1%		15.4%	
Average blanket power fraction	42.7%		27.7%	
Average discharge burnup (MWd/kg)	161.6	83.0	110.2	77.5
Peak radiation damage (DPA)	194	196	201	201
TRU/HM at BOEC (wt%)	30.4	-	15.2	-
Seed CR at BOEC	0.51		1.03	
HM at BOEC (tons)	5.7	53.5	18.5	46.4
Specific power (MWt/tHM)	99.8	8.0	39.1	6.0

TRU feed rate (kg/EFPY)	92.3	-	0.0	-
DU feed rate (kg/EFPY)	116.3	-	259.3	-
Thorium feed rate (kg/EFPY)	0.0	1876.4	0.0	1304.6
Trans-Th feed rate (kg/EFPY)	0.0	-152.5	0.0	-102.3
Reprocessing capacity (kg/GWt-EFPY)	1295.0		2392.5	

There is another synergism between a low CR seed and the S&B core concept: the blanket fissile contents are built up over the cycle and partially compensate for the reactivity loss due to the TRU consumption in the seed, as illustrated in Figure 3-1. The net effect is that the burnup reactivity swing of the CR 0.5 Th S&B core is -2.9% per EFPY while that of the CR 0.5 ABR is -4.8% per EFPY [43]. Whereas the cycle length of CR 0.5 ABR is limited to 7 months by the burnup reactivity swing constraint of 3.5%, it is 13.5 months in the CR 0.5 Th S&B core. The lower specific power density of the blanket fuel in the S&B core (Table 3-1) also contributes to the longer fuel cycle. The longer fuel cycle is expected to improve the S&B reactor capacity factor. Figure 3-2 shows that the k_∞ of the innermost blanket batch near the interface between the seed and the blanket is close to 1.0.

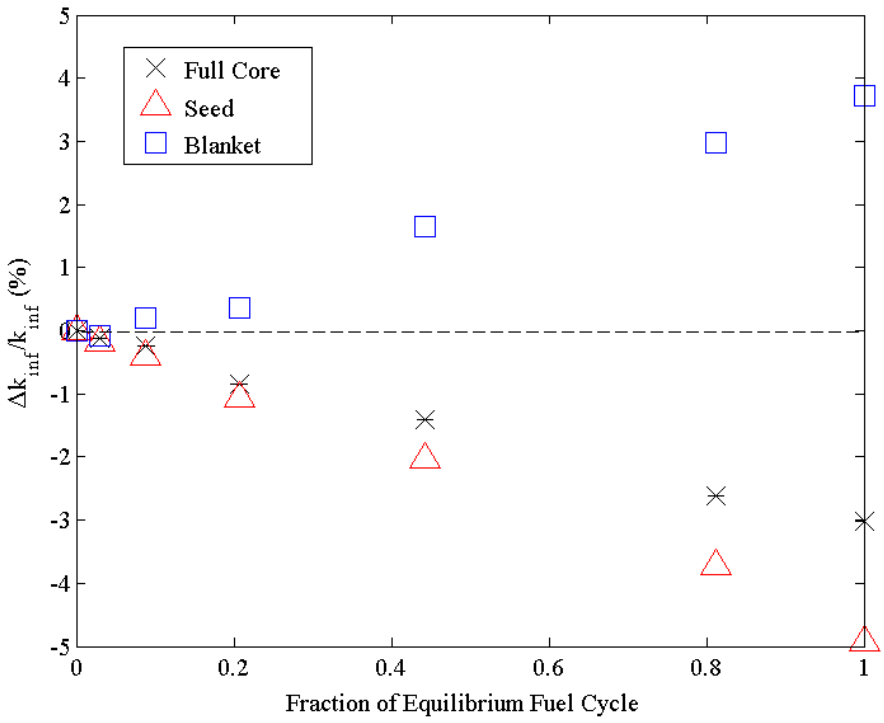

Figure 3-1 Reactivity gain and loss of seed, blanket, and core average for CR 0.5

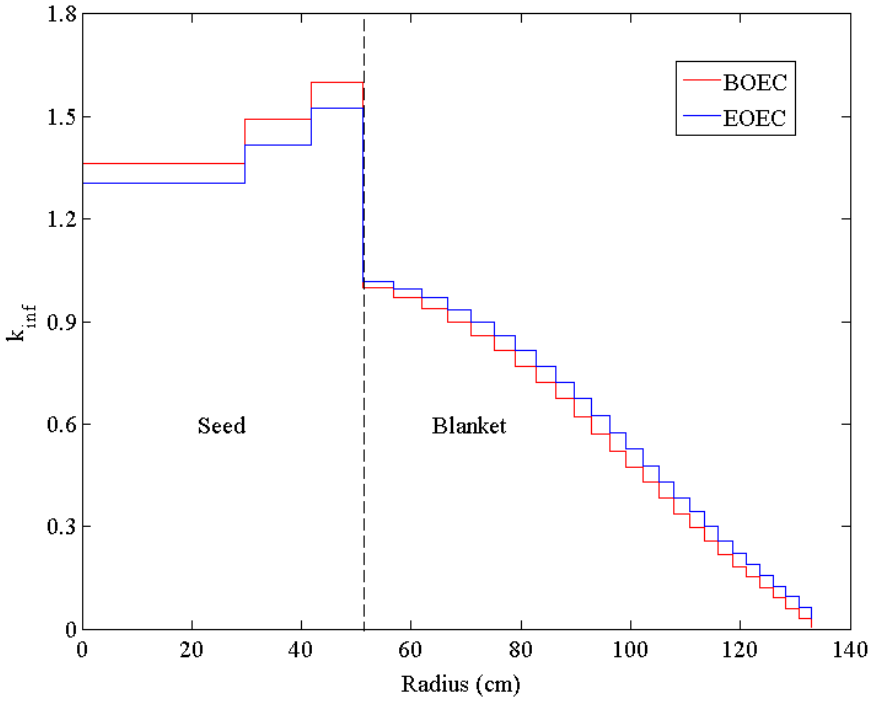

Figure 3-2 Seed and blanket radial distribution of infinite multiplication factor for CR 0.5

3.2. Parametric study of subcritical blankets

3.2.1. Neutron balance analysis of uranium vs. thorium system

In the breeding process, ^{238}U and ^{232}Th are converted into ^{239}Pu, and ^{233}U, respectively, as shown in (Equation 1-1). Uranium fuel has good neutron economy and this is attributed to a couple of reasons: (1) at high-energy, the number of fission neutrons per absorption (η value) in ^{233}U is smaller than that from ^{239}Pu (Figure 3-3); (2) the fast fission cross-section of ^{232}Th has a higher threshold energy and smaller magnitude than that of ^{238}U (Figure 3-4).

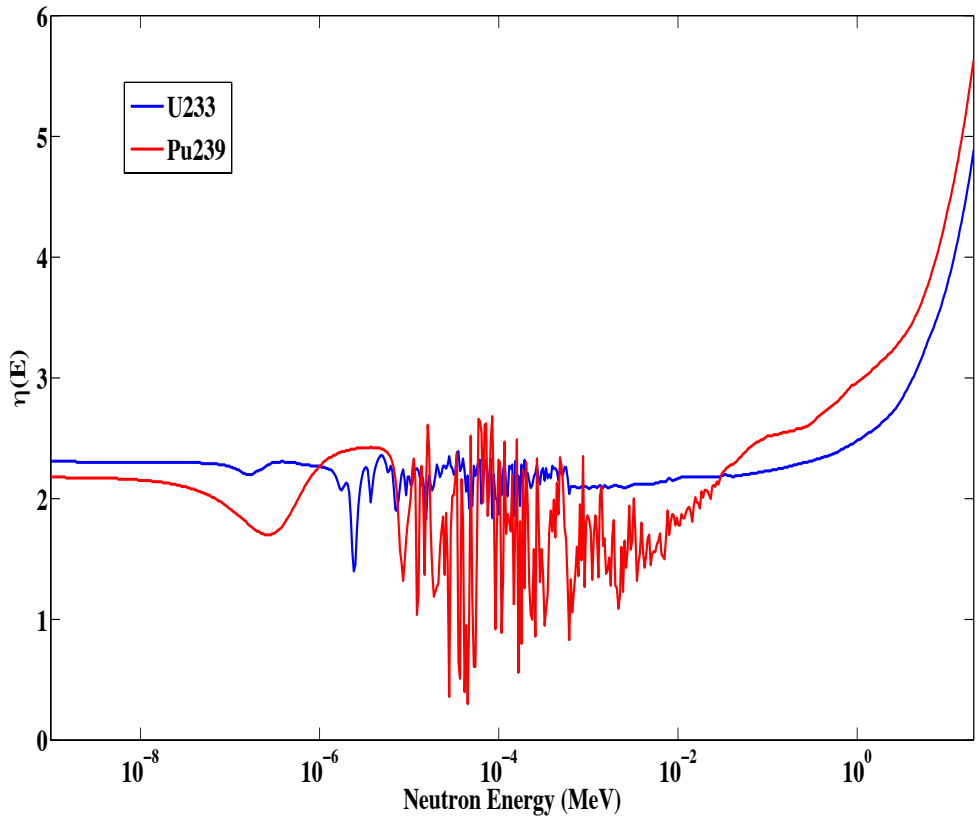

Figure 3-3 Fission neutrons per absorption (η value) by ^{233}U and ^{239}Pu

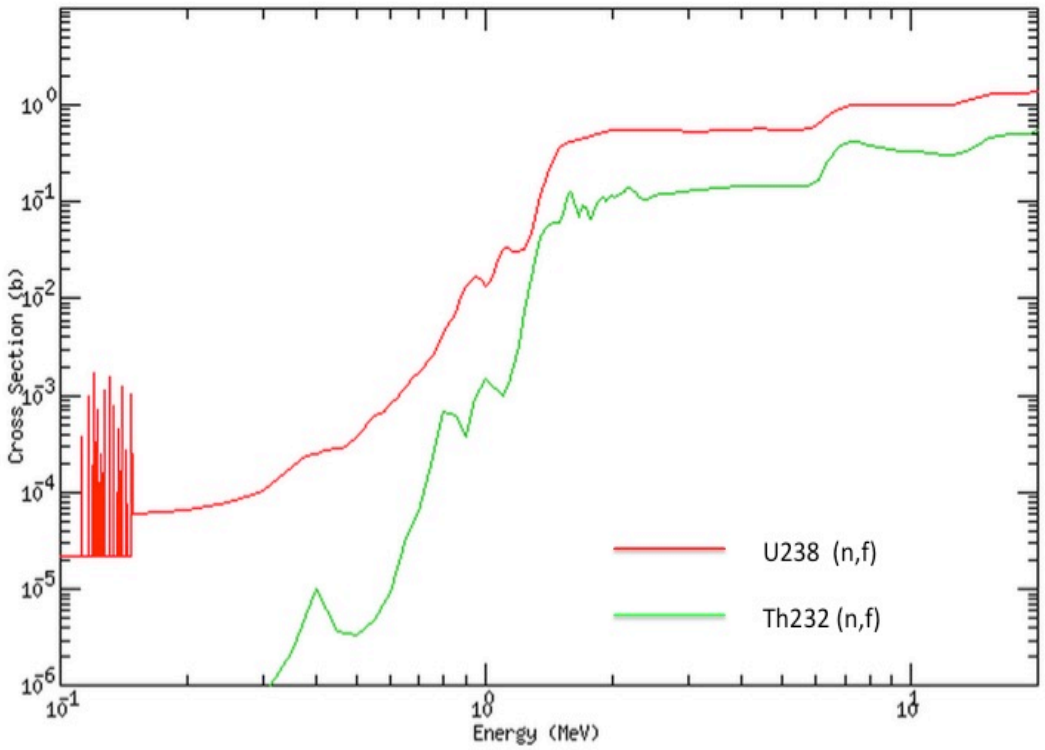

Figure 3-4 Fission cross-sections of ^{232}Th and ^{238}U from ENDF VII.0 at 300K [80]

Figure 3-5 compares the k_∞ evolution of depleted uranium and thorium in 0-D model. The depleted uranium system uses a metallic alloy U-10wt%Zr (theoretical density of 15.7 g/ cm^3 and smear density of 75%) and has a tight pitch-to-diameter ratio of 1.122; the corresponding volume fractions of fuel/gap/cladding/coolant are 37.5%/12.5%/22.0%/28.0% respectively. The thorium system uses a metallic alloy thorium (theoretical density of 11.7 g/ cm^3 and smear density of 75%) with same volume fractions as the uranium system.

The neutron balance of the two systems is also compared in Figure 3-5. The concept of neutron balance was introduced in [36, 81, 82] to estimate the minimum burnup required for establishing the B&B mode of operation in a critical system. The fissile contents have to be built up in the fertile feed fuel until $k_\infty \times P_{NL} \times P_{RC}$ reaches unity such that the fuel can become a net neutron producer. In the above, P_{NL} is the neutron non-leakage probability and P_{RC} is the probability that neutrons will not be absorbed by control elements to

compensate for excess reactivity. The net number of excess neutrons that accumulate with burnup can be estimated from (Equation 3-1 [34]).

$$N_{HM}\int_0^{BU} dBU'[1-\frac{1}{k_\infty(BU')\times P_{NL}\times P_{CR}}]\bar{\nu}(BU')$$

(Equation 3-1)

A 0-D model is applied to compare the neutron balance of thorium versus depleted uranium fueled blanket. Figure 3-5a shows that the minimum BU required to sustain the B&B mode of operation using depleted uranium feed fuel is about 20% FIMA. The net number of excess neutrons can be still positive until 50% FIMA (Figure 3-5a). However, thorium fueled blanket cannot sustain a B&B mode of operation (Figure 3-5b). This is because the $\eta(^{233}U) < \eta(^{239}Pu)$ at high neutron energies and the thorium fast fission cross section has a higher effective threshold energy and smaller magnitude than that of the ^{238}U. It is for the latter reason that the k_∞ value of the depleted uranium at zero burnup is ~0.2 versus close to 0.0 for the thorium (Figure 3-5). It is concluded that a sustainable breed-and-burn mode of operation cannot be established by using metallic thorium as the feed. Nevertheless, it is possible to operate a subcritical thorium blanket in the B&B mode with the help of excess neutrons that leak from the seed. Based on the above neutron balance analysis it is expected that more external neutrons are required to drive a thorium than depleted-uranium fueled blanket to the same burnup.

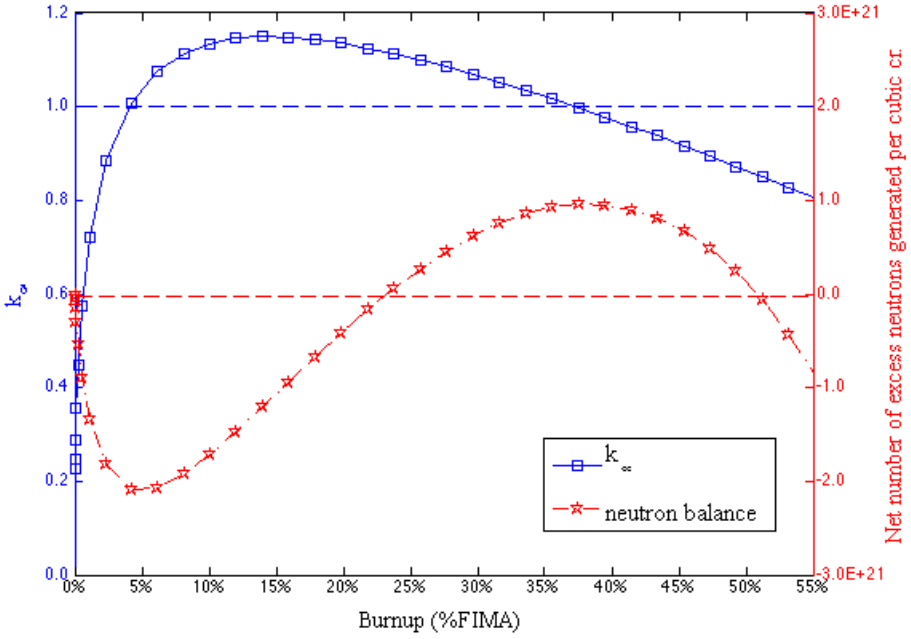

(a)

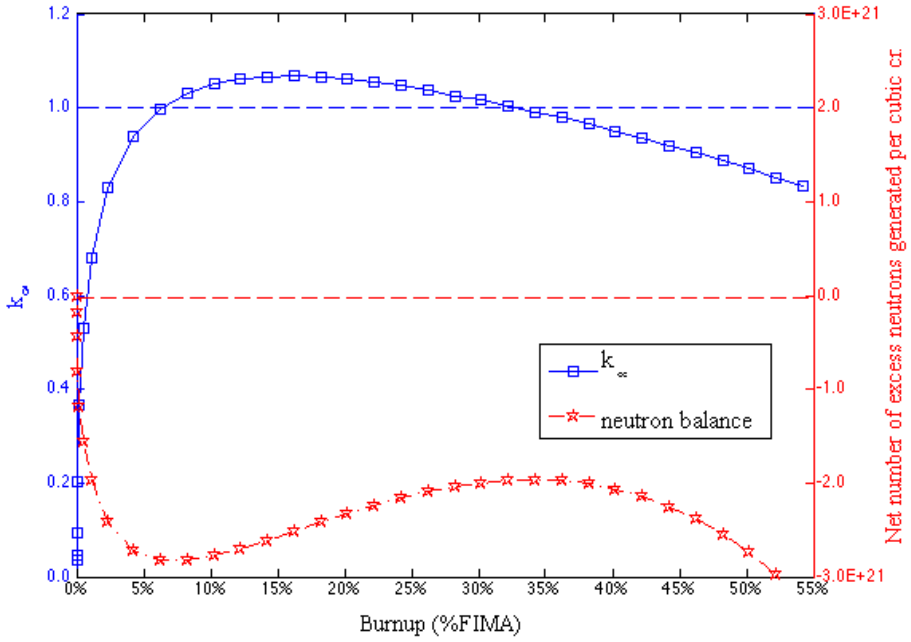

(b)

Figure 3-5 k_∞ (blue) and neutron balance (red) evolution with burnup for depleted uranium (a) and thorium (b) fueled B&B cores

3.2.2. Comparison of uranium vs. thorium blanket

A parametric study was conducted to assess the effect of the blanket fuel on the S&B core performance. The subcritical blanket is driven by a CR 0.5 seed similar to that used for the previous tradeoff study (Section 3.1). Table 3-2 compares the S&B core performance with depleted uranium versus thorium blankets. It is found that the cycle average power fraction that can be generated from the depleted uranium blanket – 51.1%, is larger than the 42.7% the thorium blanket can generate. As less power is generated from the seed, the reprocessing capacity required per unit of electricity generated is lower in the core with the uranium blanket – 1026.2 kg/GWt-EFPY vs. 1295.0 kg/GWt-EFPY for thorium. Based on this observation it is expected that it is economically superior to have a depleted uranium blanket in the S&B core.

It is also found that the TRU consumption rate per unit of electricity generated in the seed is practically independent of the fertile fuel used for the blanket. However, the depleted uranium blanket produces TRU at a rate that far exceeds the TRU destruction rate in the seed. When the primary objective is to minimize total TRU inventory, a thorium blanket is the preferred approach to the S&B core design.

Table 3-2 Performance Characteristics of 1000 MWt S&B Cores with Thorium and Depleted Uranium Blankets

Property	Thorium blanket		Uranium blanket	
	Seed	Blanket	Seed	Blanket
Fuel form	U-TRU-10Zr	Th	U-TRU-10Zr	U-10Zr
Target TRU CR of seed	0.5		0.5	
Number of batches	4	26	3	17
P/D ratio	1.368	1.187	1.510	1.220
Fuel volume fraction	22.29%	37.62%	18.29%	35.61%
Permissible assembly power (MWt)	16.8	9.0	21.0	10.5
Peak-to-permissible power ratio	0.97	0.98	0.69	0.98
Seed diameter (cm)	102.5		102.5	
Core power (MWt)	1000		1000	
Cycle length (EFPD)	405		560	
k_{eff} at BOEC	1.041±0. 0.001		1.036±0.001	
k_{eff} at EOEC	1.007±0. 0.001		1.001±0.001	
Burnup reactivity swing (%Δk/k)	-3.26		-3.41	
Burnup reactivity swing rate (%Δk/k /EFPY)	-2.94		-2.22	
Radial leakage probability from	25.1%		23.7%	

seed				
Average blanket power fraction	42.7%		51.1%	
Average discharge burnup (MWd/kg)	161.6	83.0	174.0	77.1
Peak radiation damage (DPA)	194	196	198	203
TRU/HM at BOEC (wt%)	30.4	-	31.7	-
Seed CR at BOEC	0.51		0.51	
HM at BOEC (tons)	5.7	53.5	4.7	62.4
Specific power (MWt/tHM)	99.8	8.0	103.6	8.2
TRU feed rate (kg/EFPY)	92.3	0.0	77.3	-201.7
DU feed rate (kg/EFPY)	116.3	0.0	97.3	2416.4
Thorium feed rate (kg/EFPY)	0.0	1876.4	0.0	0.0
Trans-Th feed rate (kg/EFPY)	0.0	-152.5	0.0	0.0
Reprocessing capacity (kg/GWt-EFPY)	1295.0		1026.2	

3.3. Reactivity coefficients and kinetic parameters

Safety related parameters of the S&B cores at BOEC are summarized in Table 3-3. The coolant densities in the seed and blanket were perturbed separately to calculate the reactivity response to sodium voiding. Large positive coolant density coefficient and sodium void worth are observed for all the three cases. Since the S&B cores are designed to minimize the leakage in the axial direction and the large amount of relatively high reactivity blanket batches surrounding the seed reduces the net radial leakage probability, the negative feedback from enhanced neutron leakage induced by coolant expansion is of a small magnitude. The void reactivity worth of these S&B cores is between 10$ to 12$ and close to that of a large 3000 MWt SFR [38]; they are significantly larger than that of a self-sustaining compact shape (coolant void worth ~7$) [83] as well as the reference CR 0.5 ABR design (coolant void worth of ~9$) [43].

The core with thorium blanket has less positive coolant void worth than the core with depleted uranium blanket. This is due to the smaller increase in η for ^{233}U than for ^{239}Pu upon spectrum hardening and the higher fission threshold energy of ^{232}Th relative to ^{238}U. For the same reasons the thorium blanket also offers a less positive coolant void worth and is therefore preferable over a depleted uranium blanket. As more power is generated from the thorium blanket in the CR 0.5 core, this core tends to have a smaller coolant void worth.

The axial expansion coefficient accounts for the reactivity change due to the fuel expansion and the corresponding reduction of fuel density. The value is calculated conservatively without considering an effective insertion of control rods which remain

stationary during core expansion [54]. The radial expansion coefficient represents the reactivity change due to the expansion of the core supporting structure – which is induced by the grid temperature change when the inlet coolant temperature increases. The assembly pitch increases with temperature according to the thermal expansion coefficient of the structure material; the fuel and structure densities decrease to preserve the initial mass. In the core with CR 0.5 seed, the larger P/D ratio enhances the neutron leakage out from the seed so that the thermal expansion coefficients are more negative compared with those in the CR 1.0 core. The Doppler coefficient was obtained for fuel temperature increase of 300°C. Due to the smaller ^{238}U-to-TRU ratio, the CR 0.5 cores generally feature less negative Doppler feedback.

Safety related parameters of the S&B cores with thorium and uranium blanket at BOEC are summarized in Table 3-3. The effective delayed neutron fractions β_{eff} is smaller for core with thorium blanket. This is attributed to the fact that the delayed neutron yields of ^{238}U and ^{232}Th are significantly larger than those of ^{239}Pu and ^{233}U, but the fission probability of ^{232}Th is much smaller than that of ^{238}U (Figure 3-4).

Table 3-3 Comparisons of Safety Characteristics of 1000 MWt S&B Cores with Thorium and Uranium Blanket Driven by Self-sustaining Seed and TRU Transmutation Seed

Blanket fuel	Thorium blanket	Thorium blanket	Uranium blanket
Target TRU CR of seed	0.5	1.0	0.5
Effective delayed neutron fraction	0.0028±0.0002	0.0033±0.0002	0.0038±0.0002
Sodium void worth ($)			
Seed only	12.05±0.08	13.10±0.06	10.67±0.06
Blanket only	-1.24±0.08	-0.39±0.06	2.03±0.06
Full core	10.48±0.08	12.65±0.06	12.69±0.05
Sodium density coefficient (¢/°C)			
Seed only	0.37±0.02	0.31±0.02	0.26±0.02
Blanket only	0.00±0.02	0.01±0.02	0.03±0.02
Full core	0.32±0.02	0.31±0.02	0.32±0.02
Doppler coefficient (¢/°C)	-0.05±0.03	-0.09±0.02	-0.07±0.02
Axial expansion coefficient (¢/°C)	-0.33±0.04	-0.29±0.03	-0.34±0.03
Radial expansion coefficient (¢/°C)	-0.19±0.03	-0.14±0.02	-0.15±0.02

Chapter 4

4. Study of ABR with Internal/External Thorium Blanket

4.1. Promising S&B cores featuring annular drivers

In order to enhance radial neutron leakage probability, reduce radial power peaking and further improve performance [84], the feasibility of S&B cores with annular seed was evaluated. The seed is located in between an inner blanket placed at the center of the core, and an outer blanket (Figure 4-1). Fresh thorium fuel is fed to the outermost blanket location; at the end of each cycle blanket fuel is shuffled inward; the fuel is shuffled from the innermost batch of the outer blanket to the outermost batch of the inner blanket. The innermost blanket batch is discharged at the end of cycle. The annular seed features a larger surface-to-volume ratio than a central cylindrical seed and thus larger neutron leakage probability into the thorium blanket. Based on observations in Chapter 3, a larger neutron leakage is expected to improve the fraction of core power generated by the blanket, reduce the coolant expansion and sodium voiding positive reactivity feedbacks.

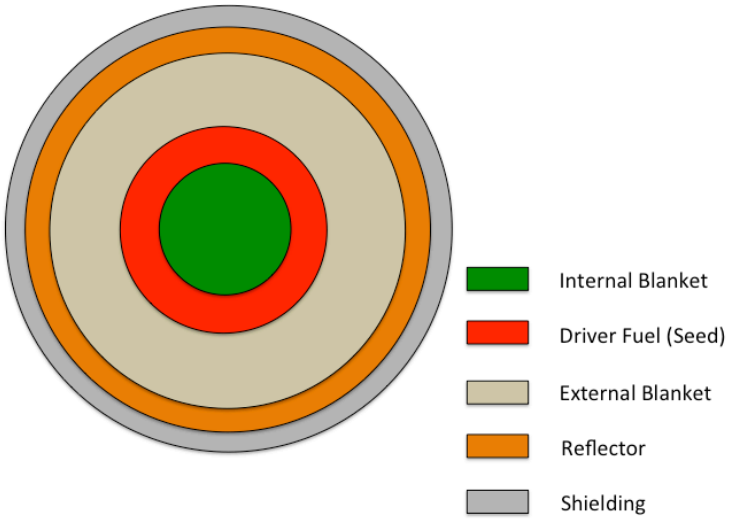

Figure 4-1 Schematic core configuration of annular S&B design

4.2. Parametric study of ABR with internal blanket

A parametric study was performed to understand the effect of the internal blanket dimensions on the core performance and to quantify the required volume for the annular seed. The number of fuel assemblies and batches in the internal blanket are design variables, whereas the number of the seed batches is kept at four. As more thorium assemblies are loaded in the internal blanket, the number of fuel assemblies in seed increases in order to assure criticality throughout the cycle.

Table 4-1 compares selected performance characteristics of three annular seed cores and of the reference cigar-shape CR 0.5 seed design described in Section 3.1. It is found that loading more thorium assemblies in the internal blanket (1) increases the fraction of power generated by the blanket up to 46.4%, (2) reduces the blanket radial power peaking factor from 5.08 to 2.51, (3) lowers the peak seed assembly power by up to about 40% (Figure 4-2), (4) decreases the burnup reactivity swing to almost zero, and (5) extends the cycle length to more than double the reference—and about four times that of the ABR with CR 0.5 [43].

The sodium void worth of the annular seeds is lower, by more than 50%, compared to the reference central cigar-shape seed design. This is due to the enhanced neutron leakage from the seed. On the contrary, the sodium void worth of the blanket increases with the inner blanket size as coolant voiding enhances neutrons leakage from the inner blanket into the high reactivity seed. The net result of these two competing effects is a reduction in the total coolant void feedback with larger inner blanket.

The smaller burnup reactivity swing of the S&B designs is more pronounced in the annular seed cases because a larger fraction of the core power is generated by the internal blanket that is nearly critical and is located in a relatively high neutron importance region. The nearly zero burnup reactivity swing of the large inner blanket cores suggests that it is feasible to design S&B cores with annular seed to have an extended cycle length for enhanced capacity factor ("ultra-long" case), or a lower CR for higher TRU transmutation rate ("high transmutation" cases). Such options are explored in the following sub-sections.

Table 4-1 Comparison of Performance Characteristics and Safety Parameters of S&B Cores with Annular Seed as a Function of Inner Blanket Dimension

Property	Reference	Case 1	Case 2	Case 3
Fuel form		U-TRU-10Zr/Th		
Target TRU CR of seed	0.5	0.5	0.5	0.5
Number of assemblies				

Inner blanket	0	13	35	62
Seed	37	61	61	65
Outer blanket	234	197	175	144
Number of batches				
Inner blanket	0	1	2	3
Seed	4	4	4	4
Outer blanket	26	15	10	7
P/D ratio	1.368/1.187	1.392/1.222	1.265/1.166	1.190/1.124
Permissible assembly power (MWt)	16.8/9.0	17.8/10.6	12.5/8.0	9.1/6.0
Peak-to-permissible power ratio	0.97/0.98	0.58/0.89	0.80/0.93	0.98/0.96
Shuffling mode for blanket	out-in scheme			
Core power (MWt)	1000	1000	1000	1000
Cycle length (EFPD)	405	635	760	865
Tot. residence time (EFPD)	1620/10530	2540/10160	3040/9120	3460/8650
k_{eff} at BOEC	1.041±0.001	1.036±0.001	1.020±0.001	1.001±0.001
k_{eff} at EOEC	1.007±0.001	1.007±0.001	1.006±0.001	1.001±0.001
Burnup reactivity swing (%Δk/k)	-3.30	-2.80	-1.30	-0.01
Burnup reactivity swing rate (%Δk/k /EFPY)	-2.97	-1.61	-0.62	0.00
Radial leakage probability from seed at BOEC				
to external blanket	25.1%	23.3%	25.1%	26.4%
to internal blanket	0.0%	1.4%	3.7%	6.1%
total	25.1%	24.7%	28.8%	32.5%
Average blanket power fraction	42.7%	41.0%	44.4%	46.4%
Radial peaking factor at BOEC	1.01/5.08	1.03/5.10	1.04/3.74	1.05/2.51
Average discharge burnup (MWd/kg)	161.6/83.0	167.4/91.0	154.7/80.5	139.7/75.7
Peak radiation damage (DPA)	194/196	197/205	195/201	186/208
TRU/HM at BOEC (wt%)	30.4	30.7	29.7	29

Seed CR at BOEC	0.51	0.51	0.50	0.50
HM at BOEC (tons)	5.7/53.5	9.0/45.1	10.9/49.7	13.3/52.3
Specific power (MWt/tHM)	99.8/8.0	65.9/9.1	50.9/8.9	40.4/8.9
TRU feed rate (kg/EFPY)	92.3/0.0	94.9/0.0	90.2/0.0	87.0/0.0
DU feed rate (kg/EFPY)	116.3/0.0	119.8/0.0	112.7/0.0	108.9/0.0
Thorium feed rate (kg/EFPY)	0.0/1876.4	0.0/1643.8	0.0/2011.4	0.0/2238.1
Trans-Th feed rate (kg/EFPY)	0.0/-152.5	0.0/-138.1	0.0/-160.6	0.0/-171.3
Reprocessing capacity (kg/GWt-EFPY)	1295.0	1286.6	1312.4	1399.7
Safety Parameters at BOEC				
Effective delayed neutron fraction	0.0028±0.0002	0.0031±0.0002	0.0034±0.0002	0.0032±0.0002
Sodium void worth ($)				
Seed only	12.05±0.08	10.96±0.06	6.95±0.06	5.44±0.06
Blanket only	-1.24±0.08	0.99±0.06	2.40±0.06	3.08±0.06
Full core	10.48±0.08	11.66±0.06	9.18±0.06	8.64±0.06
Doppler coefficient (¢/°C)	-0.05±0.03	-0.10±0.02	-0.05±0.02	-0.12±0.02
Axial expansion coefficient (¢/°C)	-0.33±0.04	-0.33±0.03	-0.25±0.03	-0.36±0.03
Radial expansion coefficient (¢/°C)	-0.19±0.03	-0.18±0.02	-0.15±0.02	-0.19±0.02

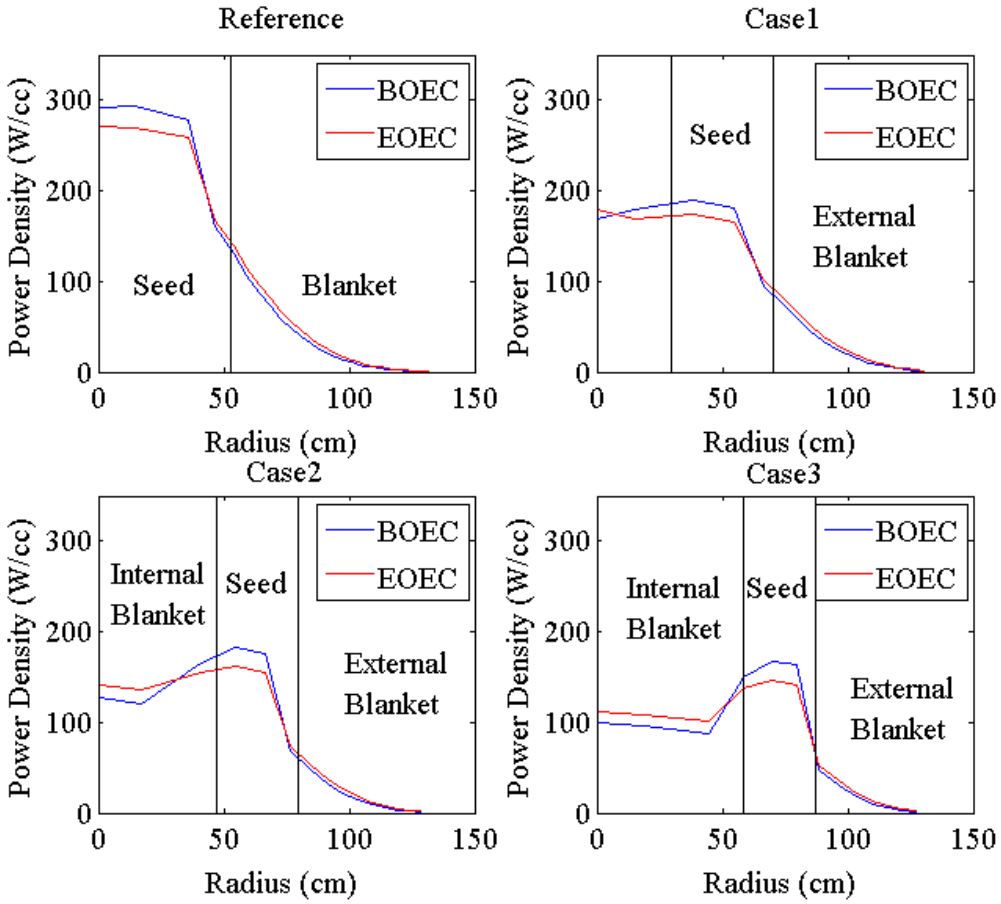

Figure 4-2 Comparison of radial power distribution of S&B cores as a function of inner blanket dimension

4.3. Design of ultra-long cycle length core

The ultra-long cycle S&B core with thorium blanket is designed by setting the annular seed to operate in a single batch mode while featuring same TRU CR of 0.5 as the reference ABR. The number of blanket batches is reduced as well to one internal and two external batches. Performance characteristics of the ultra-long cycle S&B core arrived at are compared in Table 4-2 against those of the reference ABR core design with CR 0.5.

It was found possible to design a core to have a cycle length of 88 months or 7 years — 12 times as that of the ABR [43]. This would significantly improve the capacity factor of a typical ABR. The fraction of power generated by the blanket is more than 40% and thus the reprocessing capacity required for the S&B core is about 62% that for the ABR. The

sodium void worth decreases to +7.6$ -- smaller than that of the reference ABR design (+9.2$) and of previous S&B design (+10.5$).

Table 4-2 Comparison of Performance Characteristics of Ultra-long Cycle S&B and ABR Cores

Property		Ultra-long	ABR
Fuel form		U-TRU-10Zr/Th	U-TRU-10Zr
Target TRU CR of seed		0.5	0.5
Number of assemblies			
	Inner blanket	42	-
	Seed	61	144
	Outer blanket	168	-
Number of batches			
	Inner blanket	1	-
	Seed	1	6/6/7
	Outer blanket	2	-
P/D ratio		1.261/1.151	1.293
Permissible assembly power (MWt)		12.3/7.3	-
Peak-to-permissible power ratio		0.96/0.99	-
Core power (MWt)		1000	1000
Cycle length (EFPD)		2630	221
Tot. residence time (EFPD)		2630/7890	1326/1326/1547
k_{eff} at BOEC		1.039±0.001	-
k_{eff} at EOEC		1.004±0.001	-
Burnup reactivity swing (%Δk/k)		-3.39	-2.90
Burnup reactivity swing rate (%Δk/k /EFPY)		-0.47	-4.79
Average blanket power fraction		42.5%	0.0%
Average discharge burnup (MWd/kg)		123.2/65.0	131.9
Peak radiation damage (DPA)		175/204	-[5]
TRU/HM at BOEC (wt%)		29.9	33.3
Seed CR at BOEC		0.46	0.5
HM at BOEC (tons)		12.3/51.4	9.4
Specific power (MWt/tHM)		46.8/8.3	106.4
TRU feed rate (kg/EFPY)		93.2/0.0	173.8
DU feed rate (kg/EFPY)		117.0/0.0	217.5

[5] The peak radiation damage on the cladding of the ABR design is constrained by peak fast fluence of 4E+23 n(>0.1 MeV)/cm^2.

Thorium feed rate (kg/EFPY)		0.0/2386.0	0.0
Trans-Th feed rate (kg/EFPY)		0.0/-174.5	0.0
Reprocessing capacity (kg/GWt-EFPY)		1703.6	2767.2
Safety Parameters at BOEC			
Effective delayed neutron fraction		0.0032±0.0002	0.003
Sodium void worth ($)			
	Seed only	5.90±0.06	-
	Blanket only	1.05±0.00	-
	Full core	7.55±0.06	9.17
Doppler coefficient (¢/°C)		-0.03±0.02	-0.08
Axial expansion coefficient (¢/°C)		-0.34±0.03	-0.52
Radial expansion coefficient (¢/°C)		-0.19±0.02	-0.41

4.4. Design of high TRU transmutation core

Two design variants were examined: one has TRU CR of 0.25 seed and the other has TRU CR of 0.0 seed. Performance characteristics and safety parameters of the two S&B core designs arrived at are summarized in Table 4-3 together with the reference ABR. The TRU transmutation rate of the CR=0 design is 373.5 kg/GWt-EFPY per unit of electricity generated by the seed, which is more than two times that of the reference ABR; when normalized by the total core power, the TRU consumption rate — 158.1 kg/EFPY, is almost 10% smaller than that of the ABR — 173.8 kg/EFPY. The high fissile content in the CR 0.0 seed reduces the number of driver assemblies and increases the P/D ratio. As a result, an enhanced neutron leakage into the blanket leads to a higher blanket power fraction — 57.7%, the highest of all S&B design options considered so far. The higher TRU concentration in the seed also results in a lower flux magnitude for a given fission rate such that the seed fuel could be discharged at an average burnup of 312.4 MWd/kg without exceeding the cladding radiation damage limit. The high discharge burnup along with the high fraction of core power generated by the blanket reduce the required reprocessing capacity for the CR 0.0 core to 494.5 kg/GWt-EFPY -- only about one sixth of that required by the ABR. The smaller capacities for reprocessing and remote fuel fabrication are expected to reduce the fuel cycle cost (more details are provided Section 4.5 and 7.4). The high leakage probability from the seed to the blanket also results in a relatively small sodium void worth for the seed (+4.2$). The full core coolant void worth is +6.6$, smaller than that of the ABR (+9.2$) [43]. The non-fertile fuel usually causes some concerns for positive Doppler coefficient. It is observed that the Doppler coefficient for the seed fuel only in the high-transmutation case with CR 0.0 is -0.02 ¢/°C while the corresponding value is -0.07 ¢/°C by perturbing the fuel temperature of the full core; the large fraction of core power generated from the thorium blanket results in a net negative feedback to an increase in the fuel temperature.

Table 4-3 Comparison of Performance Characteristics of the High-transmutation S&B and ABR Cores

Property	High-transmutation S&B		ABR
Fuel form	U-TRU-10Zr/Th		U-TRU-10Zr
Target TRU CR of seed	0.25	0.0	0.5
Number of assemblies			
Inner blanket	39	96	-
Seed	40	30	144
Outer blanket	192	145	-
Number of batches			
Inner blanket	2	2	-
Seed	4	2	6/6/7
Outer blanket	10	3	-
P/D ratio	1.316/1.164	1.406/1.104	1.293
Permissible assembly power (MWt)	14.7/7.9	18.3/5.1	-
Peak-to-permissible power ratio	0.93/0.99	0.97/0.99	-
Core power (MWt)	1000	1000	1000
Cycle length (EFPD)	685	1550	221
Total residence time (EFPD)	2740/8220	3100/7750	1326/1326/1547
k_{eff} at BOEC	1.026±0.001	1.041±0.001	-
k_{eff} at EOEC	1.004±0.001	1.003±0.001	-
Burnup reactivity swing (%Δk/k)	-2.11	-3.60	-2.90
Burnup reactivity swing rate (%Δk/k /EFPY)	-1.12	-0.85	-4.79
Average blanket power fraction	50.0%	57.7%	-
Average discharge burnup (MWd/kg)	213.5/74.0	312.4/70.2	131.9
Peak radiation damage (DPA)	206/193	185/207	-[6]
TRU/HM at BOEC (wt%)	45.9	99.5	33.3
Seed CR at BOEC	0.25	0.01	0.5
HM at BOEC (tons)	6.4/55.0	4.2/63.7	9.4
Specific power (MWt/tHM)	77.9/9.1	100.8/9.1	106.4
TRU feed rate (kg/EFPY)	127.5/0.0	158.1/0.0	173.8
DU feed rate (kg/EFPY)	56.8/0.0	0.2/0.0	217.5
Thorium feed rate (kg/EFPY)	0.0/2467.0	0.0/3024.2	0.0
Trans-Th feed rate (kg/EFPY)	0.0/-191.2	0.0/-223.3	0.0

[6] The peak radiation damage on the cladding of the ABR design is constrained by peak fast fluence of 4E+23 n(>0.1 MeV)/cm^2.

Reprocessing capacity (kg/GWt-EFPY)	854.8	494.5	2767.2
Safety Parameters at BOEC			
Effective delayed neutron fraction	0.0035±0.0002	0.0031±0.0002	0.003
Sodium void worth ($)			
Seed only	5.11±0.06	4.24±0.07	-
Blanket only	2.34±0.06	2.40±0.07	-
Full core	7.37±0.06	6.56±0.07	9.17
Doppler coefficient (¢/°C)	-0.11±0.02	-0.07±0.02	-0.08
Axial expansion coefficient (¢/°C)	-0.35±0.03	-0.34±0.03	-0.52
Radial expansion coefficient (¢/°C)	-0.18±0.02	-0.23±0.02	-0.41

4.5. Preliminary study of fuel cycle cost

4.5.1. Fuel cycle cost methodology

The total cost of electricity from nuclear power plants consists of the reactor capital, operation and maintenance (O&M), and fuel cycle costs. Since next generation nuclear plants are still undergoing research, development, and demonstration, the capital and O&M costs are unknown for commercial scale reactors. This study compares the fuel cycle costs that include front-end, back-end, and fuel recycling costs and are estimated to contribute ~20% of the total Costs of Electricity (COE) from a typical SFR [85]. Costs of major fuel cycle facilities and processes are obtained from [85] and reproduced in Table 4-4. Figure 4-3 shows a flow chart of the detailed fuel cycle considered. The fuel cycle cost components for fast reactors are presently subjected to large uncertainties due to lack of commercial experience.

The TRU transmuted in the ABR and S&B cores is considered as an existing large stockpile of waste from the current once-through LWRs. Nevertheless, reprocessing LWR's UNF, extracting TRU, and disposing of the separated FPs in geologic repository require extra cost. The saving from avoided direct geological disposal of UNF ($1,000/kg HM) is equivalent to the cost of aqueous reprocessing. To obtain 1 kg of TRU, 87.1kg of LWR's UNF has to be reprocessed; 4.5 kg of FP will be sent to aqueous HLW conditioning facility ($2,000/kg FPs) and final geological repository ($10,000/kg FPs); 81.6 kg of Recycled Uranium (RU) is sent to conditioning facility ($93/kg RU); therefore, the net cost for 1 kg of LWR TRU is about $61,588/kg TRU. As the responsibility to pay for the TRU separation is presently unknown, the fuel cycle cost of the S&B reactors and ABR is reported in two ways: (1) the TRU separation cost is fully charged to the fast reactor utilities; (2) the TRU separation is paid for by the Nuclear Waste Fund as the solution of UNF and fast reactor utilities obtain TRU for free. The cost

of TRU separation might very well be covered by a combination of Nuclear Waste Fund and fast reactor utilities, in which case the cost of TRU transmuting cores will be between the two values reported here. Depleted uranium is added to the seed fuel as makeup and the cost is negligible considering the current large stockpile of depleted uranium in the US. The thorium fuel fed to the blanket is much cheaper than metallic U-TRU fuel charged to the seed. The fuel fabrication cost of natural thorium is assumed to be as of natural uranium. Since the blanket is operated in the B&B mode, the discharged thorium fuel is sent to geological repository assuming same cost per unit of mass as of current UOX discharged fuels although the discharge burnup for thorium blanket fuel — 70 to 80 MWd/kg is slightly higher than that for PWR UOX fuel — 50 MWd/kg. According to the waste management analysis in Section 7.5, the radioactivity at 10 years of the spent fuel from thorium blanket is 0.73 MCi per metric ton which is close to the corresponding value of the spent fuel from PWR -- 0.56 MCi per metric ton.

Table 4-4 Costs of Fuel Cycle Major Facilities and Processes [85] Assumed for the Studies

Activities of Fuel Cycle	Cost
Natural Uranium Mining and Milling, $/kg-U	60
Natural Thorium Mining and Milling, $/kg-Th	100
Conversion Processes, $/kg-U	10
Enrichment, $/SWU	105
LWR UO_2 Fuel Fabrication, $/kg-U	240
UREX Aqueous Separation, $/kg HM	1,000
Reprocessing - Electrochemical & Remote Fuel Fabrication, $/kg-HM	5,000
Aqueous HLW Conditioning (FPs+Ln), $/kg-FPs	2,000
Recycled Uranium conditioning, $/kg-RU	93
UOX fuel conditioning, $/kg-HM	100
Geologic Repository (PWR UNF), $/kg-HM	1,000
Geologic Repository (HLW FPs+Ln+Tc), $/kg-FPs	10,000

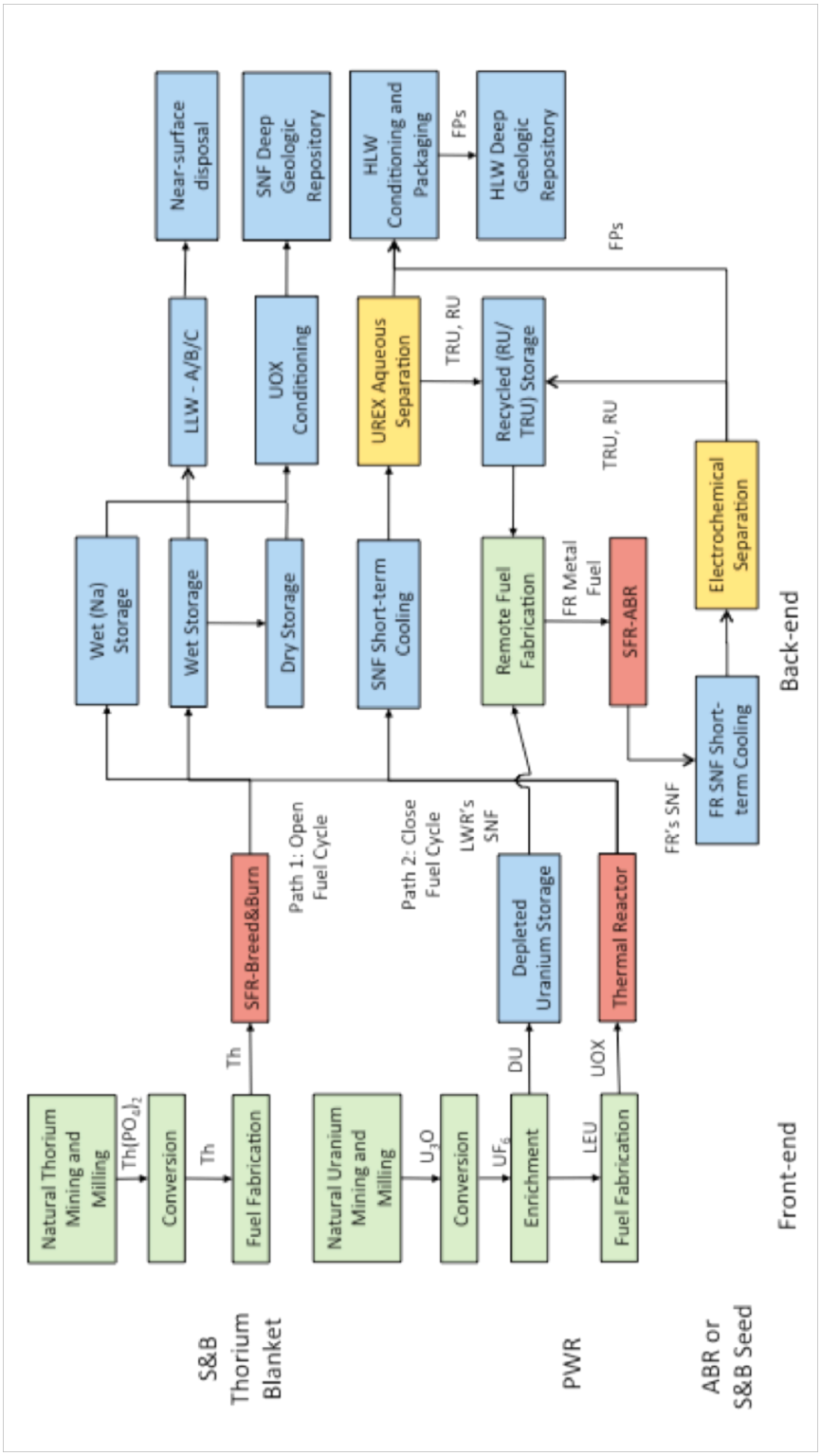

Figure 4-3 Fuel cycle flow chart for S&B SFR, ABR, and PWR

4.5.2. Fuel cycle cost of the S&B cores

Figure 4-4 shows the fuel cycle cost estimation of several S&B core designs discussed in previous sections. The S&B cores driven by TRU burner (CR 0.5 or less) have a significant lower cost for fuel reprocessing and remote fuel fabrication per unit of electricity generated. The S&B core with TRU burner (CR 0.5) and uranium blanket features the lowest fuel cycle cost due to the largest fraction of core power generated by the blanket. For the fuel self-sustaining core (CR 1.0), the fuel cycle cost is mainly composed of fuel reprocessing and remote fuel fabrication due to the relatively lower discharge burnup of the seed fuel. When TRU separation cost is included, the fuel cycle costs per unit of electricity generated of all the S&B designs tend to be comparable. The S&B cores with high TRU transmutation rate are still preferable since they provide a solution to the large stockpile of existing UNF from LWR fleet.

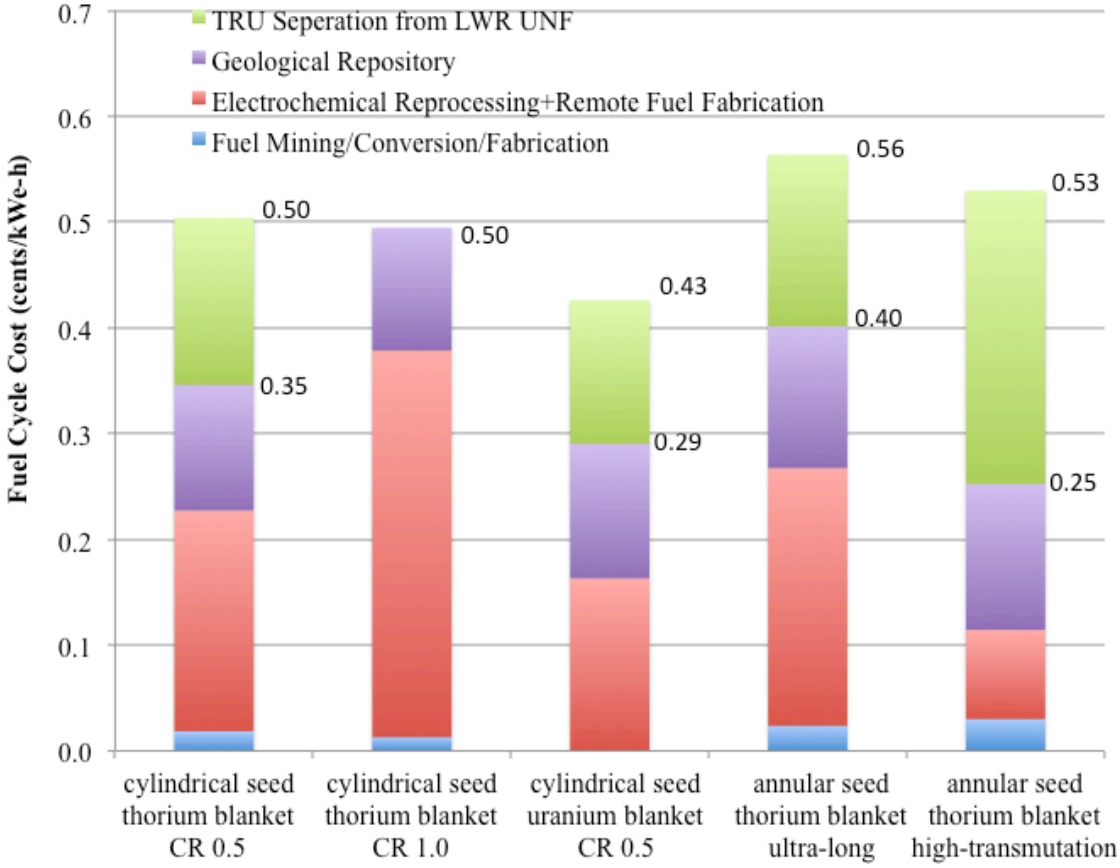

Figure 4-4 Comparison of fuel cycle costs for selected S&B core designs

4.5.3. Comparison of fuel cycle costs of S&B, ABR, and PWR

The fuel cycle cost of S&B cores is compared in Figure 4-5 with those of the reference ABR and a contemporary PWR [18] that operate on the once-through fuel cycle. The high-transmutation (CR=0.0) design (Section 4.4) is used as the representative of S&B cores since it features a similar TRU transmutation rate as the reference ABR per unit of electricity generated from the core. For the PWR, ^{235}U is assumed enriched to 4.5wt% and the depleted uranium stream contains 0.2wt% ^{235}U. This requires a total separation work of 7.61 SWU per kg of LEU and, thus, the cost of UOX enrichment is 800 $/kg LEU. The PWR fuel is discharged with average burnup of 50 MWd/kg and is eventually sent to geological repository. Thermal efficiency of 40% is assumed for both ABR and S&B designs, whereas 33% is used for the PWR.

Figure 4-5 compares the fuel cycle cost of the three reactors. Since the total reprocessing capacity of the S&B core is only about one sixth of that for ABR per unit of core energy; the cost of reprocessing and remote fuel fabrication for the S&B is about one sixth of the ABR. Both the ABR and S&B cores have comparable costs for TRU separation from LWR UNF due to the similar effective TRU transmutation rate per unit of core power. The thorium blanket is fed with natural thorium and no enrichment facility is required; therefore, the front-end cost of thorium blanket is significantly lower compared with typical PWR. As the thorium blanket discharges the fuel at ~50% higher burnup (~70 MWd/kg) than that of PWR (50 MWd/kg) and the seed operates on closed fuel cycle with only FPs in waste stream, the overall cost of geologic repository for the S&B is lower than that for the PWR. When fully accounting for the cost of LWR TRU separation in the fast reactor fuel cycle, the S&B fuel cycle cost is estimated to be 0.53 cents/kWe-h versus 0.73 cents/kWe-h of the reference ABR. The S&B fuel cycle cost is also lower than the fuel cycle cost of current PWRs — 0.69 cents/kWe-h.

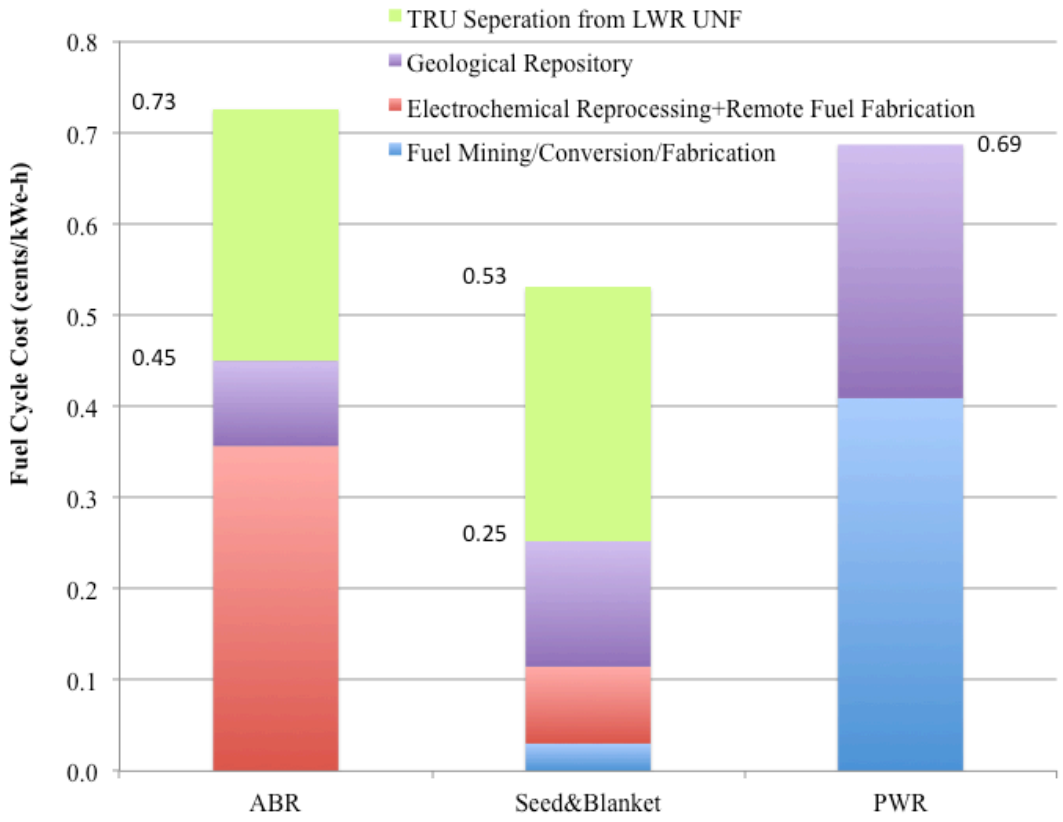

Figure 4-5 Comparison of fuel cycle cost of ABR, S&B, and PWR

4.6. Unique synergism between the seed and blanket of the S&B core concept

The study of the S&B SFR core concept has demonstrated remarkable difference in the performance of S&B cores relative to the performance of standard ABR cores. These differences are attributed to the unique synergism that exists between a TRU transmuting seed and a thorium breed-and-burn blanket combined with a core layout that enables an effective beneficial utilization of the seed excess neutrons. This unique synergism is further elaborated upon below.

4.6.1. TRU transmutation, discharge burnup, and fuel reprocessing capacity

As the seed is designed to have a lower TRU conversion ratio, the TRU/HM ratio of the seed fuel increases along with the seed k_∞. Therefore, the seed enables to contribute a

larger fraction of its fission neutrons to leak into the blanket such that the fraction of core power generated by the blanket increases (Section 3.1). The effect is enhanced when using an annular seed.

Another advantage of a higher TRU/HM ratio seed is a higher attainable burnup for a given radiation damage constraint because for a given HM specific power the neutron flux amplitude along with DPA rate decline as TRU/HM increases. The higher discharge burnup of the seed together with the larger fraction of core power generated by the blanket result in a smaller capacity of fuel reprocessing and fabrication required per unit of electricity generated by the core and these lower the fuel cycle cost (Figure 4-5). The amount of TRU that will end up in waste streams get also smaller when the fuel recycling capacity gets smaller.

The excess neutrons from the seed enable to extract a significant fraction of the thorium energy by using the breed-and-burn mode that is without enrichment and thorium reprocessing technologies. A critical core cannot sustain a B&B mode of operation if fueled with thorium due to the relatively small η value of ^{233}U and low fission probability of thorium at the SFR spectrum (Section 3.2.1).

4.6.2. Burnup reactivity swing

Designing conventional SFR cores with TRU CR of 0.0 is not practical as the ABR cannot be passively safe [48]. The large burnup reactivity swing of low CR ABR cores will also force impractically short cycle length [43]. However, the thorium blanket enables to design S&B cores using non-fertile fuel (TRU-10Zr) to have a relatively slow burnup reactivity drop and, in fact, much longer cycles than of standard ABR cores (Section 4.4) whose corresponding CR is even higher. The relatively slow reactivity drop with time of S&B cores is due to a combination of a couple of phenomena: the blanket reactivity increases with burnup and this partially compensates for the drop in the seed reactivity over the cycle (Figure 3-1). In addition, the low average specific power of the S&B core – due to the high inventory of HM for the same core power as of the ABR cores, enables very long cycles for the same burnup reactivity drop (Section 4.3).

Even though the HM inventory of the reference S&B core is significantly higher than of a conventional SFR core, the HM inventory of the seed is smaller than that of a typical SFR. The cost of the blanket fuel is a very small fraction of the cost of the seed fuel. At the same time, longer cycles enable higher capacity factor and, therefore, lower operation-and-maintenance contribution to the cost-of-electricity is also expected.

4.6.3. Radial power flattening

The use of internal blanket enables to greatly flatten the radial power distribution in the S&B core. As in the equilibrium core the blanket fuel adjacent to the seed has pretty high fissile contents -- the k_∞ is close to 1.0, there is a relatively smooth transition in the power density across the seed-blanket boundaries. Unlike most blanket in conventional SFR designs, the large inventory of fissile contents in the blanket at BOEC contribute to the relatively smaller fractional change in the blanket power density over the equilibrium cycle. There are no fundamental differences in this aspect between a thorium and a depleted uranium blanket.

4.6.4. Reactivity coefficients

Even though the S&B cores examined above feature significantly large volume and lower leakage than the ABR cores, the positive reactivity effect of coolant voiding of the S&B cores is surprisingly comparable to that of typical ABR design. This is due to the tight neutronics coupling between the seed and the blanket combined with the physics characteristics of thorium. The thorium fueled SFRs feature less positive feedback to the spectrum hardening due to the following two reasons: the increase in the number of fission neutrons generated per neutron absorbed in ^{233}U (the "η" value) with neutron energy is significantly smaller than in ^{239}Pu; the increase in the fission probability of ^{232}Th with neutron energy is significantly smaller than of ^{238}U. With depleted uranium fueled blanket, the coolant voiding reactivity effect of the S&B core would have been significantly more positive (Section 3.3).

Chapter 5

5. Heterogeneous Compact S&B Design

The previously considered S&B cores feature an active core height of 250cm to minimize the neutron leakage in the axial direction. This section describes a conventional compact core that incorporates thorium fueled blanket assemblies interspersed between U-TRU-10%Zr driver fuel assemblies. The objective is to compare the performance characteristics of such a more conventional compact S&B core against those of the large S&B cores discussed in Chapter 4. It is to reveal if and to what extent the proposed S&B core concept offers sufficient advantages over the presently accepted SFR core designs.

5.1. Compact ABR and the benchmark

Reactor physics and safety considerations enable designing conventional sodium-cooled advanced TRU burner reactors to have a conversion ratio as low as ~0.2 for cycle length of ~7 months or as low as ~0.6 for cycle length of ~12 months [48]. A metallic fuel ABR design that features a conversion ratio of ~0.7 [41] is recommended by ANL as the preferable TRU burner because its fuel had undergone successful irradiation and, therefore, is licensable in the near-term [48].

The design of the S&B cores has been done so far in this study using a homogenized R-Z model. The homogenized R-Z model is not applicable for the heterogeneous compact core which requires assembly level resolution. The ARC computational package developed for fast reactor analysis (described in Section 2.5.2) is consistently applied to both the reference ABR and to the compact S&B core in order to eliminate the computational bias.

The reference ABR (shown in Figure 5-1) is reproduced in this section for the benchmark purpose based on the detailed information that was provided by Dr. T.K. Kim from ANL. Table 5-1 compares our results against the results reported by ANL; acceptable agreement is observed.

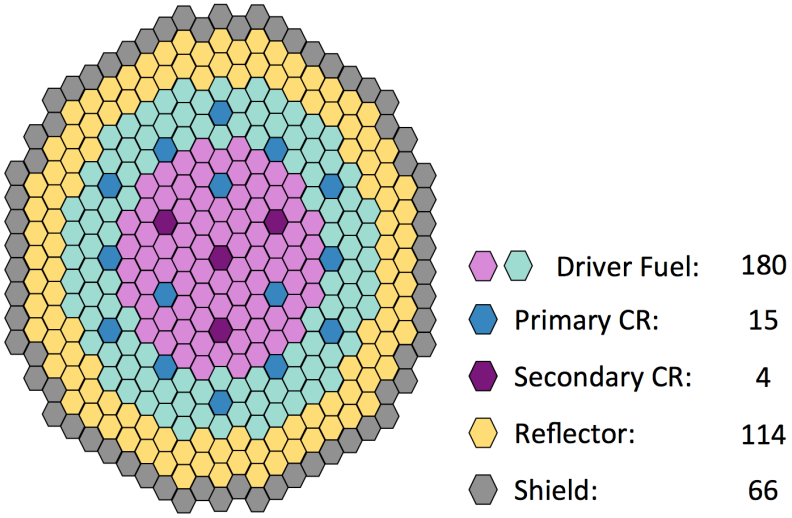

Figure 5-1 Core layout of ABR with TRU CR of 0.73 [41]

Table 5-1 Performance Characteristics of Benchmark CR=0.73 ABR in UCB

	ABR Results	UCB Results
TRU Feed Primary feed make-up feed	Recovered TRU LWR-SNF	Recovered TRU LWR-SNF
Cycle length, month	12	12
Number of batches	4	4
TRU enrichment in inner/outer zone, %	18.3/25.0	19.1/26.2
TRU conversion ratio	0.73	0.72
HM/TRU inventory at BOEC, MT	13.2/2.9	13.2/3.0
Discharge burnup (ave/peak), MWd/kg	93/138	91/135
Specific power density (MW/MT)	73.2	73.2
Peak discharge fast fluence, 10^{23}/cm^2	4.09	3.99
Burnup reactivity loss, Δk	0.022	0.023
Core average flux, 10^{15}/cm^2-sec	3.23	3.23
Fast flux fraction	0.68	0.67
TRU consumption rate, kg/year	81.6	84.9

5.2. Compact S&B core vs. reference ABR

Two compact S&B cores were designed for this comparative study; their layout is depicted in Figure 5-2. Case 1 has 54 thorium blanket assemblies loaded at the periphery of the reference ABR core. The blanket assemblies stay in the core for six fuel cycles before reaching the fast fluence constraint. The resulting core diameter is the same as of the metallic fuel S-PRISM core [44]. This case is used to demonstrate the performance of a compact core with a conventional radial blanket. Case 2 has thorium blanket assemblies interspersed over the entire core in addition to blanket assemblies at the radial periphery. Every cycle 12 blanket assemblies are shuffled from the periphery to the center. The total residence time of blanket assemblies are eight fuel cycles – six at the periphery followed by two at the inner core. There are a couple of TRU enrichment levels in the driver assemblies of both cores as commonly done to flatten the radial power distribution. The TRU weight fraction in the driver fuel is adjusted in order to achieve the desirable conversion ratio and ensure the criticality through one cycle. The active height of the two cores is 81.3cm, same as of the reference ABR [41]. Either half (Case 1) or one fourth (Case 2) of the driver fuel is recycled after each cycle.

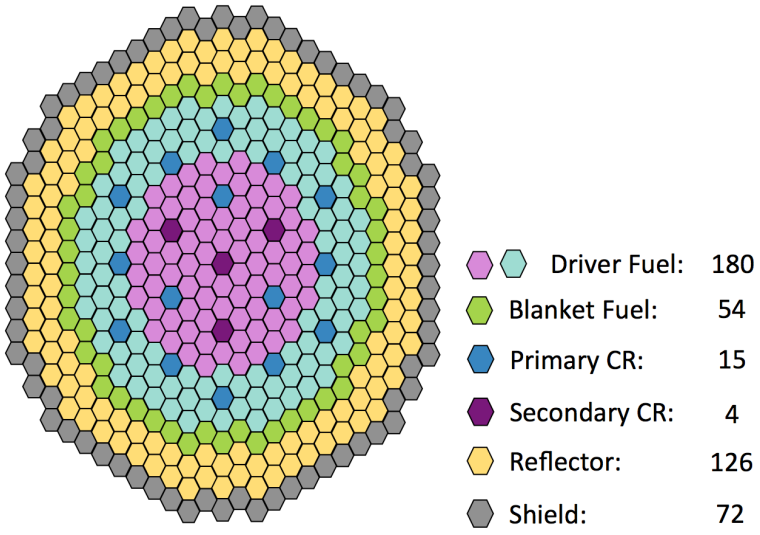

(a)

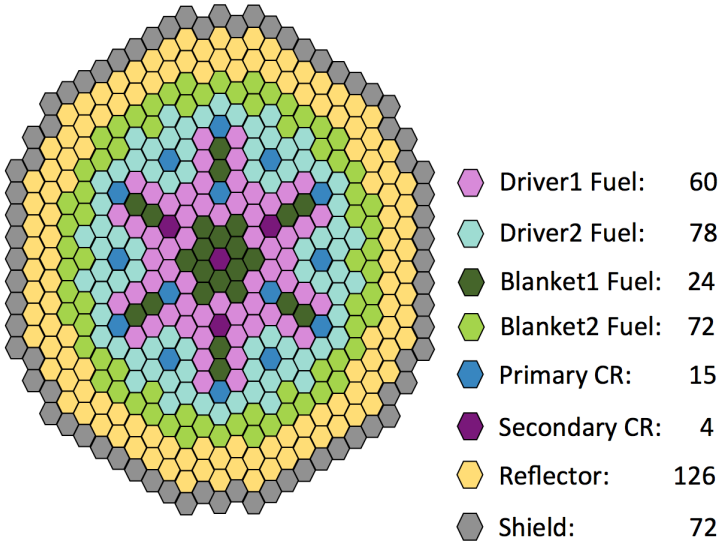

(b)

Figure 5-2 Core layout of compact S&B designs with TRU CR of the seed fuel at 0.73 (a) and 0.5 (b)

The design variables are the cycle length, number of batches, number of seed/blanket assemblies, TRU loading to the seed and P/D ratios for the seed and blanket fuel assemblies. Same optimization strategy used in previous studies (Section 2.9) is applied: the maximum acceptable P/D ratio is searched for the driver assemblies to maximize neutron leakage into the blankets while maintaining criticality; likewise, the P/D ratio of blanket assemblies is the minimum required to safely accommodate the peak assembly power. Design constraints are considered as in Section 2.4 with two exceptions: the pressure drop through the system is 0.5 MPa and the radiation damage constraint is the peak fast neutron fluence of less than $4x10^{23}$ n(E<0.1 MeV)/cm^2.

Selected performance characteristics of the two compact S&B cores and of the ANL designed reference core are compared in Table 5-2. Case 1 features a longer cycle that results in a larger burnup reactivity swing. A two-batch scheme is applied for the driver fuel without violating the burnup reactivity swing constraint and the cycle length is extended to 650 EFPD. The smaller burnup reactivity swing of this core is due to the unique synergism of the S&B concept (discussed in Section 4.6): the reactivity gained over the cycle in the blanket assemblies partially compensates the reactivity loss in the driver fuel. Case 2 has fewer driver assemblies with thorium assemblies interspersed near the center of the core and therefore has to have higher TRU loading which results in

lower conversion ratio and higher transmutation rate. With four-batch scheme for the driver fuel, Case 2 has cycle length of 300 EFPD, similar to that of reference ABR.

It is also found that using a conventional radial blanket (Case 1) the thorium blanket contributes only 5.9% of the total core power. By interspersing blanket assemblies in between driver fuel assemblies (Case 2), the thorium blanket contributes 13.6% of the total core power. However, more TRU has to be loaded in the driver assemblies to sustain the core criticality. Both Case 1 and Case 2 demonstrate that the use of thorium blanket reduces the radial and total neutron leakage probability by ~5% (absolute value); their impact on the axial leakage probability is ignorable.

Table 5-2 Performance Characteristics of the Compact S&B Cores

	Reference ABR	Case 1	Case 2
Active core height, cm	81.3	81.3	81.3
Effective core diameter, cm	242.3	270.2	270.2
Number of assemblies (seed/blanket)	180/-	180/54	138/96
Number of batches (seed/blanket)	4	2/6	4/8
Cycle length, EFPD	328.5	650	300
Burnup reactivity loss, Δk/k	0.022	0.038	0.024
P/D ratio, (seed/blanket)	1.180	1.181/1.031	1.240/1.098
Ave./Peak TRU enrichment, %	22.1/25.0	22.5/24.6	32.1/33.1
TRU conversion ratio	0.73	0.73	0.49
TRU consumption rate, kg/EFPY	-81.6	-77.0	-142.1
Average discharge burnup (seed/blanket), MWd/kg	93/-	83.4/37.6	101.8/34.5
Radial peaking factor (seed/blanket)	1.26/-	1.33/1.49	1.36/2.14
Peak discharge fast fluence (seed/blanket), 10^{23}/cm^2	4.09	3.88/3.68	3.93/4.08
Fraction of power from blanket	0.0%	5.9%	13.6%
Axial neutron leakage probability	14.9%	15.2%	15.7%
Radial neutron leakage probability	12.7%	7.9%	7.4%
Safety parameters at EOEC			
Sodium void worth (Δk/k)	0.022	0.026	0.022
Doppler coefficient (pcm/°C)	-0.326	-0.377	-0.320

5.3. Compact S&B core vs. elongated S&B core

A comparison between the compact S&B core (Case 2) and the large S&B core ("Ultra-Long" case in Section 4.3) is given in Table 5-3. Both cases have a similar seed conversion ratio of ~0.5 and the same effective diameter but the large S&B core is approximately 3 times higher. As P/D ratios of the two cores are similar, the HM inventory of the long S&B core is approximately three times larger although its seed HM inventory is only 30% larger. The TRU/HM ratios in the seed fuel of the two cores are comparable. The discharge burnup of the large S&B core is 20% higher than that of the compact core due to the different radiation damage constraints applied. A sensitivity analysis summarized in Section 6.5 indicates that the constraint of peak fast fluence is more conservative. Same reason can also explains the smaller discharge burnup for the blanket of the compact core. In addition, the neutron spectrum gets softer and the DPA per fast neutrons (> 0.1MeV) gets smaller towards the radial periphery of the large S&B cores. The spectrum in the blanket of the compact core is generally same as that of the driver fuel and this partially results in a lower discharge burnup. Due to the higher HM inventory, higher discharge burnup and the larger fraction of core power from the blanket -- 42.5% for the large core versus 13.6% for the compact core, the cycle length of the large S&B core is almost nine times that of the compact core. The burnup reactivity rate of the large S&B core -- 0.0049 $\Delta k/k$ per year, is only one sixth of that for the compact core -- 0.0292 $\Delta k/k$ per year. The longer cycles will enable higher capacity factor. The reprocessing capacity required to support 1 GWth of the large S&B core – 1703.6 kg/EFPY, is nearly half that required to support the compact S&B core at identical power – 3097.8 kg/EFPY. Nevertheless, the TRU transmutation rate of the large S&B core is only about two thirds that of the compact core where all the power is generated from the driver fuel. As the cost of the thorium blanket fuel is very small compared with the cost of the TRU containing seed fuel and the blanket fuel is not reprocessed, the fuel cycle cost of the large S&B core is expected to be lower than that of the compact core.

The potential advantages of the large S&B core are derived from the more efficient utilization of the excess neutrons generated from the seed. Whereas the axial neutron leakage probability of the compact core is 15.7%, that of the large S&B core is merely 2.9%. The radial neutron leakage probability of the large S&B core is also lower – 3% versus 7.4% for the compact core. It is possible to reduce the compact core radial leakage probability by adding a second and, even more, a third raw of blanket assemblies near the periphery of the core. However, in order to accommodate this suggestion, the core has to have either higher TRU content driver fuel or increased core diameter.

Table 5-3 Comparison of Compact vs. Large S&B Core Designs

	Case 2	Ultra-Long
Active core height, cm	81.3	250.0
Effective core diameter, cm	270.2	270.2
Cycle length, EFPD	300	2630
Number of batches (seed/blanket)	4/8	1/3
Burnup reactivity loss, Δk/k	0.024	0.035
P/D ratio, (seed/blanket)	1.240/1.098	1.261/1.151
Average TRU enrichment	30.8%/33.1%	27.8%/27.8%/34.1%
TRU conversion ratio	0.49	0.46
TRU consumption rate, kg/EFPY	-142.1	-93.2
Average discharge burnup (seed/blanket), MWd/kg	101.8/34.5	123.2/65.2
Reprocessing capacity (seed fuel), kg/EFPY	3097.8	1703.6
HM inventory (seed/blanket), Mt	9.3/9.0	12.3/51.4
TRU inventory (seed), Mt	3.0	3.7
TransTh inventory (blanket), Mt	0.2	1.0
Peak assembly power (seed/blanket), MW		
BOEC	8.0/3.5	11.8/4.4
EOEC	7.5/4.2	8.3/7.2
Average power density (seed/blanket), W/cc	359.5/185.2	172.9/38.4
Average specific power (seed/blanket), W/g	93.1/15.2	46.8/8.3
Radial peaking factor (seed/blanket)	1.36/2.14	1.21/3.34
Pressure drop, MPa	0.5	0.9
Peak discharge fast fluence (S/B), 10^{23}/cm^2 or DPA	3.93/4.08	175/204
Fraction of power from blanket	13.6%	42.5%
Neutron leakage out of active core		
axial	15.7%	2.9%
radial	7.4%	3.0%

The compact S&B cores discussed in this chapter are not necessarily the optimal cores of their category. Moreover, the distortion may have been introduced by the use of a different measure for the radiation damage induced by the fast neutrons. A more consistent analysis is provided in Section 6.2 that reports the study of the sensitivity of the core performance to the active S&B core height.

Chapter 6

6. Sensitivity Analysis of S&B Cores

The S&B cores studied in Chapter 4 were designed to have active core height of 2.5m in order to minimize the axial neutron leakage and maximize the fraction of excess neutrons that leak radially from the seed. It makes beneficial use of these leaking neutrons to the subcritical blanket -- close to 60% of the core power can be generated by a thorium fueled blanket driven by an annular non-fertile (TRU-10Zr) fueled seed. The performance characteristics of the reference S&B core reported in Chapter 4 were designed to give an upper bound on the improvements that can be provided by this core concept. This core significantly deviates from design practices followed by the SFR community in several aspects – the core height and pressure drop are more than twice the commonly used values. In addition, the reference seed conversion ratio is zero versus 0.5 to 0.75 of typical ABR [41]. To get a zero conversion ratio, it requires use of inert matrix fuel with which there is limited experience. Typical ABR cores targeting for early licensing are designed to be much more compact and their TRU-to-HM ratio does not exceed ~30% [43]. A study was therefore undertaken to quantify the tradeoff between S&B core design variables and the core performance. The objective of this section is to investigate the performance implications of designing S&B cores using more accepted design practices, including the non-fertile seed fuel with Zr fraction of 40wt%, smaller S&B active core height, lower coolant pressure drop and different radiation damage constraints.

6.1. Zr fraction in non-fertile seed fuel

The S&B core used as the reference core for this sensitivity analysis is derived from the "High Transmutation" case described in Section 4.4 with one exception -- the seed fuel is TRU-40Zr instead of TRU-10Zr alloy. TRU-40Zr was assumed for the seed fuel because it can be supported by the existing data based on inert matrix fuel. The Fuel Cycle Research & Development program of the early 2000 [50] successfully irradiated fuel rods made of Pu-40Zr and Pu-10Am-10Np-40Zr up to burnup of 22.6%FIMA and 17.7%FIMA, respectively. These fuels could possibly retain their integrity up to even higher burnup. As the TRU content of a metallic transmutation fuel alloy increases, the fuel melting temperature decreases. A zirconium concentration of 40wt% is required in order to offset the decrease of melting temperature.

Table 6-1 compares selected design and performance characteristics of the new reference S&B core with the "High Transmutation" core of Section 4.4 and of a standard ABR core that features a TRU conversion ratio of 0.5. Due to the higher Zr concentration in the reference seed fuel, the number of the seed assemblies had to be doubled compared with that of the original "High Transmutation" core to enable criticality. The cycle length is

cut by half to meet the burnup reactivity swing constraint and the number of batches is increased from two to four for the seed fuel management. The increase in the seed thickness reduces the neutron leakage probability from the seed to the blanket. As a result, the fraction of core power generated from the blanket decreases from 57.5% to 50.7%. However, due to its higher Zr and lower TRU concentrations, the reference seed has somewhat softer spectrum and can achieve a higher discharge burnup for the same radiation damage constraint. As a result, the reprocessing capacity required per unit of electricity generated is even slightly lower in the new reference core than in the "High Transmutation" core. Compared with the ABR core [43] with approximately same TRU transmutation rate, the reference core features about one sixth of the ABR reprocessing capacity and, therefore, a significantly lower fuel cycle cost. The reference S&B reactor features a four times longer cycle and is expected to have a higher capacity factor and, possibly, better economics. The safety parameters of the reference S&B core -- including delayed neutron fraction, sodium void worth, and Doppler coefficients, are comparable to those of the ABR.

Table 6-1 Performance Characteristics of the S&B Cores with TRU-10Zr and TRU-40Zr Seed Fuel and Advanced Burner Reactor (ABR) [43]

	High Transmutation	Reference	ABR
	Seed/Blanket	Seed/Blanket	
Fuel form	TRU-10Zr/Th	TRU-40Zr/Th	U-TRU-10Zr
Target TRU CR of seed	CR=0.0	CR=0.0	CR=0.5
Number of assemblies			
Inner blanket	96	63	-
Seed	30	61	144
Outer blanket	145	147	-
Number of batches			
Inner blanket	2	3	-
Seed	2	4	6/6/7
Outer blanket	3	7	-
P/D ratio	1.406/1.104	1.216/1.132	1.293
Permissible assembly power (MWth)	18.3/5.1	10.3/6.4	-
Fraction of max. permissible	0.97/0.99	0.92/0.99	-
Core power (MWth)	1000	1000	1000
Core height (cm)	250	250	101.6
Leakage probability			
Axial	2.8%	3.5%	-
Radial	4.2%	3.9%	-

Core pressure drop (Mpa)	0.9	0.9	-
Cycle length (EFPD)	1550	840	221
Tot. residence time (EFPD)	3100/7750	3360/8400	1326/1326/1547
k_{eff} at BOEC	1.041±0.00095	1.042±0.00093	-
k_{eff} at EOEC	1.003±0.00085	1.007±0.00085	-
Burnup reactivity swing (%Δk/k)	-3.60	-3.33	-2.90
Burnup reactivity swing rate (%Δk/k /EFPY)	-0.85	-1.45	-4.79
Average blanket power fraction	57.7%	50.7%	0.0%
Average discharge burnup (MWd/kg)	312.4/70.2	374.0/79.8	131.9
Peak radiation damage (DPA)	185/207	196/208	-[7]
TRU/HM at BOEC (wt%)	99.5	99.3	33.3
Seed CR at BOEC	0.01	0.00	0.5
HM at BOEC (tons)	4.2/63.7	4.4/52.6	9.4
Specific power (MWt/tHM)	100.8/9.1	111.3/9.6	106.4
TRU feed rate (kg/EFPY)	158.1/0.0	182.4/0.0	173.8
DU feed rate (kg/EFPY)	0.2/0.0	0.3/0.0	217.5
Thorium feed rate (kg/EFPY)	0.0/3024.2	0.0/2317.0	0.0
Trans-Th feed rate (kg/EFPY)	0.0/-223.3	0.0/-182.1	0.0
Reprocessing capacity (kg/GWt/Yr)	494.5	481.3	2767.2
Safety Parameters at EOEC			
Effective delayed neutron fraction	0.0030±0.0002	0.0029±0.0002	0.003
Sodium void worth (Δk/k)			
Seed only	0.012±0.0002	0.017±0.0002	-
Blanket only	0.014±0.0002	0.013±0.0002	-
Full core	0.026±0.0002	0.029±0.0002	0.029
Doppler coefficient (¢/°C)	-0.08±0.02	-0.06±0.03	-0.09
Axial expansion coefficient (¢/°C)	-0.27±0.03	-0.27±0.04	-0.54
Radial expansion coefficient (¢/°C)	-0.16±0.02	-0.10±0.03	-0.43

It is concluded that in order to achieve high TRU transmutation rate the seed in the S&B cores can be charged with TRU-40Zr fuel suggested by the irradiation experiment [50]. The major benefits claimed by the S&B cores in previous chapters are preserved, like the smaller reprocessing capacity per unit of electricity generated. The fraction of power generated by blanket decreases slightly but still significant. It suggests that the future

[7] The peak radiation damage on the cladding of the ABR design is constrained by peak fast fluence of $4x10^{23}$ n(>0.1 MeV)/cm^2.

high TRU transmutation cases should be charged by this non-fertile fuel with Zr fraction of 40wt%.

6.2. Core height

The reference S&B core was designed to have unconventionally tall core of 250 cm in order to minimize the axial leakage out from the core while maximizing the radial leakage from the seed into the subcritical radial blanket [49, 84, 86]. Conventional SFR cores, like ANL's ABR [43] and GE's S-PRISM [44], feature core height of about 100 cm. Compared with these compact SFR cores, the large S&B core is expected to increase the SFR capital cost as it would require a higher reactor vessel and a more challenging seismic design. A parametric study was undertaken to quantify the effect of reducing the core height on the S&B core performance.

Table 6-2 compares the performance characteristics of the S&B cores optimized to have an active core height in the range from 250 cm to 90 cm. The P/D ratio for the seed and blanket fuel assemblies of the shorter cores are approximately the same as of the reference core. Therefore, the shorter cores also feature a lower pressure drop. As the core height decreases, the axial leakage probability significantly increases and more seed fuel assemblies are required to establish criticality. As the result, the radial leakage probability from the seed to the blanket decreases together with fraction of core power generated by the blanket. Compared with the reference core, the shorter S&B cores feature: (1) a higher fraction of neutrons leaking out without constructive use; (2) smaller fraction of core power generated by the blanket; (3) smaller HM inventory and, therefore, higher specific power; (4) larger burnup reactivity swing per year and therefore increased number of seed batches and (5) shorter cycles; (6) higher average seed fuel discharge burnup due to the smaller axial power peaking factor; (7) slightly larger reprocessing capacity per unit of electricity but still about one fifth that for ANL's ABR [43]; (8) significantly less positive feedback to coolant voiding due to the enhanced leakage induced by coolant expansion; and (9) more negative feedback to core axial and radial expansion due to the larger core leakage.

The study of active core height indicates that it is possible to shorten the S&B core down to ~120 cm with only 15% reduction in the fraction of core power generated by the blanket (from 50.7% of 250 tall core to 43.1%) and only 10% increase in the required reprocessing capacity, despite of the increase in the fraction of fission neutrons that is lost via leakage in the axial direction. The discharge burnup of the seed fuel slightly increases due to the smaller axial peaking factor. The cycle length significantly decreases with core height reduction due to a combination of reduction in the HM inventory along with an increase in the required number of the seed batches. The increase in the number of seed fuel batches is dictated by an increase in the rate of reactivity decline per unit time. The

latter is attributed to the higher specific power that is inversely proportional to the HM inventory. The shorter cores feature a smaller pressure drop and a smaller coolant voiding reactivity worth. For core height of 120 cm it is possible to design S&B cores to have one year long cycles and the total blanket fuel residence time is approximately 14 years – close to half that for the reference core.

Table 6-2 Performance Characteristics of 1000MWth S&B Cores with Different Active Fuel Height

Property	Reference	Height180	Height120	Height90
	Seed/Blanket			
Fuel form	TRU-40Zr/Th			
Target TRU CR of seed	0.0	0.0	0.0	0.0
Core height (cm)	250	180	120	90
Number of assemblies				
Inner blanket	63	57	57	37
Seed	61	61	71	79
Outer blanket	147	153	143	155
Number of batches				
Inner blanket	3	3	4	4
Seed	4	4	5	6
Outer blanket	7	8	10	17
P/D ratio	1.216/1.132	1.208/1.128	1.190/1.117	1.204/1.125
Permissible assembly power (MWth)	10.3/6.4	10.0/6.2	9.1/5.7	9.2/6.1
Fraction of max. permissible	0.92/0.99	0.98/1.00	1.00/0.97	0.97/1.00
Leakage probability				
Axial	3.5%	5.9%	10.7%	15.0%
Radial	3.9%	3.5%	3.6%	2.8%
Core pressure drop (MPa)	0.9	0.8	0.7	0.66
Cycle length (EFPD)	840	600	350	220
Total residence time (EFPD)	3360/8400	2400/6600	1750/4900	1320/4620
k_{eff} at BOEC	1.042±0.001	1.046±0.001	1.041±0.001	1.056±0.001
k_{eff} at EOEC	1.007±0.001	1.004±0.001	1.000±0.001	1.007±0.001
Burnup reactivity swing (%Δk/k)	-3.33	-4.03	-3.98	-4.64
Burnup reactivity swing	-1.45	-2.45	-4.15	-7.70

rate (%Δk/k /EFPY)				
Average blanket power fraction	50.7%	48.6%	43.1%	37.0%
Average discharge burnup (MWd/kg)	374.0/79.8	382.3/83.0	396.6/84.5	416.5/96.4
Peak radiation damage (DPA)	196/208	192/205	189/197	192/202
TRU/HM at BOEC (wt%)	99.3	99.4	99.4	99.4
HM at BOEC (tons)	4.4/52.6	3.2/38.1	2.5/24.6	2.0/17.4
Specific power (MWt/tHM)	111.3/9.6	159.3/12.8	226.6/17.5	315.5/21.2
TRU feed rate (kg/EFPY)	182.4/0.0	189.9/0.0	210.0/0.0	231.9/0.0
DU feed rate (kg/EFPY)	0.0/0.0	0.0/0.0	0.0/0.0	0.0/0.0
Thorium feed rate (kg/EFPY)	0.0/2317.0	0.0/2138.3	0.0/1863.8	0.0/1402.5
Trans-Th feed rate (kg/EFPY)	0.0/-182.1	0.0/-172.6	0.0/-153.5	0.0/-120.9
Reprocessing capacity (kg/GWt/yr)	481.3	490.3	523.4	551.7
Safety Parameters at EOEC				
Effective delayed neutron fraction	0.0029±0.0002	0.0030±0.0002	0.0030±0.0002	0.0023±0.0002
Sodium void worth (Δk/k)				
Seed only	0.017±0.0002	0.015±0.0002	0.014±0.0002	0.014±0.0002
Blanket only	0.013±0.0002	0.010±0.0002	0.005±0.0002	0.002±0.0002
Full core	0.029±0.0002	0.025±0.0002	0.018±0.0002	0.016±0.0002
Doppler coefficient (¢/°C)	-0.06±0.03	-0.10±0.03	-0.07±0.02	0.00±0.03
Axial expansion coefficient (¢/°C)	-0.27±0.04	-0.27±0.03	-0.31±0.03	-0.34±0.04
Radial expansion coefficient (¢/°C)	-0.10±0.03	-0.18±0.03	-0.22±0.02	-0.29±0.03

It is concluded that the performance characteristics of the S&B cores deteriorate as the active core height decreases. In the compact core, relatively more seed fuel has to be loaded in the core to compensate the larger neutron leakage out of the core and, therefore,

the fraction of power generated by the blanket decreases. When the S&B core is designed as typical SFR core at the core height of 120cm, the fraction of power by blanket decrease but the reprocessing capacity per unit of electricity generated is comparable with the large S&B core. This is attributed to the slightly higher achievable burnup of the seed due to the smaller axial peaking factor in the compact core.

6.3. Pressure drop

The S&B cores studied so far have a coolant pressure drop of 0.9 MPa which is higher than the value used for most SFR core designs – the experimental SFR cores are designed with pressure drop of 0.3 MPa while the demonstration SFR cores are designed with pressure drop of 0.5-0.7 MPa [15]. The lower pressure drop system is preferable for the natural circulation. This section summarizes the findings of a study that investigates the effect of the coolant pressure drop reduction on the S&B core performance. The pressure drop is adjusted by changing the distance between fuel pins while preserving the reference core height. Three cases with larger P/D ratios for both seed and blanket fuel assemblies are optimized to achieve a coolant pressure drop of 0.7, 0.5 and 0.3 MPa.

The sensitivity of the S&B core performance to the pressure drop was investigated for the reference 250cm tall S&B core through which the pressure drop is 0.9 MPa. The pressure drop is reduced by a smaller fuel pin diameter – that is, increasing the coolant cross-section area. The outer diameter of all cores is not changed so the fuel inventory in the core decreases as the pressure drop is reduced. Table 6-3 compares the performance characteristics of the S&B cores optimized to have different coolant pressure drops. As the neutron economy of S&B cores deteriorates with a reduction in the fuel volume fraction, it is observed that the performance of the core will degrade with the reduction of the pressure drop. Therefore, in order to maintain criticality more seed fuel assemblies are required for the S&B cores with lower coolant pressure drop. Compared with the reference core, the lower pressure cores are found to have: (1) more seed fuel assemblies and fewer internal blanket assemblies; (2) larger number of seed batches due to the larger burnup reactivity swing per year; (3) shorter cycle length; (4) smaller fraction of core power from the thorium blanket; (5) slightly higher fuel reprocessing capacity; (6) more positive feedback to coolant voiding due to the higher TRU fuel content loaded in the core. Nevertheless, the impairment of the S&B core performance due to reduction in the pressure drop constraint is relatively small – the pressure drop reduction from 0.9 MPa all the way to 0.3 MPa results in a decrease of the fraction of core power generated by the blanket from 50.7% to 44.0% and a corresponding increase in the required reprocessing capacity from 481.3 to 515.0 kg/GWt/Yr; the latter is less than one fifth that of the reference ABR (Table 6-1). The cycle length is somewhat reduced with lower pressure drop due to a reduction in the HM inventory in the fixed volume core. However, even for the core designed to have a pressure drop of 0.3 MPa, the cycle length is three times that

of ABR design (TRU CR of 0.5). The reactivity effect of sodium voiding increases as the coolant pressure drop decreases.

Table 6-3 Sensitivity of the S&B Core Performance to the Coolant Pressure Drop

	Reference	Pressure0.7	Pressure0.5	Pressure0.3
Fuel form	Seed/Blanket TRU-40Zr/Th	Seed/Blanket TRU-40Zr/Th	Seed/Blanket TRU-40Zr/Th	Seed/Blanket TRU-40Zr/Th
Target TRU CR of seed	CR=0.0	CR=0.0	CR=0.0	CR=0.0
Number of assemblies				
Inner blanket	63	62	60	43
Seed	61	64	71	84
Outer blanket	147	145	140	144
Number of batches				
Inner blanket	3	3	3	3
Seed	4	4	4	5
Outer blanket	7	7	7	10
P/D ratio	1.216/1.132	1.241/1.145	1.293/1.175	1.398/1.262
Permissible assembly power (MWth)	10.3/6.4	10.0/6.1	10.0/6.1	10.0/6.8
Fraction of max. permissible	0.92/0.99	0.94/1.00	0.86/1.01	0.78/0.99
Core power (MWth)	1000	1000	1000	1000
Core height (cm)	250	250	250	250
Leakage probability				
Axial	3.5%	3.6%	3.8%	4.6%
Radial	3.9%	4.1%	4.6%	5.2%
Core pressure drop (Mpa)	0.9	0.7	0.5	0.3
Cycle length (EFPD)	840	780	780	630
Tot. residence time (EFPD)	3360/8400	3120/7800	3120/7800	3150/8190
k_{eff} at BOEC	1.042±0.001	1.039±0.001	1.041±0.001	1.047±0.001
k_{eff} at EOEC	1.007±0.001	1.009±0.001	1.006±0.001	1.004±0.001
Burnup reactivity swing (%Δk/k)	-3.33	-2.89	-3.37	-4.04
Burnup reactivity swing rate (%Δk/k	-1.45	-1.35	-1.58	-2.34

/EFPY)				
Average blanket power fraction	50.7%	48.7%	47.6%	44.0%
Average discharge burnup (MWd/kg)	374.0/79.8	355.0/74.0	356.3/78.8	397.2/94.3
Peak radiation damage (DPA)	196/208	182/192	179/195	191/202
TRU/HM at BOEC (wt%)	99.3	99.3	99.3	99.4
Seed CR at BOEC	0.00	0.00	0.00	0.00
HM at BOEC (tons)	4.4/52.6	4.5/50.7	4.6/46.4	4.4/37.5
Specific power (MWt/tHM)	111.3/9.6	113.8/9.6	114.2/10.2	126.1/11.7
TRU feed rate (kg/EFPY)	182.4/0.0	189.6/0.0	193.4/0.0	205.8/0.0
DU feed rate (kg/EFPY)	0.3/0.0	0.3/0.0	0.3/0.0	0.4/0.0
Thorium feed rate (kg/EFPY)	0.0/2317.0	0.0/2403.6	0.0/2204.4	0.0/1700.5
Trans-Th feed rate (kg/EFPY)	0.0/-182.1	0.0/-186.5	0.0/-175.6	0.0/-145.4
Reprocessing capacity (kg/GWt/Yr)	481.3	527.4	537.2	515.0
Safety Parameters at EOEC				
Effective delayed neutron fraction	0.0029±0.0002	0.0027±0.0002	0.0031±0.0002	0.0027±0.0002
Sodium void worth (Δk/k)				
Seed only	0.017±0.0002	0.018±0.0002	0.021±0.0002	0.029±0.0002
Blanket only	0.013±0.0002	0.013±0.0002	0.013±0.0002	0.011±0.0002
Full core	0.029±0.0002	0.031±0.0002	0.034±0.0002	0.040±0.0002
Doppler coefficient (¢/°C)	-0.06±0.03	-0.03±0.03	-0.10±0.02	-0.10±0.03
Axial expansion coefficient (¢/°C)	-0.27±0.04	-0.32±0.04	-0.34±0.03	-0.36±0.04
Radial expansion coefficient (¢/°C)	-0.10±0.03	-0.18±0.03	-0.20±0.02	-0.18±0.03

It is concluded that the performance characteristics of the S&B cores are not very sensitive to the pressure drop constraint. When the S&B core is designed to have a pressure drop comparable to most demonstration SFR designs – 0.5MPa, the fraction of core power generated by the blanket decreases slightly but the reprocessing capacity per unit of electricity generated increases only slightly.

6.4. Radiation damage constraint and phased development of the B&B reactors

The radiation damage on the cladding and structural materials of both seed and blanket of the S&B core designs considered so far is constrained to 200 DPA. Efforts are being made to increase this constraint [87] – by extending the irradiation experiments to higher fluence and by developing improved structural materials, up to close to 500 DPA – the level required for making critical B&B cores practical [8]. The objective of the sensitivity study summarized in this section is to quantify the improvement in the S&B core performance made possible by a successful R&D of structural materials that will enable increasing the radiation damage constraint from 100 and 200 to 300 or 400 DPA. The DPA value of the seed fuel is kept at 200 DPA since the discharge burnup of the non-fertile fuel (approaching 400 MWd/kg) is already higher than the feasible value (~ 200 MWd/kg) demonstrated so far [50].

Table 6-4 summarizes the performance characteristics of the S&B cores optimized for a blanket peak radiation damage of 100, 200, 300, and 400 DPA. As the blanket fuel is discharged at a higher DPA value and, hence, higher burnup, the reactivity of the blanket fuel increases and as the result: (1) more blanket assemblies are loaded in the internal blanket region; (2) the cycle length is extended as the result of smaller burnup reactivity swing; (3) a larger fraction of core power is generated from the blanket. The positive feedback to coolant voiding also decreases due to a larger power fraction from the thorium blanket. At 400 DPA, the B&B blanket can generate 64.2% of the core power while utilizing about 17% of the natural thorium energy value without the need for a thorium reprocessing technology The corresponding decrease in the reprocessing capacity required to support the S&B core operation from 481.3 to 373.4 kg/GWt/Yr is only 13.5% the capacity of 2767.2 kg/GWt/Yr required for the reference ABR core. The HM inventory in the seed slightly increases with DPA as the reduction of the seed power enables designing the seed to have a slightly tighter lattice pitch and, therefore higher fuel volume fraction. The sodium void reactivity worth slightly decreases as a larger fraction of core power is generated from the thorium blanket.

Table 6-4 Sensitivity of the S&B Core Performance to the Blanket Cladding Radiation Damage Constraint

	DPA100	Reference	DPA300	DPA400
Fuel form	Seed/Blanket TRU-40Zr/Th	Seed/Blanket TRU-40Zr/Th	Seed/Blanket TRU-40Zr/Th	Seed/Blanket TRU-40Zr/Th
Target TRU CR of seed	CR=0.0	CR=0.0	CR=0.0	CR=0.0
Number of assemblies				
Inner blanket	32	63	92	123
Seed	61	61	61	61
Outer blanket	178	147	118	87
Number of batches				
Inner blanket	2	3	4	7
Seed	6	4	3	4
Outer blanket	11	7	4	5
P/D ratio	1.280/1.155	1.216/1.132	1.184/1.132	1.154/1.119
Permissible assembly power (MWth)	13.2/7.5	10.3/6.4	8.8/6.4	7.4/5.8
Fraction of max. permissible	0.90/0.92	0.92/0.99	0.96/0.92	0.94/0.90
Core power (MWth)	1000	1000	1000	1000
Core height (cm)	250	250	250	250
Leakage probability				
Axial	4.1%	3.5%	3.3%	3.1%
Radial	2.7%	3.9%	5.2%	6.5%
Core pressure drop (MPa)	0.9	0.9	0.9	0.9
Cycle length (EFPD)	380	840	1390	1215
Tot. residence time (EFPD)	2280/4940	3360/8400	4170/11120	3645/14580
k_{eff} at BOEC	1.034±0.001	1.042±0.001	1.043±0.001	1.024±0.001
k_{eff} at EOEC	1.002±0.001	1.007±0.001	1.008±0.001	1.005±0.001
Burnup reactivity swing (%Δk/k)	-3.01	-3.33	-3.30	-1.82
Burnup reactivity swing rate (%Δk/k /EFPY)	-2.89	-1.45	-0.87	-0.55
Average blanket power fraction	36.4%	50.7%	58.2%	64.2%
Average discharge burnup (MWd/kg)	368.2/35.1	374.0/79.8	362.8/121.3	349.6/171.6
Peak radiation damage (DPA)	184/106	196/208	195/306	190/405

TRU/HM at BOEC (wt%)	99.4	99.3	99.3	99.2
Seed CR at BOEC	0.00	0.00	0.00	0.00
HM at BOEC (tons)	3.9/51.0	4.4/52.6	4.8/51.9	5.0/51.9
Specific power (MWt/tHM)	161.5/7.1	111.3/9.6	87.0/11.2	71.9/12.4
TRU feed rate (kg/EFPY)	235.5/0.0	182.4/0.0	154.6/0.0	131.9/0.0
DU feed rate (kg/EFPY)	0.4/0.0	0.3/0.0	0.3/0.0	0.2/0.0
Thorium feed rate (kg/EFPY)	0.0/3784.4	0.0/2317.0	0.0/1750.2	0.0/1366.1
Trans-Th feed rate (kg/EFPY)	0.0/-239.5	0.0/-182.1	0.0/-148.7	0.0/-120.4
Reprocessing capacity (kg/GWt/Yr)	630.7	481.3	421.0	373.4
Safety Parameters at EOEC				
Effective delayed neutron fraction	0.0025±0.0002	0.0029±0.0002	0.0033±0.0002	0.0027±0.0002
Sodium void worth (Δk/k)				
Seed only	0.024±0.0002	0.017±0.0002	0.012±0.0002	0.009±0.0002
Blanket only	0.008±0.0002	0.013±0.0002	0.016±0.0002	0.019±0.0002
Full core	0.032±0.0002	0.029±0.0002	0.028±0.0002	0.027±0.0002
Doppler coefficient (¢/°C)	-0.07±0.03	-0.06±0.03	-0.12±0.02	-0.10±0.03
Axial expansion coefficient (¢/°C)	-0.44±0.04	-0.27±0.04	-0.28±0.03	-0.28±0.04
Radial expansion coefficient (¢/°C)	-0.33±0.03	-0.10±0.03	-0.17±0.02	-0.12±0.03

It is concluded that the benefits from our S&B core concept are expected to increase with an increase in the radiation damage constraint that the structural materials will be certified to operate at. A phased development of S&B core designs is therefore expected. This phased development can be initiated using presently available technology. At the end of such a phased development plan it is hoped that critical B&B reactors could be licensed and become commercial.

6.5. Sensitivity to the definition of radiation damage constraint

The radiation damage constraint used in this study is measured by the displacement per atom; this DPA value is calculated by using the model developed by Norgett, Robinson, and Torrens assuming the displacement energy of 40eV (Section 2.7.1). The DPA value is estimated by taking into account the specific shape of the fast neutron spectrum which

is different for the seed and the blanket (Figure 2-9). A detailed discussion of the used method is given in Section 2.7. The comparison analysis was conducted on a 0-D FFTF model with MCNP. The calculated ratio between DPA and fast fluence – 39.8 DPA per 10^{23} n(>0.1MeV)/cm^2 in Section 2.7.2, is close to the values (41-45 DPA per 10^{23} n/cm^2) reported for the samples irradiated in FFTF [72].

However, the fast fluence constraint is widely accepted by the SFR community. The 200 DPA constraint is inconsistent with the radiation damage constraint of $4x10^{23}$ n(>0.1 MeV)/cm^2 used by the ANL SFR designers. The maximum cell average fast fluence pertaining to 200 DPA in Table 2-7 is higher than the fast fluence constraint of $4.0x10^{23}$ n/cm^2 used by the fast reactor design community by up to 25% and 40% for the seed and blanket, respectively. The estimation of the DPA value depends on the assumption of the displacement energy for steel -- 40eV [68, 70]. Lower displacement energy value – 28eV, is recommended by the experts from ANL [75].

The objective of this study is to compare these two constraints and their effects on the S&B core performance. The sensitivity of the S&B core performance to the radiation damage constraint was established by redesigning the reference S&B core with one of the following radiation damage constraints: (1) DPA calculated using a displacement energy of 40eV – the reference case in Section 6.1; (2) a peak fast fluence of $4x10^{23}$ n(>0.1MeV)/cm^2, which is widely accepted by the fast reactor community – Case 1; (3) DPA calculated using a displacement energy of 28eV which is suggested by ANL [75] – Case 2. The optimization strategy is that described in Section 2.9.

Table 6-5 summarizes the performance characteristics of the three S&B cores designed with different radiation damage constraints. Both Case 1 and Case 2 have comparable number of the internal and external blanket assemblies as the reference. However, the total residence time of the seed and blanket fuel is significantly shorter in Case 1 and 2 cores than the corresponding values in the reference case. When using the fast fluence constraint, the fraction of core power generated by the blanket is reduced from 50.7% to 41.9% (Case 1). The achievable seed/blanket discharge burnup decrease from 374.0/79.8 MWd/kg to 311.2/46.5 MWd/kg (Case 1). As a result the reprocessing capacity increases from 481.3 to 681.5 kg/GWth-Yr (Case 1). The latter is still far lower – only about one fourth, than the ABR reprocessing capacity – 2767.2 kg/GWth-Yr.

Table 6-5 Effect of Radiation Damage Constraint on the Performance of the S&B Cores

	Reference	Case 1 (Fast_Fluence)	Case 2 (DE 28eV)
Fuel form	Seed/Blanket TRU-40Zr/Th	Seed/Blanket TRU-40Zr/Th	Seed/Blanket TRU-40Zr/Th

Target TRU CR of seed	CR=0.0	CR=0.0	CR=0.0
Number of assemblies			
Inner blanket	63	59	65
Seed	61	63	63
Outer blanket	147	149	143
Number of batches			
Inner blanket	3	2	3
Seed	4	3	3
Outer blanket	7	5	5
P/D ratio	1.216/1.132	1.229/1.124	1.236/1.124
Permissible assembly power (MWth)	10.3/6.4	10.9/6.0	11.2/6.0
Fraction of max. permissible	0.92/0.99	1.00/0.94	0.96/0.84
Core power (MWth)	1000	1000	1000
Core height (cm)	250	250	250
Core pressure drop (Mpa)	0.9	0.9	0.9
Cycle length (EFPD)	840	850	730
Tot. residence time (EFPD)	3360/8400	2550/5950	2190/5840
k_{eff} at BOEC	1.042±0.001	1.046±0.001	1.043±0.001
k_{eff} at EOEC	1.007±0.001	1.002±0.001	1.005±0.001
Burnup reactivity swing (%Δk/k)	-3.33	-4.24	-3.62
Burnup reactivity swing rate (%Δk/k /EFPY)	-1.45	-1.82	-1.81
Average blanket power fraction	50.7%	41.9%	41.9%
Average discharge burnup (MWd/kg)	374.0/79.8	311.2/46.5	263.1/45.7
Peak radiation damage (DPA) with displacement energy of 40eV	196/208	162/139	138/146
Peak radiation damage (DPA) with displacement energy of 28eV	280/297	231/199	197/208
Peak fast neutron fluence (10^{23} n/cm^2)	4.97/5.88	4.04/3.98	3.43/4.00
TRU/HM at BOEC (wt%)	99.3	99.3	99.3
Seed CR at BOEC	0.00	0.00	0.00
HM at BOEC (tons)	4.4/52.6	4.8/53.2	4.8/53.2
Specific power (MWt/tHM)	111.3/9.6	122.0/7.9	120.1/7.9
TRU feed rate (kg/EFPY)	182.4/0.0	215.5/0.0	215.3/0.0
DU feed rate (kg/EFPY)	0.3/0.0	0.4/0.0	0.4/0.0
Thorium feed rate (kg/EFPY)	0.0/2317.0	0.0/3285.7	0.0/3347.6
Trans-Th feed rate (kg/EFPY)	0.0/-182.1	0.0/-222.6	0.0/-223.8
Reprocessing capacity (kg/GWt/Yr)	481.3	681.5	805.5
Safety Parameters at EOEC			

Sodium void worth (Δk/k)	0.029±0.0002	0.029±0.0002	0.029±0.0002
Doppler coefficient (¢/°C)	-0.06±0.03	-0.14±0.02	-0.09±0.03
Axial expansion coefficient (¢/°C)	-0.27±0.04	-0.36±0.03	-0.42±0.04
Radial expansion coefficient (¢/°C)	-0.10±0.03	-0.19±0.02	-0.20±0.03

It is concluded that the performance characteristics of the S&B cores are sensitive to the radiation damage constraint applied. The fast fluence constraint is the most conservative one but ignores the specific shape of the fast neutron spectrum. Nevertheless, the DPA calculated with the displacement energy of 40eV is used up to so far and supported by several references from nuclear material community; it gives the best performance of the S&B cores compared with the other two constraints.

Chapter 7

7. Fuel Cycle Analysis of S&B Cores

7.1. Introduction

Previous chapters found that it is feasible to design Seed-and-Blanket (S&B) cores made of elongated TRU burner seed from which most of the excess neutrons leak in the radial direction and drive a subcritical radial blanket. While the seed recycles its fuel, the blanket operates in the once-through Breed-and-Burn (B&B) mode. Using a low conversion ratio (CR) seed it was found possible to generate over 50% of the core power from a thorium blanket. A unique synergism was found between the low CR seed and the thorium blanket – while the seed "drives" the blanket fuel in the B&B mode without exceeding the cladding radiation-damage constraint of 200 DPA, the blanket reactivity increase over the cycle compensates for part of the seed reactivity loss. This, along with the low power density of the blanket and low DPA/burnup of high TRU loaded seed, enables significantly increasing the cycle length and seed discharge burnup. As a result of the high discharge burnup along with high fraction of core power generated by the blanket the reprocessing capacity required for the seed fuel can be as low as one sixth that of a conventional ABR (Advanced Burner Reactor) of comparable transmutation capability. The studies summarized in this chapter evaluate the implications of the improved S&B core performance on the fuel cycle related characteristics.

7.2. Methodology

7.2.1. Metrics

The metrics used in this study are made of five parts: (1) fuel cycle performance characteristics pertaining to the equilibrium cycle and including fuel loading, specific power, average discharge burnup, reprocessing capacity, and cycle length; (2) fuel cycle cost accounting for both front-end and back-end activities; (3) waste characteristics including radioactivity, inhalation radiotoxicity, and ingestion radiotoxicity of the used nuclear fuel and High Level Waste (HLW) — all at short term (10 years) and long term (100,000 years) after fuel discharge; (4) proliferation resistance related characteristics such as plutonium throughput, fissile plutonium fraction, ^{238}Pu fraction, specific plutonium decay heat, spontaneous fission rate, and material attractiveness; (5) fuel utilization — the natural uranium and thorium required per unit of electricity generated.

7.2.2. Assumptions

The major assumptions and constraints used for the ABR and the S&B core designs are summarized in Chapter 2. Additional assumptions used for this fuel cycle analysis are: the thermal efficiency is 40% for the SFR and 33% for PWR; the discharge fuel from the ABR and the seed of the S&B core goes through 5-years cooling before recycling; 1.2% of the discharged heavy metal that is recycled is lost into waste stream during the reprocessing and fuel fabrication.

For the fuel cycle analysis of the transmuting reactors, a two-tier system is assumed — Tier-1 consists of PWRs whereas Tier-2 is composed of either the ABR or the S&B reactor. An equilibrium system is assumed such that the TRU generation rate in Tier-1 PWRs is equal to the TRU consumption rate by Tier-2 reactors. All TRU transmuting cores were designed to recycle their heavy metal (HM).

7.3. Description of ABR, S&B, PWR models for the fuel cycle analysis

The specific S&B core design used for this fuel cycle analysis is the annular seed design described in section 4.4. Both seed and blanket are operating with multi-batch fuel management scheme; half of the seed fuel is discharged and recycled after each cycle; fresh thorium fuel is charged to the outermost blanket batch and the blanket fuel is gradually shuffled inward after each cycle. The blanket batch closest to the outer boundary of seed is shuffled to the batch location closest to the inner seed boundary. At end of cycle, the innermost batch of the internal blanket is discharged. The seed region has a TRU conversion ratio of 0.0 and transmutes TRU at the rate of 383.3 kg/GWe-EFPY (normalized by the seed power). The high fissile content of the low CR seed enables reducing the number of driver assemblies as well as increasing the Pitch-to-Diameter ratio (P/D) and thereby enhancing neutron leakage into the subcritical blanket. As a result, the fraction of core power generated by the blanket is 57.7% — the highest of all S&B cores designed so far. The higher TRU concentration of the lower CR seed also results in a lower flux amplitude for a given fission rate and a higher average discharge burnup without violating the cladding radiation damage constraint. The higher average discharge burnup along with the high fractions of core power generated by the blanket reduce the reprocessing capacity and the fuel cycle cost.

ANL's ABR design featuring a TRU CR of 0.5 [43] is used for comparison. The core is to transmute TRU from LWR's UNF and has no blanket assemblies. The ABR is designed with three zones and operates on multi-batch fuel management scheme. At end of cycle, a certain number of assemblies are discharged from the core and reprocessed; TRU and depleted uranium (DU) are added as the makeup fuel. All the heavy metals are

recycled and fission products are disposed in a geological repository. The studies in [43] designed ABR to have a conversion ratio of 0.5 but this implies undesirably short cycle length when imposing the commonly used burnup reactivity swing constraint of 3.5% Δk/k. The TRU transmutation rate of the CR=0.5 ABR is comparable to that of the S&B core at identical power.

The PWR core used as a reference is fueled with 4.5wt% enriched uranium dioxide (UOX) and discharged at a burnup of 50 MWd/kg. It operates with a three-batch fuel management with an out-in shuffling scheme. The discharged fuel is sent to the geological repository after interim storage on site.

Figure 7-1 shows a schematic view of the ABR and the S&B fuel cycles considered. As the ABR core and the S&B seed are designed to incinerate TRU recovered from LWR's UNF, they operate in a closed fuel cycle. The first stage consists of a typical PWR fed by 4.5% ^{235}U enriched UOX fuel that is burned up to 50 MWd/kg followed by 10-years cooling. The TRU recovered from the PWR is used, after mixing with DU, to feed the second stage cores — either the driver fuel in the S&B or the ABR. The fuel mass loaded in stage i reactors per unit of electricity generation was obtained from

$$M^i = \frac{P_{th}^i}{BU(i) \times P_{el}^i} \cdot \frac{365d}{1yr}$$

(Equation 7-1)

where

M^i = the fuel mass charged per GWe-EFPY to stage i; it is equal to the mass of fuel sent to the reprocessing facility per GWe-EFPY,

P^i_{th} = the thermal power of stage i (GWt),

P^i_{el} = the electrical power of stage i (GWe),

BU(i) = the discharge burnup for stage i (GWd/Mt).

At the equilibrium state, the TRU mass discharge rate from stage 1 equals to the TRU incineration rate in stage 2. That is,

$$F_{el}^1 \times TRU_P^1 = F_{el}^2 \times TRU_D^2$$

(Equation 7-2)

where

F^{i}_{el} = the fraction of the system electricity generated from stage i reactors such that

$$F^{1}_{el} + F^{2}_{el} = 1$$

(Equation 7-3)

$$\frac{F^{1}_{el}}{1 - F^{1}_{el}} = \frac{TRU^{2}_{D}}{TRU^{1}_{P}}$$

(Equation 7-4)

where

TRU^{1}_{P} = the amount of TRU produced in stage 1 reactors per unit of electricity generated (kg/GWe-EFPY) — the typical TRU production rate for PWR with discharge burnup of 50 MWd/kg is 251.3 kg/GWe-EFPY,

TRU^{2}_{D} = the amount of TRU incinerated in stage 2 reactors per unit of electricity generated (kg/GWe-EFPY).

The support-ratio, S, is defined as the ratio of electricity generated by stage 1 reactors to the electricity generated by stage 2 reactors. That is,

$$S = \frac{F^{1}_{el}}{F^{2}_{el}} = \frac{TRU^{2}_{D}}{TRU^{1}_{P}}$$

(Equation 7-5)

A transmuting reactor with a smaller conversion ratio can be designed to have a higher support ratio and, therefore, contribute smaller fraction of power in the two-tier system. There are approximately two PWRs per one ABR or S&B of identical electrical power.

Table 7-1 compares the equilibrium fuel cycle parameters of the three cores. Due to the higher TRU transmutation rate of the ABR per unit of electricity generated, smaller fraction of power is generated from stage 2 of the PWR-ABR system, than of the PWR-S&B system. The driver fuel of the S&B core is designed to have nearly 100% TRU loading and its discharged burnup is over two times that of the ABR. The high discharge burnup along with the nearly 60% of core power generated from the once-through B&B blanket significantly reduces the electro-chemical reprocessing capacity required per unit of electricity — 487.7 kg/GWe-EFPY for the PWR- S&B versus 2446.7 kg/GWe-EFPY for the PWR-ABR system.

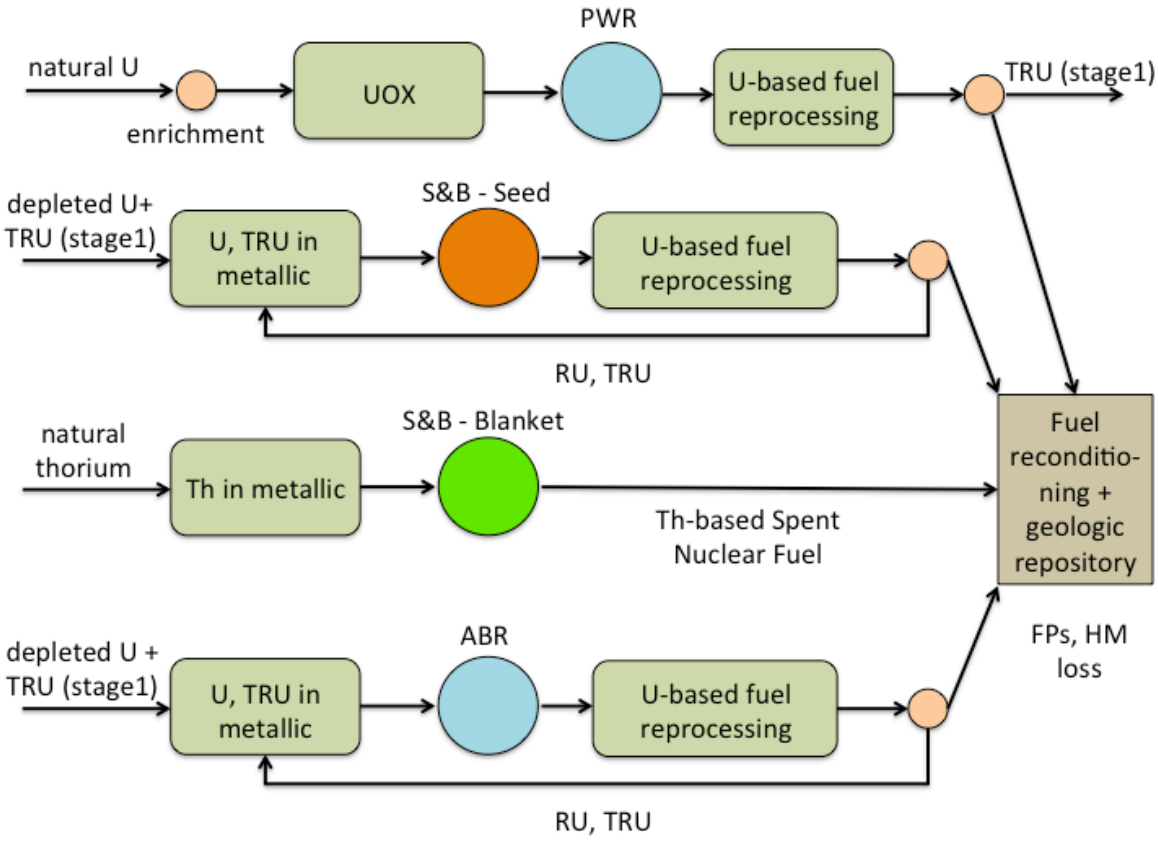

Figure 7-1 Schematic view of the PWR-S&B and the PWR-ABR fuel cycles

Table 7-1 Fuel Cycle Parameters of PWR-ABR, PWR-S&B, and PWR

Parameter	ABR	S&B (seed/blanket)	PWR
Capacity factor, %	85	85	90
Average discharge burnup, GWd/t	131.9	312.4/70.2	50
Specific power, MWth/t	105.8	100.7/9.1	33.8
Number of batches	6/6/7	2/5	3
HM inventory in core, t	9.5	4.2/63.4	116.1
HM mass per batch, t	1.7	2.1/12.7	38.7
Fuel residence time, EFFD	1326/1326/1547	3100/7750	1478
Cycle length, EFPD	221	1550	493
Burnup reactivity swing, %Δk/k	-2.9	-3.6	-

TRU transmutation rate, kg/GWe-EFPY	458.7	383.3	-
Power Fraction, %			
Stage1 (PWR)	64.6	60.4	100.0
Stage2	35.4	39.6	-
Reprocessing capacity, kg/GWe-EFPY			
PWR UNF from 1st stage	14154.8	13233.9	-
SFR UNF from 2nd stage	2446.7	487.7	-
Pu from 2nd stage	580.5	266.2	-
TRU from 2nd stage	651.6	322.9	-
Charge mass fraction, %			
Th-232	-	-/100.0	
TransTh[8]	-	-/-	4.5
U-238	66.7	2.8/-	95.5
TRU	33.3	97.2/-	
Discharge mass fraction, %			
Th-232	-	-/84.9	
TransTh	-	1.1/7.9	1.3
U-238	59.02	0.3/-	92.4
TRU	26.63	66.4/-	1.1
FPs	14.36	32.2/7.2	5.2
Fuel mass at time of recycle, %			
Th-232	-	-/84.9	
TransTh	-	1.3/7.9	1.3
U-238	59.02	0.3/-	92.4
TRU	26.63	66.2/-	1.1
FPs	14.36	32.2/7.2	5.2

7.4. Fuel cycle cost for the S&B, the ABR, and the PWR

The total cost of electricity is usually measured by the levelized electricity cost, which is composed of the reactor capital, operation-and-maintenance, and fuel cycle costs. This study focuses on the fuel cycle cost including the front-end and back-end activities. The PWR described above represents the current nuclear industry practice. The nominal values reported in [85] and reproduced in Table 4-4 are used for the fuel cycle cost analysis. In lack of commercial experience there are large uncertainties in the cost components involving fuel recycling and waste disposal but quantifying these

[8] The TransTh includes the actinide bred from thorium fuel cycle, like ^{233}U, ^{234}U, ^{235}U, but not ^{238}U and TRU; they also include ^{235}U of the enriched uranium.

uncertainties is beyond the scope of this preliminary study. The detailed flow chart of the fuel cycle evaluated is shown in Figure 4-3.

Although extra shielding may be required to fabricate the driver fuel of the S&B core due to the higher TRU contents, this study assumes that the cost of fuel reprocessing and remote fabrication is independent of the TRU contents. The fabrication cost of natural thorium in blanket of the S&B core is assumed the same cost as of UOX fuel. The fuel discharged from the thorium B&B blanket is sent to geological repository; the blanket UNF disposal cost is assumed same as of the PWR UNF disposal considering the comparable discharge burnup (70-80 MWd/kg for thorium blanket and 50 MWd/kg for UOX fuel in PWR). For PWR, ^{235}U is enriched to 4.5wt% from natural uranium and depleted uranium stream contains 0.2wt% ^{235}U. This requires a total separation work of 7.6 SWU per kg of enriched Uranium. Thus, the cost of UOX enrichment is approximately 800 $/kg LEU.

Figure 7-2 compares the fuel cycle cost of the PWR-ABR, the PWR-S&B, and the PWR systems. The total fuel reprocessing capacity of the S&B core is only one fifth that for the ABR per unit of core energy; therefore, the cost of reprocessing and remote fuel fabrication for the S&B is about one fifth that of the ABR. The two cores have comparable costs for TRU separation from LWR UNF due to the similar effective TRU transmutation rate. The thorium blanket is fed with fresh thorium that is not radioactive and no enrichment is required; therefore, the front-end cost of the thorium blanket is much lower compared with that of a typical PWR. As the seed region in the S&B core operates in a closed fuel cycle, its geological repository cost is lower relative to PWR. The net result is that the fuel cycle cost of the PWR-S&B energy system is about 0.60 cents/kWe-h versus about 0.73 cents/kWe-h for the PWR-ABR system. In fact, The fuel cycle cost of PWR-S&B system is even lower than that of current PWRs -- 0.68 cents/kWe-h.

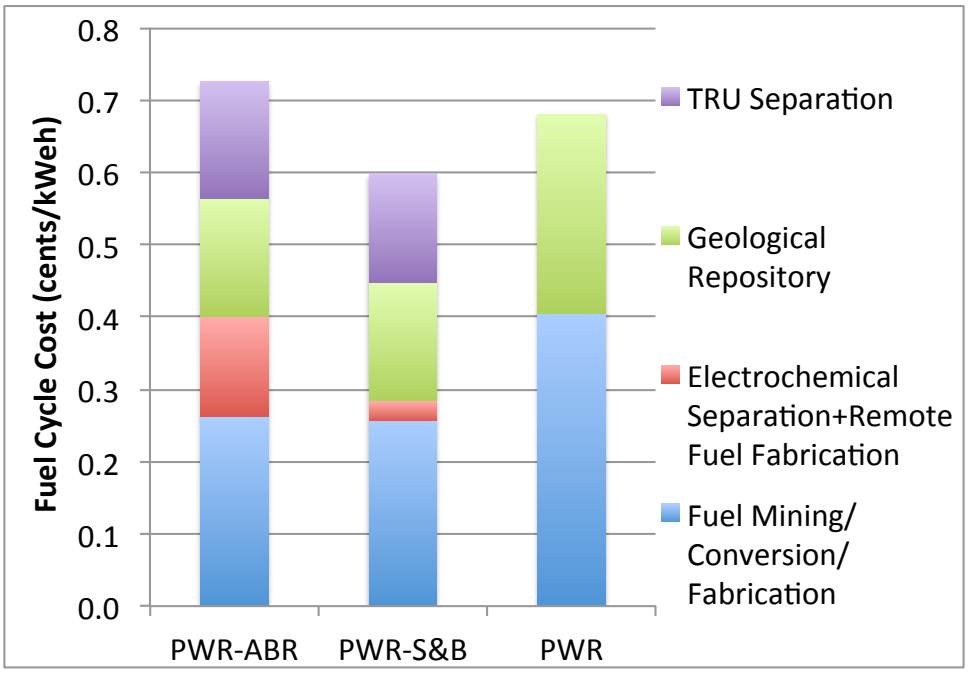

Figure 7-2 Fuel cycle cost of PWR-ABR, PWR-S&B, and PWR

7.5. Waste management analysis: radioactivity and radiotoxicity

7.5.1. Radioactivity

Radioactivity of UNF and High Level Waste (HLW) was quantified at short term (10 years) and long term (100,000 years) after the fuel is discharged from the core. The fresh fuel loaded into the equilibrium cycle of each core was depleted using ORIGEN2.2 up to the average discharge burnup to get an estimation of the concentration of those isotopes that were not tracked in the MCNP neutronics model for full core analysis; the cross-sections used for depletion calculation are prepared by MocDown; the depletion time in ORIGEN2.2 is the total residence time of the fuel; the flux magnitude is determined by the target average burnup. Then, the waste characteristics, like isotopic inventories, radioactivity and the decay heat of the discharged fuel were calculated with ORIGEN2.2 accounting for 879 fission products and 128 actinides. It was assumed that 1% of the heavy metals are lost during reprocessing and 0.2% is lost during fuel fabrication and get into the HLW stream.

Figure 7-3 compares the radioactivity of UNF+HLW at 10 and 100,000 years after discharge. In the short term, fission products contribute most of the radioactivity. The

higher radioactivity of the FPs from the PWR is mainly attributed to the lower thermal efficiency compared with the fast reactors. In addition, ^{235}U fissions yield FPs with higher radioactivity than those from ^{239}Pu fissions but this makes a small difference. The disposal of ^{233}U discharged from the thorium blanket of the S&B core has no significant effect on the radioactivity in the short term because ^{233}U has a very long half-life of 159,200 years. In case of the reference PWR that operates on the once-through fuel cycle, the disposal of plutonium (mainly ^{241}Pu) contributes notable radioactivity to the waste repository.

In the long term, fuel discharged from the thorium blanket is the predominant contributor to the higher radioactivity relative to the reference PWR. The long-life ^{233}U($T_{1/2}$=159,200years) decays into highly radioactive nuclides such as ^{209}Pb($T_{1/2}$=3.253hours), ^{213}Bi($T_{1/2}$=45.59minutes), ^{217}At($T_{1/2}$=32.3ms), ^{221}Fr($T_{1/2}$=4.777minutes), ^{225}Ra($T_{1/2}$=14.9days), ^{225}Ac($T_{1/2}$=9.92days), and ^{229}Th($T_{1/2}$=7,932years); these isotopes have equal contribution to the radioactivity since the decay daughters of ^{233}U have relatively short half-life. The discharged plutonium and minor actinides from the PWR-ABR and the PWR undergo substantial decay by 100,000 years.

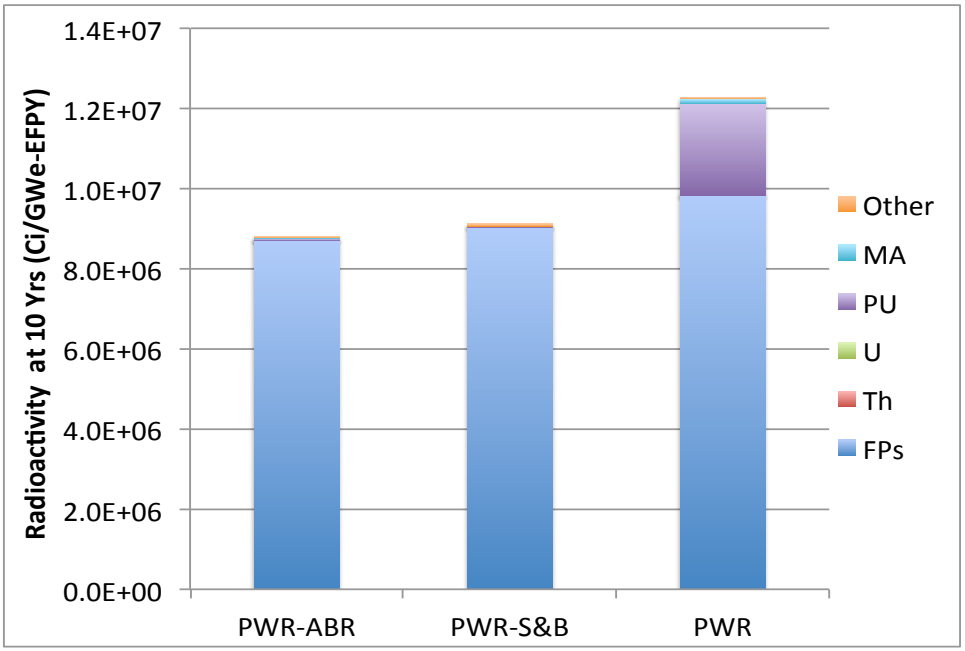

(a)

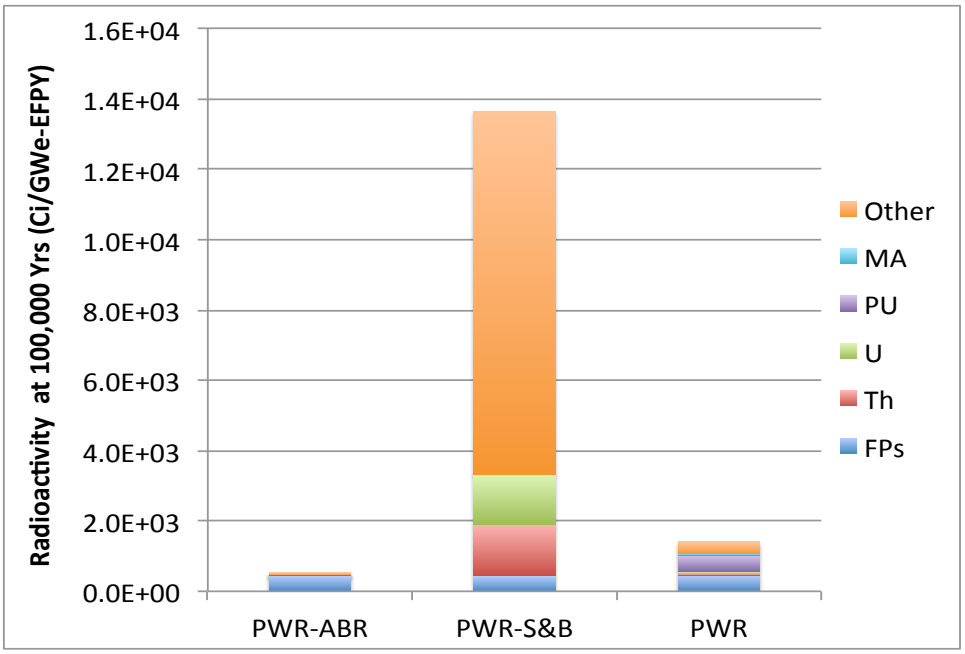

(b)

Figure 7-3 Radioactivity of UNF+HLW at 10 years (a) and 100,000 (b) years

7.5.2. Inhalation and ingestion radiotoxicity

The inhalation radiotoxicity and ingestion radiotoxicity of the UNF+HLW were calculated by considering different types of radiation on different parts of the human body. The values of the radioactivity were weighted by the inhalation and ingestion conversion factors (207 fission products and 91 actinides from [88]). The effective inhalation/ingestion coefficients were applied for a typical adult member of the public; median aerodynamic (diameter = 1 μm) radionuclides are inhaled into the blood stream via the lungs. Typical ranges of inhalation/ingestion conversion factors [88] are shown in Table 7-2. In general, the alpha-emitters heavy metals tend to contribute more radiation damage than most low atomic mass elements (like FPs) that are mostly beta-emitters. The actinides inhaled through lungs are far more hazardous than ingested via stomach [89].

Table 7-2 Range of Inhalation and Ingestion Dose Conversion Factors (Sv/Bq)

Isotope	Inhalation	Ingestion
Actinides	1.E-5 – 1.E-4	1.E-7 – 1.E-6
FPs	1.E-10 – 1.E-8	1.E-10 – 1.E-8

Figure 7-4 compares the inhalation radiotoxicity of the UNF and HLW at 10 and 100,000 years. ^{238}Pu, ^{244}Cm, ^{241}Pu, and ^{241}Am are the predominant contributors to inhalation radiotoxicity at 10 years. As the PWR disposes its plutonium and minor actinides directly, its short-term inhalation radiotoxicity is the highest. The fuel discharged from the driver of the S&B core and from the ABR core is reprocessed and only 1.2% of heavy metals get into the geological repository such that the total inhalation radiotoxicity of the PWR-S&B and the PWR-ABR systems are similarly low. The ^{233}U disposed from the thorium blanket of the S&B core contributes very small amount to the short-term inhalation radiotoxicity. However, by 100,000 years, ^{238}Pu, ^{244}Cm, ^{240}Pu, and ^{241}Am decayed out while ^{229}Th — a decay daughter of ^{233}U — that is a strong alpha-emitter with half-life time of 7932 years becomes the major contributor to the inhalation radiotoxicity of the PWR-S&B system. The PWR-ABR system exhibits by far the lowest inhalation radiotoxicity at 100,000 years due to its closed fuel cycle and absence of ^{233}U.

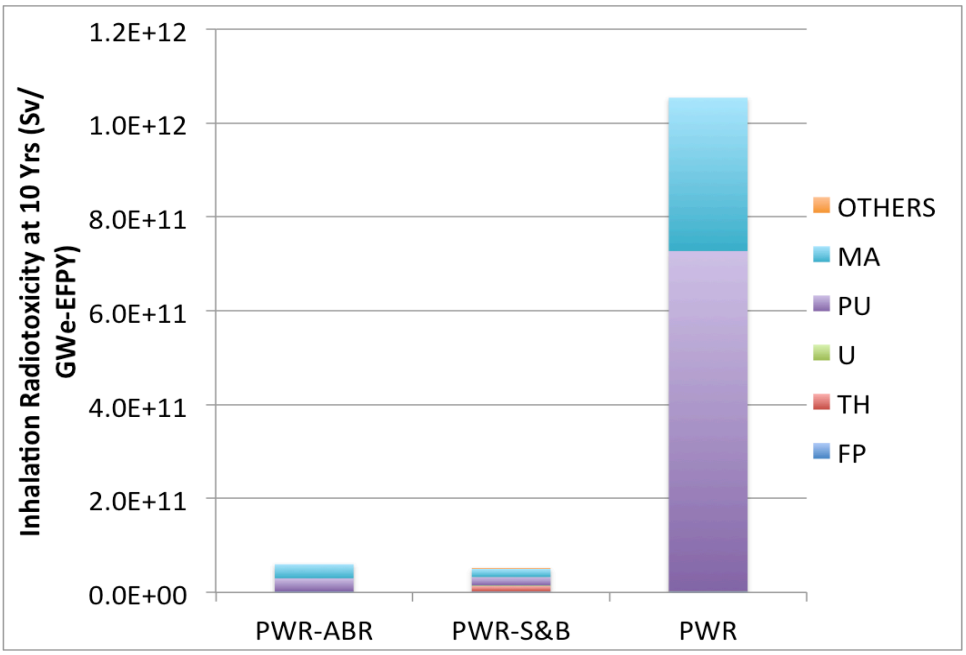

(a)

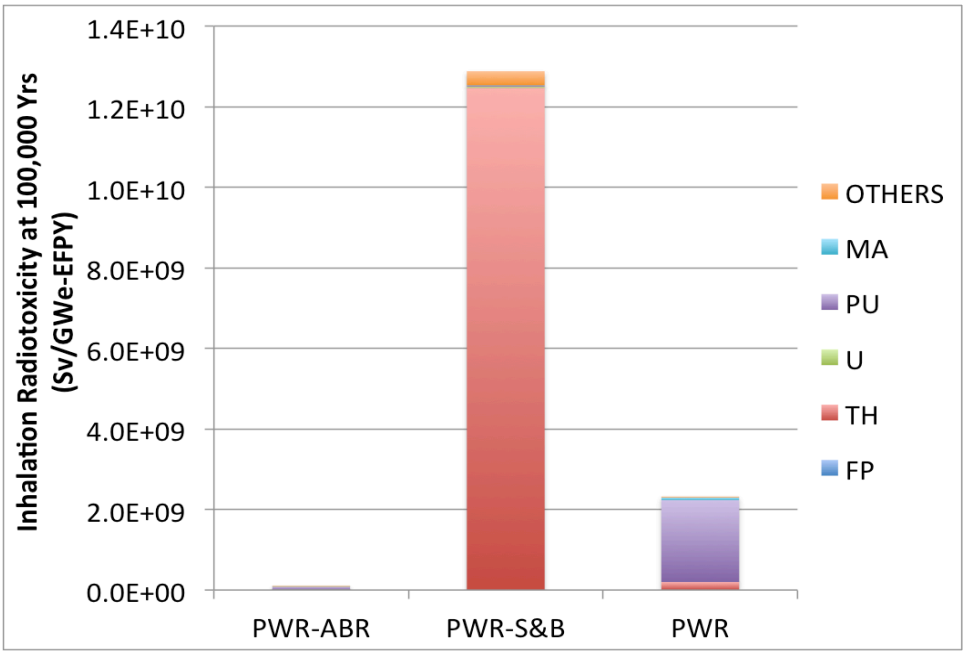

(b)

Figure 7-4 Inhalation radiotoxicity of UNF+HLW at 10 years (a) and 100,000 years (b)

As the ingestion conversion factors of actinides are generally smaller than the inhalation ones by a factor of 100, fission products dominate the short-term ingestion radiotoxicity again (shown in Figure 7-5). The comparison of ingestion radiotoxicity shows consistent trends with the radioactivity at 10 years. As most fission products decay out with relatively short half-life, heavy metals in the waste stream become the main contributors at 100,000 years. The disposal of the thorium blanket fuel contains significantly hazardous nuclides including ^{229}Th, the decay daughter of ^{233}U, so the total value of the PWR-S&B system ingestion radiotoxicity is much higher than of the other two systems.

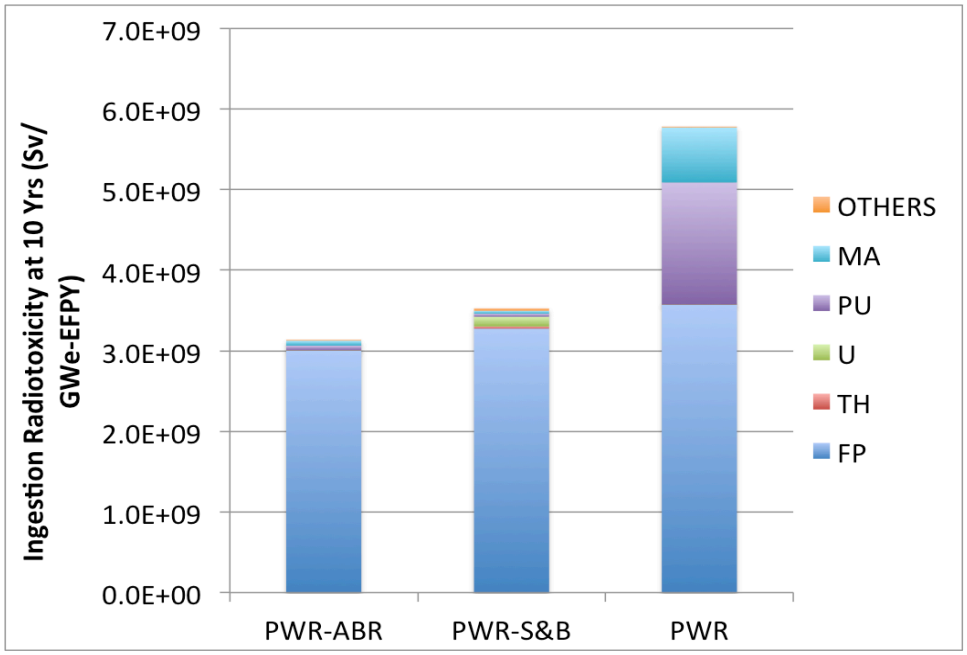

(a)

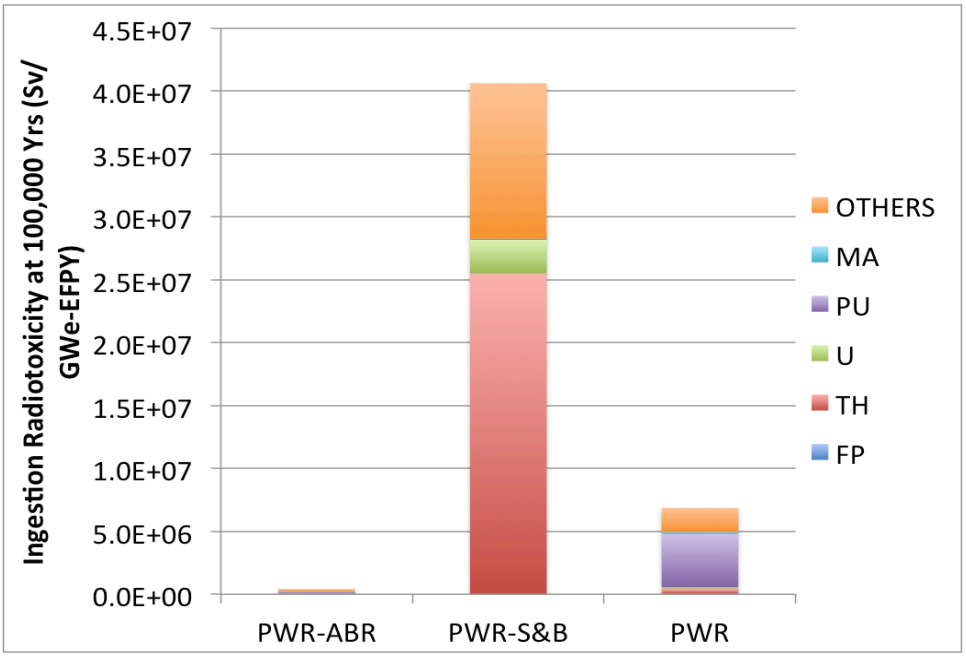

(b)

Figure 7-5 Ingestion radiotoxicity of UNF+HLW at 10 years (a) and 100,000 years (b)

7.6. Resource utilization

Table 7-3 compares the natural resources required per unit of electricity generated from the PWR-ABR, the PWR-S&B, and the PWR energy systems. Contemporary PWRs operate on once-through fuel cycle and can only fission about 0.6% of the natural uranium. It requires the largest amount of natural uranium per unit of electricity generated. Stage 2 of the 2-tier systems practically fissions all the TRU discharged from the PWR and contributes one third of the total power; this effectively increases the natural uranium utilization to ~1%. The blanket in the S&B core can utilize 7% of thorium resource without development of irradiated thorium fuel reprocessing technology; this is a factor of ~12 higher than the utilization of natural uranium in current PWRs. Overall, the improvement in resource utilization being offered by either the ABR or S&B transmuting reactors is small; a large fraction of uranium is discarded from the Stage-1 PWRs. Much higher fuel utilization is offered by self-sustaining reactors such as the ARR and the S&B core designed to have a CR=1 seed (examined in Section 3.1).

Table 7-3 Resource Utilization of PWR-ABR, PWR-S&B, and PWR

Property	PWR-ABR	PWR-S&B	PWR
Natural uranium required per energy generated, t/GWe-EFPY	117.2	109.6	181.1
Natural thorium required per energy generated, t/GWe-EFPY	0.0	3.0	0.0

By softening the blanket spectrum it is possible to significantly increase the thorium fuel utilization in the once-through blanket to more than 35 times the utilization of natural uranium in PWRs. These options are elaborated upon in Chapter 8.

7.7. Proliferation resistance and nuclear material security

The proliferation resistance is evaluated based on the plutonium inventory, fissile plutonium fraction, specific decay heat and spontaneous fission rate of the recovered plutonium, ^{238}Pu/Pu ratio, and ^{232}U/^{233}U ratio. ^{238}Pu, ^{240}Pu, and ^{242}Pu have high spontaneous fission rate which reduces the bomb yield significantly; ^{238}Pu also has a large decay heat to further complicate the design of an explosive device [9, 10]. In addition, Material Attractiveness is applied to quantify the proliferation resistance of the recovered plutonium considering critical mass, heat generation, dose rate, and intrinsic fission neutron production rate. The procedure for calculating the Material Attractiveness is described in [11]. Material for which Material Attractiveness <0 is considered as unattractive for weapons; 0< Material Attractiveness <1 is unattractive but theoretically

applicable for weapon; 1< Material Attractiveness <2 is attractive; and Material Attractiveness >2 is highly attractive.

Table 7-4 compares the proliferation resistance metrics of the three cores. The driver fuel in the S&B core is designed to have TRU CR ratio of 0.0 so its plutonium loading is much higher than of the other two cores. However, the fuel discharged from the S&B driver has the lowest fissile plutonium fraction due to its higher discharge burnup. Also due to the higher cumulative burnup, the ^{238}Pu/Pu ratio — 6.1%, is much higher than that in the ABR — 4.1%, and PWR — 3.0%. Of the three cores, the plutonium recovered from the S&B core is the least attractive; the present PWRs generate highly attractive plutonium when pre-initiation is not an issue (Material Attractiveness >2).

The thorium fuel cycle seems not to be more proliferation resistant than the uranium fuel cycle [90]. ^{233}U is applicable for weapon-use because the critical mass of ^{233}U is close to that of ^{239}Pu while spontaneous fission rate is much lower [91]. Nevertheless, the decay chain of co-product ^{232}U generates penetrating 2.6 MeV gamma rays from ^{208}Tl and can make ^{233}U a less desirable weapon material. It is very difficult to separate ^{232}U from ^{233}U due to the close atomic mass. ^{232}U decays to ^{228}Th with a half-life of 68.9 years. ^{228}Th has a half-life of 1.9 years and it practically decays into ^{208}Tl immediately as the decay daughters of ^{228}Th have very short half-life. After the in-growth of ^{208}Tl, the dose rate from ^{233}U containing 1 ppm ^{232}U is about the same as from reactor-grade plutonium [91]. The Material Attractiveness of ^{233}U with initial concentration of ^{232}U at 3200 ppm is similar to that of reactor-grade plutonium after 10 years cooling [11]. In order to achieve the IAEA criterion for self-protection of 100-rem per hour at 1 meter [92], the level of ^{232}U needs to be 2.4% [91].

The breed-and-burn thorium blanket has an intrinsic proliferation resistance as the discharged fuel is not required to be reprocessed. A recent study [93] by Los Alamos National Laboratory concludes that dilution with ^{238}U or ^{232}Th reduces the attractiveness of the material to a sub-state actor. With >80% ^{238}U or >70% ^{232}Th, the material is unattractive; therefore, if ^{233}U is not separated, the UNF from the thorium blanket of the PWR-S&B system is unattractive for weapon-use. The fuel discharged from the S&B core blanket has ^{232}U/^{233}U ratio of 2233 ppm, well above the contamination level that remote production operations would be required to extract ^{233}U on a large scale without incurring large occupational dose [91]. ^{233}U could be isotopically “denatured” by adding depleted uranium to the thorium feed or the spent thorium fuel to further improve the proliferation resistance of the fuel discharged from the thorium blanket; this option is demonstrated in Section 8.4.

Table 7-4 Proliferation Resistance Metrics of the ABR, the S&B and the PWR After 5 Years' Cooling Time

Property	ABR	S&B (seed/blanket)	PWR
Fissile plutonium fraction, %	46%	29%/-	63%
^{238}Pu/Pu ratio, %	4.1%	6.1%/-	3.0%
Specific decay heat of plutonium, W/kg	26.94	38.47/-	20.54
Spontaneous fission neutrons per kg Pu, n/sec-kg	6.5E+05	9.00E+05/-	4.4E+05
Tot. plutonium reprocessed, tons/GWe-EFPY	1.67	1.59/-	0.22
Pu/^{238}U ratio, %	40.6%	17127.7%/-	1.1%
Material Attractiveness of plutonium	1.92	1.69/-	2.09
^{232}U/^{233}U ratio, ppm	-	-/2233	-
Fissile U/U ratio, %	-	-/91%	0.7%
Fissile U/Th ratio, %	-	-/8%	-
(Pu+fissile U)/(^{238}U+Th) ratio, %	41%	17271%/8%	2%

Chapter 8

8. New Fuel Cycle Options Enabled by the S&B Concept

This chapter introduces a few new fuel options for the blanket of the S&B core. These include fueling the B&B blanket by either thorium hydride fuel, Fully Ceramic Microencapsulated (FCM) fuel, thorium dioxide fuel or PWR spent nuclear fuel for the improved fuel utilization; thorium fuel could be denatured by depleted uranium for the purpose of better proliferation resistance. Several new fuel cycle schemes enabled by the S&B core concept are also presented and discussed.

8.1. Thorium hydride fuel in the blanket of the S&B core

U-$ZrH_{1.6}$ fuel developed by Dr. Massoud Simnad has being successfully used for over 40 years in TRIGA type research reactors around the world with no safety problems [94-96]. Six hydride-fueled space reactors were built and operated, and one was placed in earth orbit for the Space Nuclear Auxiliary Power (SNAP) project [97]. It has been suggested that U-ThH_2 fuel is even more stable than U-$ZrH_{1.6}$ fuel and can operate at higher temperatures [98].

The feasibility analysis of the thorium hydride fuel in fuel self-sustaining SFR was conducted (Appendix-A). The proposed thorium-hydride fueled reactor is, essentially, a Sodium-cooled Fast Reactor (SFR) with a relatively softer spectrum. The hydrogen-to-thorium atom ratio (H/Th) is determined by, primarily, neutronics optimization and safety analysis. It is found that the SFR fueled with thorium hydride (H-to-Th ratio of 0.5) has intermediate spectrum. Due to the softer neutron spectrum, a large 3000 MWt SFR can be designed with sodium void worth of $1.15 at BOEC; the corresponding value for same SFR fueled by thorium dioxide is $8.41. The Doppler coefficient of thorium hydride fueled SFR is five times more negative than the value of thorium dioxide fueled SFR. The achievable burnup of such thorium hydride fueled SFR is only 3.3% FIMA and this is much smaller compared with typical SFR – average burnup of ARR fueled by thorium dioxide is 111 MWd/kg [99].

Nevertheless, the thorium blanket fueled by thorium hydride in the S&B configuration core can be driven by the excess neutrons from the seed and eventually discharge its fuel at very high burnup without fuel reprocessing. By incorporating hydrogen in the fuel, the neutron spectrum is an intermediate spectrum -- significantly softer than that of conventional fast reactors but harder than that of thermal reactors. The SFR is expected to have less radiation damage per unit of burnup and the blanket fueled by thorium hydride is able to discharge the fuel at very high resource utilization without fuel reprocessing.

Table 8-1 shows the performance characteristics of the thorium hydride fuel in the S&B core. The reference S&B core is the "ultra-long" case discussed in Section 4.3. Without violating the radiation damage constraint of 200 DPA, the thorium hydride fueled blanket can be irradiated up to an average burnup of 191.8 MWd/kg -- about three times higher than that of the metallic thorium fueled blanket – 65.0 MWd/kg and can generate about 49.9% of the core power – slightly higher than generated from the metallic thorium fueled blanket. Due to the softer neutron spectrum in the thorium hydride blanket, the seed region can discharge its fuel at relatively higher burnup and the reprocessing capacity per unit of electricity generated is reduced to 1240.1 kg/GWth-yr. The sodium void worth of the S&B core with thorium hydride fuel is less positive and the Doppler coefficient is fifteen folds more negative than of the reference core with metallic thorium.

A thorough parametric study is required to identify the optimal H-to-HM ratio and thorium-hydride blanket designs. These should be followed by assessing the feasibility of achieving adequate shutdown margin, a thorough safety analysis, fuel performance analysis, and a more thorough comparison between the thorium hydride fuel and metallic thorium fuel in SFR designs.

Table 8-1 Performance Characteristics of Thorium Hydride Fuel in the S&B Core

		Ultra Long	Thorium Hydride in S&B
		Seed/Blanket	Seed/Blanket
Fuel form		U-TRU-10Zr/Th	U-TRU-10Zr/ThH0.5
Target TRU CR of seed		CR=0.5	CR=0.5
Number of assemblies			
	Inner blanket	42	19
	Seed	61	61
	Outer blanket	168	191
Number of batches			
	Inner blanket	1	2
	Seed	1	5
	Outer blanket	2	20
P/D ratio		1.261/1.151	1.212/1.208
Permissible assembly power (MWth)		12.3/7.3	10.1/9.9
Fraction of max. permissible		0.96/0.99	0.90/0.89
Core power (MWth)		1000	1000
Cycle length (EFPD)		2630	700
Tot. residence time (EFPD)		2630/7890	3500/15400
k_{eff} at BOEC		1.039±0.001	1.038±0.001

k_{eff} at EOEC	1.004±0.001	1.010±0.001
Burnup reactivity swing (%Δk/k)	-3.39	-2.73
Burnup reactivity swing rate (%Δk/k /EFPY)	-0.47	-1.42
Average blanket power fraction	42.5%	49.9%
Average discharge burnup (MWd/kg)	123.2/65.0	147.3/191.8
Peak radiation damage (DPA)	175/204	190/209
TRU/HM at BOEC (wt%)	29.9	29.2
Seed CR at BOEC	0.46	0.50
HM at BOEC (tons)	12.3/51.4	11.9/38.6
Specific power (MWt/tHM)	46.8/8.3	42.1/13.0
TRU feed rate (kg/EFPY)	93.2/0.0	80.8/0.0
DU feed rate (kg/EFPY)	117.0/0.0	101.0/0.0
Thorium feed rate (kg/EFPY)	0.0/2386.0	0.0/950.4
Trans-Th feed rate (kg/EFPY)	0.0/-174.5	0.0/-80.6
Reprocessing capacity (kg/GWt/Yr)	1703.6	1240.1
Safety Parameters at BOEC		
Sodium void worth ($)	7.55±0.06	4.13±0.06
Doppler coefficient (¢/°C)	-0.03±0.02	-0.45±0.02

8.2. FCM fuel for the blanket of the S&B core

The objective of the Laser Inertial Fusion Energy (LIFE) project initiated by Lawrence Livermore National Laboratory (LLNL) and active until few years ago [100, 101] was using fusion neutrons to drive a subcritical blanket fueled with pebbles containing TRistructural-ISOtropic (TRISO) particles in a breed-and-burn mode of operation. The rationale for selecting this fuel type is the experimental evidence that TRISO fuel particles can withstand very high burnup without releasing their fission products. In addition, TRISO particles make a chemically stable waste form that promise to maintain its integrity in a high level waste repository for a long time. More recently, the Fuel Cycle Evaluation and Screening conducted by the Department of Energy [18] considered a number of variants of the LIFE reactor concept. Specifically, 3 out of the 40 or so Evaluation Groups (EG) – EG06, EG07 and EG08, are subcritical cores (or "blankets") fueled by either thorium or natural uranium that are driven to very high burnup by an external neutron sources. The attractive feature of all these concepts is that they are to extract a significant fraction of the energy value of the natural resource without fuel enrichment and reprocessing.

The objective of this study is to assess the neutronic feasibility of using excess neutrons from fast fission reactors instead from fusion or accelerator driven spallation neutron sources to drive the subcritical breed-and-burn blanket to very high burnup. Specifically it is proposed to use the recently conceived Seed-and-Blanket (S&B) Sodium-cooled Fast Reactor (SFR) core configuration [86] for this application.

Instead of pebbles used for the LIFE project [100, 101] it is proposed to use Fully Ceramic Microencapsulated (FCM) fuel consisting of TRISO fuel particles embedded in Silicon Carbide (SiC) matrix [102]. The SiC matrix has good thermal conductivity, can withstand high fast neutron fluence and is environmentally stable [103]. FCM fuel has been developed by the Oak Ridge National Laboratory to improve the accident tolerance of Light Water Reactors (LWRs) fuel [103, 104].

8.2.1. Model

The S&B core used in this study is that described in Section 4.3. The seed fuel used is the ternary metallic U-TRU-10wt%Zr with theoretical density of 15.7 g/cc and a smear density of 75%. The blanket is fed with FCM fuel made of thorium containing TRISO particles of the following dimensions [105]: 800 μm diameter fuel kernels; 75 μm carbon buffer layer; 20 μm thick Inner Pyro-Carbon (IPyC) and Outer Pyro-Carbon OPyC; 40 μm SiC layer. The TRISO particles packing fraction in the SiC matrix is 45%. ThN is selected for the TRISO kernel fuel for this study as it offers the highest heavy metal loading of candidate ceramic thorium compounds (Table 8-2).

Table 8-2 Theoretical Density (TD) and Heavy Metal (HM) Density of Candidate Fuel [99, 106]

Fuel	TD (g/cc)	HM Density (g/cc)
ThO_2	10.0	8.8
ThC	10.6	10.1
ThC_2	9.6	8.7
ThN	11.9	11.2

The low-swelling ferritic martensitic steel HT-9 is selected as the structural and cladding material for the seed region while SiC is used for the blanket fuel cladding material; the blanket assembly ducts are made of HT-9. The transverse dimensions of the hexagonal fuel assemblies and effective outer diameter of the active core are those of S-PRISM [44]. The effective core height is 250 cm and its effective diameter is 270 cm. A 1.9 m long fission gas plenum is located above the driver fuel; no plenum is required for the blanket fuel as the fission products are retained by the TRISO particle coatings. The

number of fuel rods per assembly and the rods diameter are design variables; they are adjusted to meet the pressure drop and peak temperatures constraints.

The core is divided into variable number of seed and blanket radial zones. Each radial zone is further divided into 6 axial nodes for burnup calculations. Both seed and blanket are operating using multi-batch fuel management; a fraction of the seed fuel, typically between 1/3 and 1 is discharged after each cycle. The heavy metal discharged from seed is fully recovered and a mixture of depleted uranium and TRU from LWR's Used Nuclear Fuel (UNF) is added as the make-up fuel. Fresh ThN FCM fuel is charged to the outermost blanket batch and the blanket batch is gradually shuffled inward after each cycle. The batch closest to the seed outer boundary is shuffled to the batch location closest to the seed inner boundary. At end of cycle, the innermost batch of the internal blanket is discharged and stored.

8.2.2. Computational methodology for FCM fuel

As the neutron mean free path in typical SFR is larger than the lattice pitch, it is common to represent each burnup node for neutronic analysis as homogenized – the fuel, cladding, other structural material and coolant are mixed by their volume fractions. The results obtained using a homogenized SFR core model are usually in acceptable agreement with those obtained using a heterogeneous mode [33, 54]. The use of the homogenized model significantly saves computational time. As the FCM fuel features double-heterogeneity and includes significant amount of low Z material (SiC), a study was performed for a single fuel pin model to quantify the significance of the self-shielding effect on such system. The simulation of an infinite unit cell is implemented with SERPENT 2.1.11 [107]. Figure 8-1 compares the infinite multiplication factor as a function of burnup obtained using three infinite unit cell models: (1) explicit model of TRISO particles, SiC matrix, cladding, and coolant; (2) homogenized TRISO particles and SiC matrix fuel; (3) fully homogeneous unit cell model. The homogenized model underestimates k_∞ below 10 MWd/kg because the fast fission probability of thorium is underestimated; at low burnup thorium contributes the majority of the fissions. As the ^{233}U concentration builds up with burnup, the homogenized models overestimate the ^{233}U breeding and, hence, k_∞ because the self-shielding effects are more pronounced on the fuel particles level as well as on the unit cell level. Starting from about 100 MWd/kg, the overestimation of k_∞ in the homogeneous models becomes burnup independent -- ~400 pcm for the partial homogenized and 800 pcm for the fully homogenized unit cell. In order to reduce the computational effort for this preliminary feasibility study, the fully homogeneous model is used and a bias of 800 pcm is applied requiring k_{eff} at EOEC to be at least 1.008.

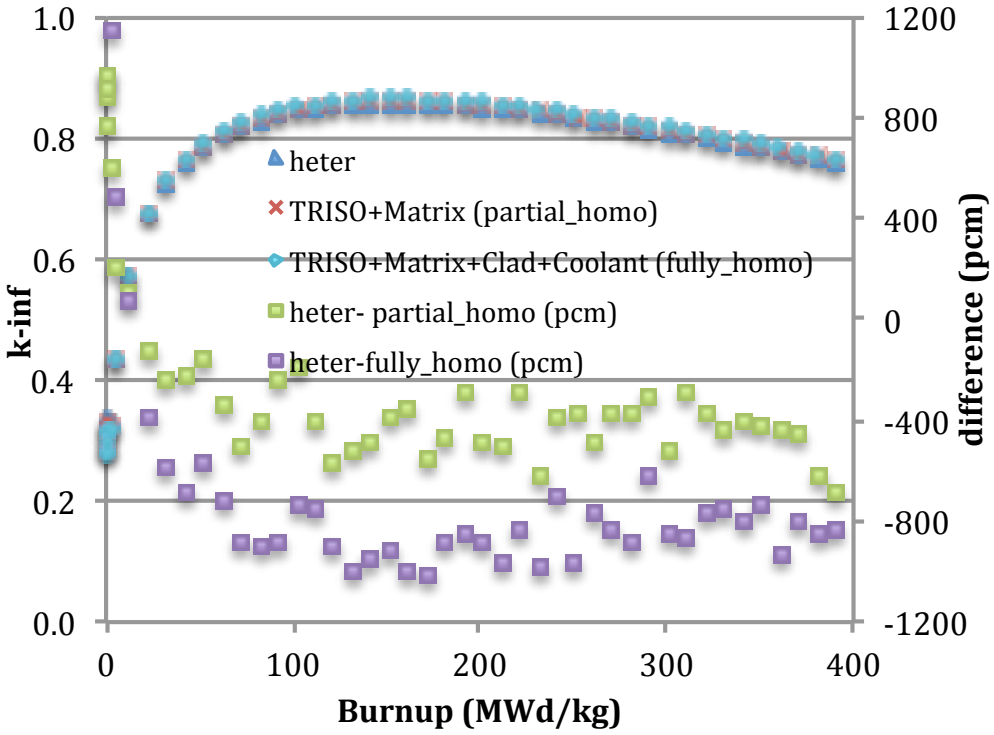

Figure 8-1 Comparison of the infinite multiplication factor as a function of burnup for different unit cell models

8.2.3. Neutron balance of thorium in FCM fuel

The performance of the ThN FCM fueled blanket in an S&B core is compared to that of a reference metallic thorium fueled blanket [84]. Figure 8-2 compares the k_∞ and neutron balance evolution with burnup of the two blanket compositions that are represented by a homogenized unit cell subjected to reflective boundary conditions. The same volume fractions were assumed for the two unit cells: 37.5%/12.5%/22.0%/28.0% for the fuel/gap/cladding/ coolant. The cladding for the FCM fuel is SiC.

Due to the significantly lower heavy metal loading and softer neutron spectrum, the k_∞ of the FCM fueled blanket is smaller than that of the metallic Th fueled blanket and never reaches unity. Therefore, more external neutrons will be required to drive the FCM blanket to a given burnup; this number is represented by the neutron balance plot on Figure 8-2; it measures the net cumulative number of excess neutrons generated per unit volume of blanket fuel as a function of burnup [34]. For example, the number of excess neutrons from seed required to drive the blanket fuel to a burnup of 20% FIMA is ~7×10^{21} n/cm^3 of the FCM blanket versus ~2×10^{21} n/cm^3 of the metallic Th blanket.

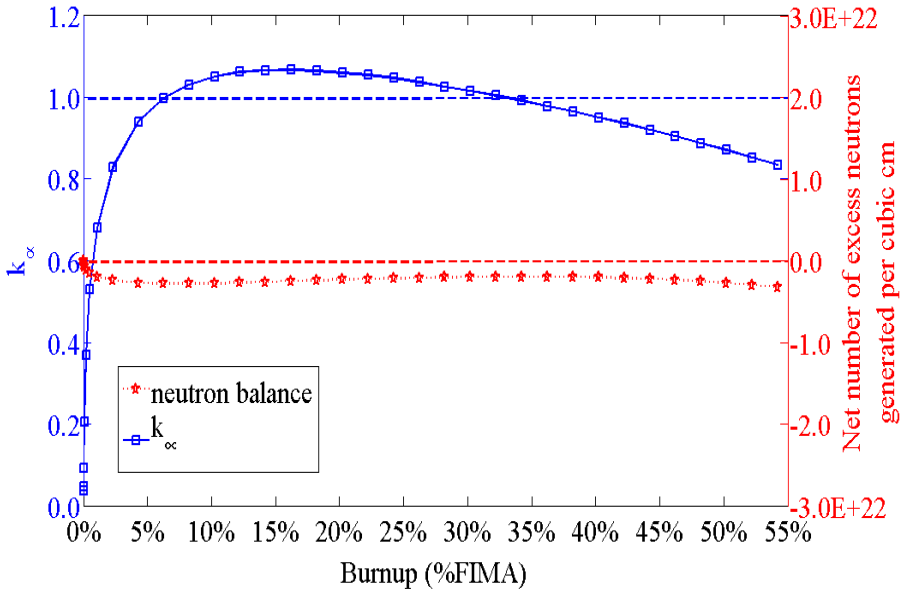

(a)

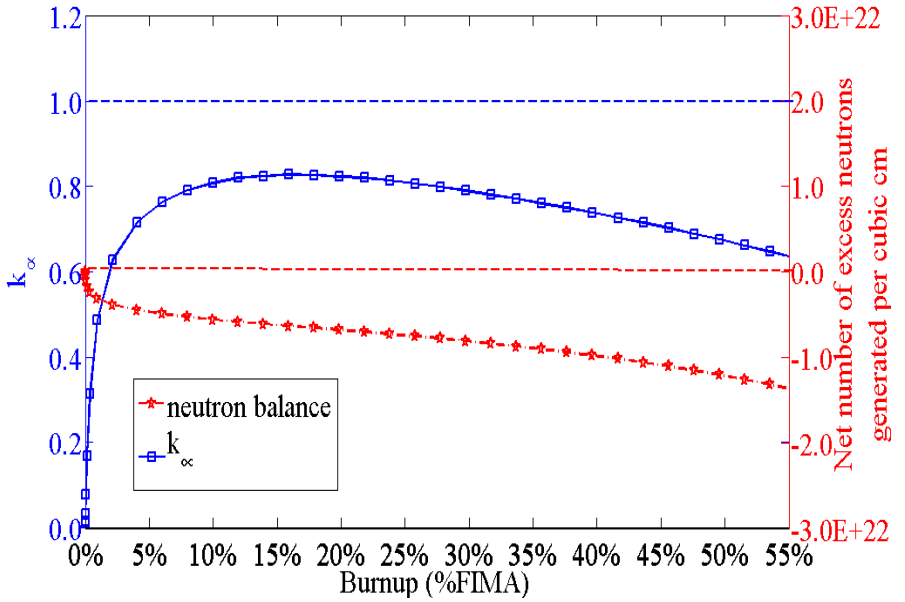

(b)

Figure 8-2 k_∞ and neutron balance evolution with burnup of metallic Th (a) and ThN FCM (b) fueled unit cells

8.2.4. Full core analysis

Table 8-3 compares selected design and performance between the S&B core with FCM blanket and the metallic Th fueled Ultra Long Cycle (ULC) (Section 4.3). The FCM fueled blanket is initially designed with the target discharge burnup of 240 MWd/kg since the k_∞ in Figure 8-2 starts decreasing from ~20%FIMA. The seed of both cores are designed to have a conversion ratio of ~0.5. However, as the FCM blanket contributes less to the core reactivity than the metallic Th blanket, its seed needs to be loaded with more fuel. For the same reason, the FCM blanket reactivity gain over the cycle does not compensate as much for the seed reactivity loss. As a result, the burnup reactivity swing per year for the FCM blanket core is about 4 times that of the ULC core and the seed has to use a 5-batch fuel management scheme and a smaller but acceptable cycle length of 750 EFPD. One third of core power is generated, at the equilibrium cycle, by the FCM blanket. This is smaller than the 42.5% that the metallic thorium blanket generates in the ULC core but quite significant. On the other hand, the FCM blanket requires about one fifth of the HM inventory and offers nearly quadruple thorium burnup -- fuel utilization. Moreover, due to the softer spectrum near the interface between the seed and blanket in the FCM core (Figure 8-3) and slightly higher TRU/HM ratio, the seed discharge burnup -- 190.6 MWd/kg, is higher versus 123.2 MWd/kg (or 137.3 MWd/kg if normalized to the same DPA value of 195). Due to the higher discharge burnup the reprocessing capacity required for the seed of the FCM core is somewhat smaller per unit of core energy. The radial power density distribution across the FCM core is displayed in Figure 8-4. The power density peaks at the interface with the inner blanket but its magnitude is easily manageable in Sodium-cooled cores.

Table 8-3 Performance Characteristics of Metallic Fuel and FCM S&B Design

		ULC	FCM1	FCM2
		Seed/Blanket	Seed/Blanket	Seed/Blanket
Seed fuel form		U-TRU-10Zr/Th	U-TRU-10Zr/ThN FCM	U-TRU-10Zr/ThN FCM
Target TRU CR of seed		0.5	0.5	0.5
Number of assemblies				
	Inner blanket	42	40	40
	Seed	61	71	71
	Outer blanket	168	160	160
Number of batches				
	Inner blanket	1	2	2

Seed	1	5	5
Outer blanket	2	8	18
P/D ratio	1.261/1.151	1.227/1.085	1.218/1.072
Permissible assembly power (MWth)	12.3/7.3	10.8/4.2	10.4/3.6
Fraction of max. permissible	0.96/0.99	0.93/0.90	0.95/0.85
Core power (MWth)	1000	1000	1000
Cycle length (EFPD)	2630	750	750
Tot. residence time (EFPD)	2630/7890	3750/7500	3750/15000
k_{eff} at BOEC	1.039±0.001	1.047±0.001	1.051±0.001
k_{eff} at EOEC	1.004±0.001	1.009±0.001	1.006±0.001
Burnup reactivity swing (%Δk/k)	-3.39	-3.60	-4.17
Burnup reactivity swing rate (%Δk/k /EFPY)	-0.47	-1.75	-2.03
Radial leakage probability from seed at MOEC	30.4%	22.1%	22.7%
Average blanket power fraction	42.5%	33.7%	34.5%
Average discharge burnup (MWd/kg)	123.2/65.0	190.6/241.2	185.0/481.5
Peak radiation damage (DPA)	175/204	195/-[9]	187/-
TRU/HM at BOEC (wt%)	29.9	31.7	31.6
Seed CR at BOEC	0.46	0.50	0.50
HM at BOEC (tons)	12.3/51.4	13.0/9.9	13.3/9.1
Specific power (MWt/tHM)	46.8/8.3	51.0/34.0	49.3/38.0
TRU feed rate (kg/EFPY)	93.2/0.0	108.7/0.0	107.7/0.0
DU feed rate (kg/EFPY)	117.0/0.0	130.8/0.0	129.0/0.0
Thorium feed rate (kg/EFPY)	0.0/2386.0	0.0/510.3	0.0/261.4
Trans-Th feed rate (kg/EFPY)	0.0/-174.5	0.0/-65.9	0.0/-31.5
Reprocessing capacity (kg/GWt/Yr)	1703.6	1269.0	1293.0
Reprocessing capacity projected to 195 DPA (kg/GWt/Yr)	1528.9	1269.0	1240.0

[9] The peak fast fluence on FCM fuel is 2.61×10^{23} n(>0.1MeV)/cm^2

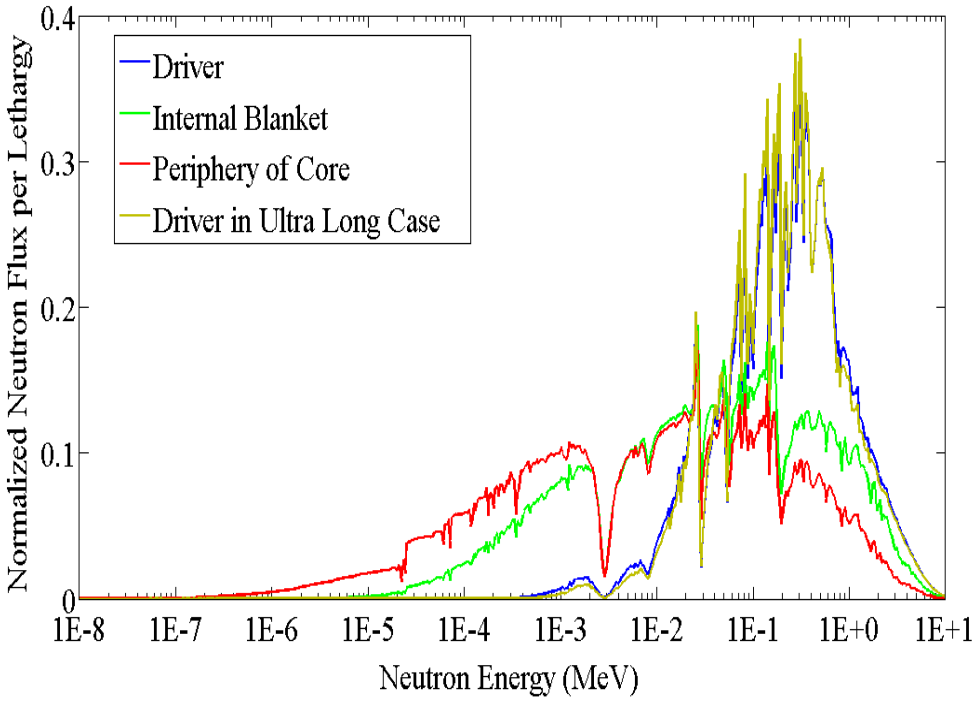

Figure 8-3 Comparison of neutron spectra between FCM1 and ULC cores

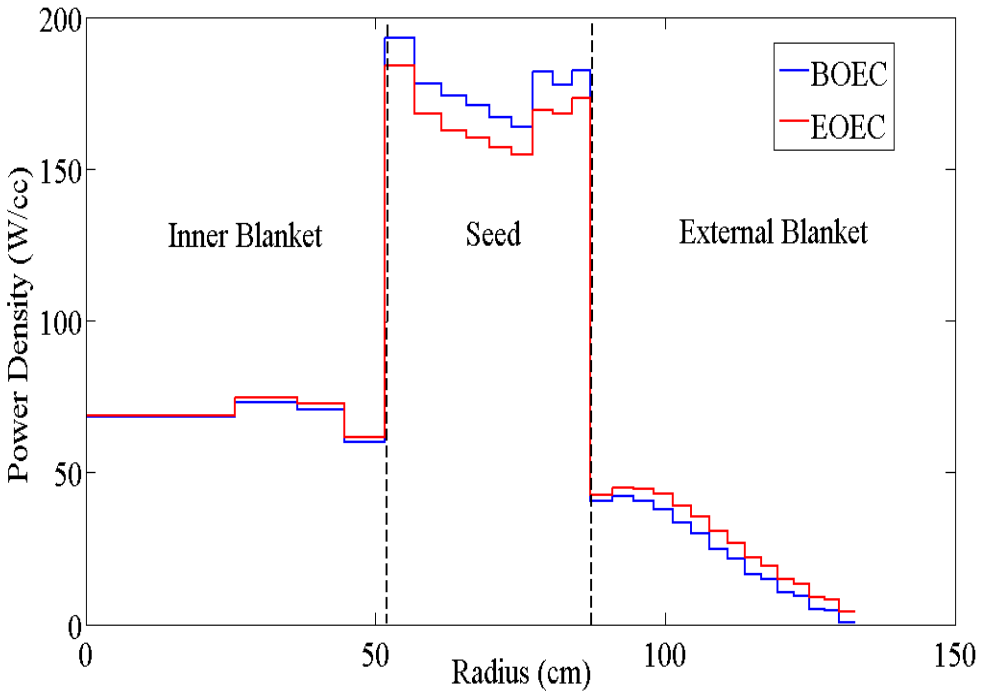

Figure 8-4 Radial power distribution across the FCM1 core

Table 8-4 compares safety related parameters of the two S&B cores. The seed of the FCM core has more positive sodium void worth – probably because more seed fuel is required. This is fully compensated by the smaller blanket feedback to the sodium void worth that is due to its softer neutron spectrum and smaller sensitivity of the blanket spectrum to sodium voiding. The Doppler coefficient of the FCM core is 10 times more negative due to its softer spectrum. This may challenge attaining adequate shutdown margin under cold zero power condition. The shutdown margin and reactivity coefficients due to axial and radial core expansion will be quantified in future study.

Table 8-4 Kinetic and Safety Related Parameters of the Metallic and FCM S&B Cores at BOEC

	ULC	FCM1	FCM2
Effective delayed neutron fraction	0.0032±0.0002	0.0031±0.0002	0.0032±0.0002
Sodium void worth ($)			
Seed only	5.90±0.06	7.26±0.06	7.10±0.06
Blanket only	1.05±0.00	0.00±0.06	0.14±0.06
Full core	7.55±0.06	7.30±0.06	7.33±0.06

Doppler coefficient (¢/°C)	-0.03±0.02	-0.34±0.02	-0.30±0.02

This preliminary study found that a thorium FCM fueled blanket can be driven by excess neutrons of a CR=0.5 seed up to the burnup of about 24% FIMA while generating one third of the S&B core power provided that the FCM fuel will be able to maintain its integrity and retain its fission products. This fuel utilization is four folds higher than that attainable with a metallic thorium fueled blanket in S&B cores and over 40 folds higher than the utilization of natural uranium in LWR. The neutronic analysis shows that the blanket fueled by FCM fuel can even achieve the discharge burnup of 481.5 MWd/kg (FCM2 case in Table 8-3); this is up to 80 folds higher than the utilization of natural uranium in LWR.

The study reported in Section 7.4 concludes that the fuel cycle cost of S&B SFR that uses metallic thorium blanket will be significantly smaller than that of a conventional SFR. Even though the fabrication cost of the FCM fuel will be probably higher than that of metallic fuel, the overall economic advantage of the S&B core is likely to be preserved when using FCM fuel because the HM inventory in the FCM fuel is one fifth that of metallic thorium blankets while its discharge burnup is much higher.

However, it is necessary to determine the radiation damage limit of the FCM fuel under the condition prevailing in the blanket of the S&B core before the feasibility of the proposed reactor concept could be reliably assessed.

8.3. Thorium dioxide fuel in the blanket of the S&B core

This section investigates the feasibility of the thoria fuel in the once-through blanket of the S&B core. Since oxide fuel is currently mature technology with well commercial experience, the thoria fuel is expected for early licensing. The spectrum in thoria fueled blanket is still fast but significantly softer [99] than the spectrum of the metallic thorium fueled blanket described in previous chapters. Without violating the 200 DPA constraint, the thoria fueled blanket driven by CR=0.5 seed fuel enables discharging the fuel at higher burnup. Same methodology is applied as previous studies with only one exception: thorium dioxide fuel (theoretical density of 10.0 g/cc [108] and the smeared density of 90%) is fed to the blanket.

Table 8-5 compares the core performance between the S&B core with thoria fueled blanket and the metallic Th fueled Ultra Long Cycle (Section 4.3). The seed of both cores are designed to have a conversion ratio of ~0.5. Since the oxide fuel has relatively softer neutron spectrum along with lower heavy metal density, the thoria blanket contributes less to the core reactivity than the metallic Th blanket. As a result, the burnup reactivity swing per year for the thoria blanket core is two times that of the Ultra Long core and,

therefore, the seed has to use a 2-batch fuel management scheme together with a smaller but acceptable cycle length of 1640 EFPD. 45.0% of the core power is generated by the thoria blanket at the equilibrium cycle and this is slightly higher than that generated by metallic thorium blanket. The seed discharge burnup – 164.0 MWd/kg, is higher versus 123.2 MWd/kg (or 145.0 MWd/kg if normalized to the same DPA value of 206); this is possibly attributed to the softer neutron spectrum coming back from the thoria blanket. The thoria blanket requires about 80% of the HM inventory and offers the thorium discharge burnup of 109.5 MWd/kg. The blanket with thoria can achieve the thorium resource utilization of about 18 times that of natural uranium in PWRs; this option requires no irradiated thorium fuel reprocessing and is based on oxide fuel for early licensing. The oxide fuel provides a softer neutron spectrum, which increases the Doppler effect by a factor of two and reduces the positive sodium void worth.

Table 8-5 Performance Characteristics of the S&B with Thorium Dioxide Fueled Blanket

	Ultra Long	Thorium Dioxide
Fuel form	Seed/Blanket U-TRU-10Zr/Th	Seed/Blanket U-TRU-10Zr/ThO_2
Target TRU CR of seed	CR=0.5	CR=0.5
Number of assemblies		
Inner blanket	42	35
Seed	61	61
Outer blanket	168	175
Number of batches		
Inner blanket	1	1
Seed	1	2
Outer blanket	2	5
P/D ratio	1.261/1.151	1.281/1.158
Permissible assembly power (MWth)	12.3/7.3	13.2/7.6
Fraction of max. permissible	0.96/0.99	0.78/0.99
Core power (MWth)	1000	1000
Core height (cm)	250	250
Core pressure drop (Mpa)	0.9	0.9
Cycle length (EFPD)	2630	1640
Tot. residence time (EFPD)	2630/7890	3280/9840
k_{eff} at BOEC	1.039±0.001	1.046±0.001
k_{eff} at EOEC	1.004±0.001	1.004±0.001
Burnup reactivity swing (%Δk/k)	-3.39	-4.04
Burnup reactivity swing rate (%Δk/k	-0.47	-0.90

/EFPY)		
Average blanket power fraction	42.5%	45.0%
Average discharge burnup (MWd/kg)	123.2/65.0	164.0/109.5
Peak radiation damage (DPA)	175/204	206/187
TRU/HM at BOEC (wt%)	29.9	30.8
Seed CR at BOEC	0.46	0.49
HM at BOEC (tons)	12.3/51.4	11.0/39.9
Specific power (MWt/tHM)	46.8/8.3	50.0/11.3
TRU feed rate (kg/EFPY)	93.2/0.0	88.5/0.0
DU feed rate (kg/EFPY)	117.0/0.0	111.4/0.0
Thorium feed rate (kg/EFPY)	0.0/2386.0	0.0/1500.6
Trans-Th feed rate (kg/EFPY)	0.0/-174.5	0.0/-142.5
Reprocessing capacity (kg/GWt/Yr)	1703.6	1223.3
Safety Parameters at EOEC		
Sodium void worth (Δk/k)	0.034±0.0002	0.030±0.0002
Doppler coefficient (¢/°C)	-0.07±0.02	-0.17±0.03

8.4. Design of denatured blanket

The proliferation analysis in Section 7.7 found that the Breed-and-Burn thorium blanket has an intrinsic proliferation resistance as the discharged fuel is not required to be reprocessed. It requires remote operation to extract the discharged ^{233}U contaminated by 2233ppm ^{232}U without incurring large occupational dose. The dilution of ^{233}U with ^{238}U to a sufficient degree adds extra difficulty to extract fissile material and helps to avoid the potential weapon-use. For mixtures of ^{233}U, ^{235}U, and ^{238}U, effectively non-weapon-usable uranium is defined by the following formula [109]:

$$\frac{wt\%^{233}U + 0.6wt\%^{235}U}{wt\%U} < 0.12$$

(Equation 8-1)

This study examined the possibility of denaturing the thorium fuel with depleted uranium in order to dilute the weapon-usable isotope ^{233}U bred in the blanket. Under the condition prevailing in the blanket of the S&B core, a mixture of 60Th-36DU-4Zr is applied to denature the ^{233}U bred in the blanket by ^{238}U below the level required for weapon usable uranium. The theoretical density of the mixture is 13.0g/cc calculated by the equation below; the smeared density of fuel in the blanket is 85%.

$$\frac{1}{\rho_{Th-U-Zr}} = \frac{wt\%(Th)}{\rho_{Th}} + \frac{wt\%(U-10Zr)}{\rho_{U-10Zr}}$$

(Equation 8-2)

where

ρ_{Th} = the theoretical density of metallic thorium at 11.7g/cc;

ρ_{U-10Zr} = the theoretical density of metallic thorium at 15.7g/cc.

The denatured blanket is driven by TRU burner with conversion ratio of 0.5. The performance characteristics of the optimized S&B core are summarized in Table 8-6 together with the "Ultra-Long" S&B core (discussed in Section 4.3) and the ANL's ABR (TRU CR of 0.5) [43]. The "Denatured" S&B core has similar performance as the regular S&B core in terms of the average blanket power fraction and the reprocessing capacity. Due to the better neutron economics of the uranium fuel (Section 3.2.1) used in the "denatured" blanket, there is large increase of the blanket reactivity and, therefore, the overall burnup reactivity swing is negligible compared with the other two cases. The existing of the uranium in the blanket results in the breeding of Pu and the amount of Pu bred in the blanket is slightly smaller than Pu destructed by the seed.

Table 8-7 compares the proliferation resistance metrics of the "denatured" S&B core with ABR and PWR. Since both ABR and the seed in the S&B core have TRU conversion ratio of 0.5, the plutonium from the ABR and the seed have similar Material Attractiveness. The fissile uranium bred in the "denatured" blanket is 11% and below the upper limit of low enriched uranium. However, the plutonium bred from the blanket has a fissile content of 93% and this is very attractive for weapon-use. To avoid the breeding of Pu, it is recommended to charge the blanket with pure thorium and then denaturing the discharged blanket fuel by mixing it with depleted uranium. A special technology or procedure needs to be developed for this option.

Table 8-6 Performance Characteristics of the S&B with 60Th-36DU-4Zr Fueled Blanket

	Ultra Long	Denatured S&B	ANL's ABR
	Seed/Blanket	Seed/Blanket	
Fuel form	U-TRU-10Zr/Th	U-TRU-10Zr/60Th-36U-4Zr	U-TRU-10Zr
Target TRU CR of seed	CR=0.5	CR=0.5	CR=0.5
Number of assemblies			

Inner blanket	42	45	-
Seed	61	63	144
Outer blanket	168	163	-
Number of batches			
Inner blanket	1	1	-
Seed	1	1	6/6/7
Outer blanket	2	1	-
P/D ratio	1.261/1.151	1.269/1.158	1.293
Permissible assembly power (MWth)	12.3/7.3	12.7/7.6	-
Fraction of max. permissible	0.96/0.99	0.99/1.00	-
Core power (MWth)	1000	1000	1000
Core height (cm)	250	250	101.6
Core pressure drop (Mpa)	0.9	0.9	-
Cycle length (EFPD)	2630	3125	221
Tot. residence time (EFPD)	2630/7890	3125/6250	1326/1326/1547
k_{eff} at BOEC	1.039±0.001	1.015±0.001	-
k_{eff} at EOEC	1.004±0.001	1.007±0.001	-
Burnup reactivity swing (%Δk/k)	-3.39	-0.82	-2.90
Burnup reactivity swing rate (%Δk/k /EFPY)	-0.47	-0.10	-4.79
Average blanket power fraction	42.5%	41.3%	0.0%
Average discharge burnup (MWd/kg)	123.2/65.0	146.7/47.9	131.9
Peak radiation damage (DPA)	175/204	206/190	-[10]
TRU/HM at BOEC (wt%)	29.9	30.4	33.3
Seed CR at BOEC	0.46	0.45	0.5
HM at BOEC (tons)	12.3/51.4	12.5/53.8	9.4
Specific power (MWt/tHM)	46.8/8.3	46.9/7.7	106.4
TRU feed rate (kg/EFPY)	93.2/0.0	95.4/-74.1	173.8
DU feed rate (kg/EFPY)	117.0/0.0	119.6/121.5	217.5
Thorium feed rate (kg/EFPY)	0.0/2386.0	0.0/1967.8	0.0
Trans-Th feed rate (kg/EFPY)	0.0/-174.5	0.0/-133.7	0.0
Reprocessing capacity (kg/GWt/Yr)	1703.6	1459.9	2767.2
Safety Parameters at EOEC			
Sodium void worth (Δk/k)	0.034±0.0002	0.040±0.0002	0.029
Doppler coefficient (¢/°C)	-0.07±0.02	-0.04±0.03	-0.09

[10] The peak radiation damage on the cladding of the ABR design is constrained by peak fast fluence of $4x10^{23}$ n(>0.1 MeV)/cm^2.

Table 8-7 Proliferation Resistance Metrics of the S&B with Denatured Thorium Fueled Blanket After 5 years Cooling Time

Property	ABR	Denatured S&B (Seed/Blanket)	PWR
Fissile plutonium fraction, %	46%	47%/93%	63%
^{238}Pu/Pu ratio, %	4.10%	3.4%/0.2%	3.00%
Specific decay heat of plutonium, W/kg	26.94	22.86/3.29	20.54
Spontaneous fission neutrons per kg Pu, n/sec-kg	6.50E+5	6.27E+5/6.61E+4	4.40E+5
^{232}U/^{233}U ratio, ppm	-	-/1715	-
Fissile U/U ratio, %	-	0%/11%	0.70%
Fissile U/Th ratio, %	-	-/8%	-
(Pu+fissile U)/(^{238}U+Th) ratio, %	41%	34%/8%	2%

8.5. PWR SNF with limited reprocessing for the blanket

The attainable burnup of contemporary PWRs is about 50-55 MWd/kg that is constrained by the criticality of the fuel. To improve the fuel utilization from current 0.6%, it is proposed to charge the PWR UNF to the blanket of the S&B cores. It is necessary to recondition the fuel but limited reprocessing may be sufficient. Instead of using aqueous or electro-chemical reprocessing, it is assumed that the Atomics International Reduction Oxidation (AIROX) process developed for uranium dioxide fuel described below is applied. After the limited reprocessing, the fuel is refabricated and loaded into the blanket. The subcritical blanket is driven by the leakage neutrons from the seed and discharges its fuel when the radiation damage on the structural material gets close to 200 DPA.

8.5.1. AIROX process

The AIROX process [110] is considered as a dry process and includes several steps: fuel de-cladding; gaseous plus volatile fission products removal; new fuel fabrication. The feasibility of similar technology, called Direct Use of Spent PWR Fuel in CANDU Reactors (DUPIC) has been demonstrated by Korea Atomic Energy Research Institute [111] for recycling the PWR SNF to Heavy Water Reactor (HWR). In AIROX, the oxidation of the UO_2 in the discharged fuel is conducted in O_2 atmosphere at 400°C to U_3O_8. The fuel pellets are converted to the fine U_3O_8 powder and part of the gaseous and volatile fission products are removed in this step. Then U_3O_8 is reduced back to UO_2 in H_2 atmosphere at 600°C. Additional fission products are removed during the fuel sintering process. Table 8-8 defines the type and amount of the removed fission products. Since the TRU are not separated from the spent fuel, the AIROX process features high proliferation resistance.

Table 8-8 Element Removal Fractions for the AIROX Process

	AIROX
Th	0%
Am	0%
Other HM	0%
FPs	100% C,Kr,Xe,I
	90% Cs,Ru
	75% Te,Cd
Gaseous FPs	100% H,He,N,O,F,Ne,Cl,Ar,Kr,Xe,Rn

8.5.2. Neutron balance analysis of AIROX processed PWR SNF

A 0-D model is applied to compare the neutron balance (Section 3.2.1) of metallic thorium versus AIROX processed PWR SNF. The corresponding volume fractions of fuel/gap/cladding/coolant are 37.5%/12.5%/22.0%/28.0% respectively. The UNF is obtained from typical PWR fueled with 4.5wt% ^{235}U in UOX and discharged at a burnup of 55MWd/kg. The depletion calculation is conducted by ORIGEN2.2 with default cross-section library for PWR. After 1000-day cooling time, the discharge fuel undergoes AIROX reprocessing. The fuel compositions and heavy metal density [112] are shown in Table 8-9.

Figure 8-5 compares the neutron economics of the two fuels. Due to the existing of the TRU and some ^{235}U in the PWR SNF, it has larger initial reactivity -- its k_∞ value is ~0.33 at burnup of 0 MWd/kg whereas the corresponding k_∞ value for metallic thorium is close to 0.0. As the fuel undergoes burnup, fissile Pu is bred in the PWR SNF and the k_∞ value increases to a maximum at about 15% FIMA. The PWR SNF after AIROX process shows similar behavior as both depleted uranium and thorium fuel (Figure 3-5) but fails to achieve criticality. Nevertheless, it is possible to operate a subcritical blanket fueled by PWR SNF with the help of excess neutrons that leak from the seed. Based on the neutron balance analysis it is expected that more external neutrons are required to drive such blanket than metallic thorium fueled blanket to the same burnup.

Table 8-9 Fuel Composition of the Metallic Thorium and the AIROX Processed PWR SNF

Fuel composition (wt%)	Metallic Th	PWR SNF after AIROX

Fissile Pu/HM	0.00%	0.69%
TRU/HM	0.00%	1.28%
Th/HM	100.00%	0.00%
U/HM	0.00%	98.72%[11]
O/HM	0.00%	14.38%
Zr/HM	0.00%	0.63%
Sr-90/HM	0.00%	0.09%
Tc-99/HM	0.00%	0.13%
Cs-135/HM	0.00%	0.01%
Cs-137/HM	0.00%	0.02%
HM atomic density[12] (#/b-cm)	3.042E-02	2.276E-02

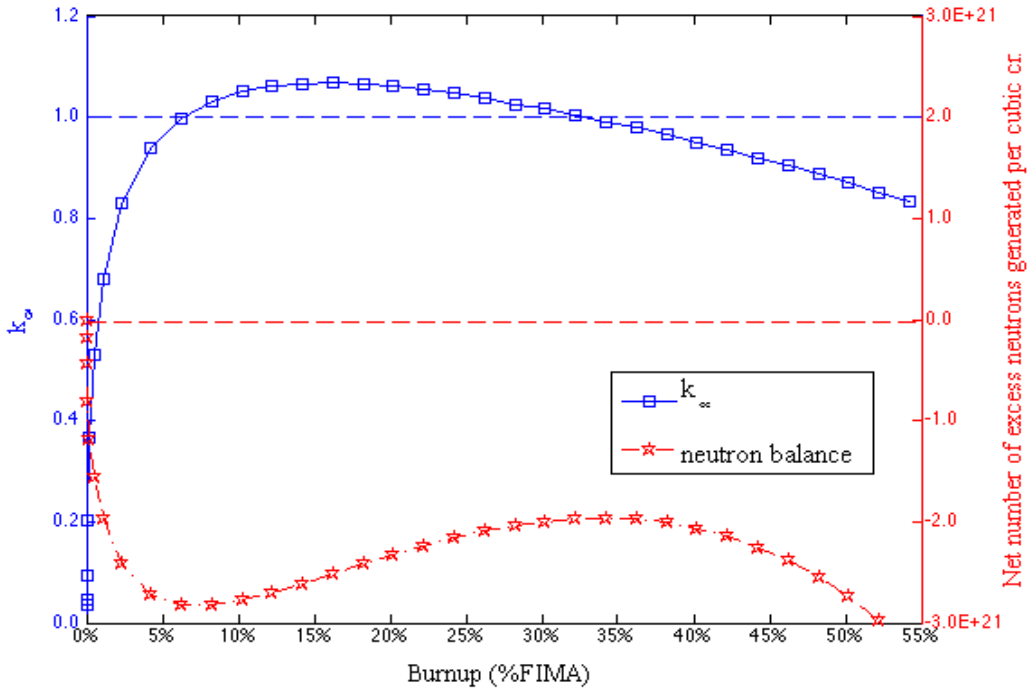

(a)

[11] The ^{235}U/U in the AIROX processed PWR SNF is about 0.6%.

[12] This is the theoretical density.

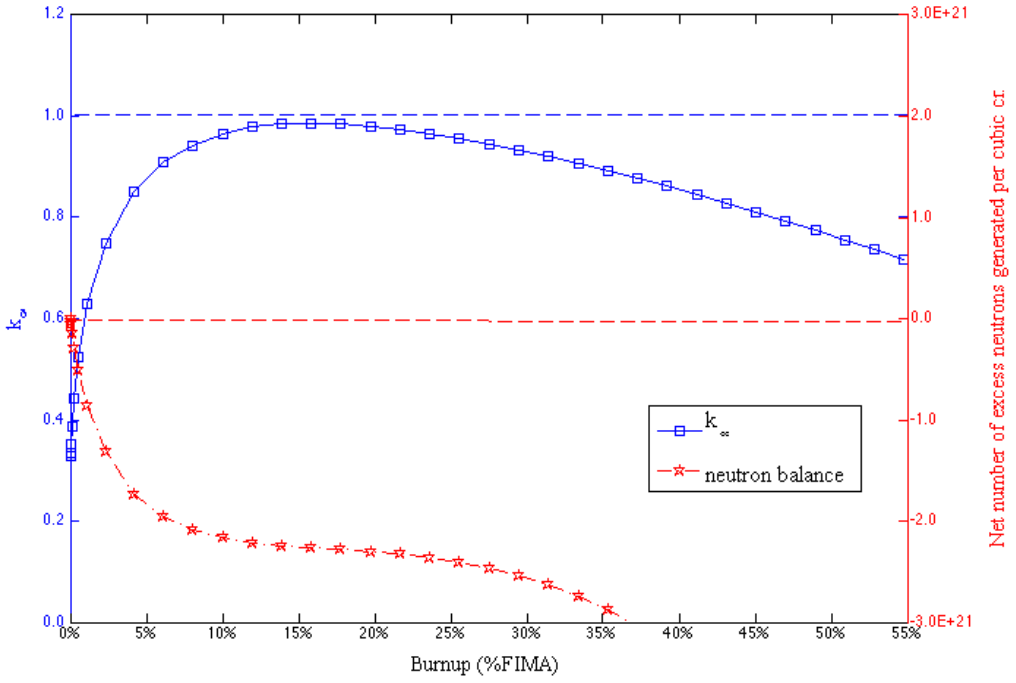

(b)

Figure 8-5 k_∞ (blue) and neutron balance (red) evolution with burnup for metallic thorium (a) and AIROX processed PWR SNF (b)

8.5.3. Full core analysis of the S&B core with PWR SNF blanket

The fuel cycle scheme of the applications of PWR UNF in the S&B core is shown in Figure 8-6. The blanket is charged by the AIROX processed PWR UNF and operates in once-through fuel cycle while the seed is designed as fuel self-sustaining. No TRU is separated from the PWR UNF under this scenario.

Table 8-10 summarizes the performance characteristics of the S&B core for the application of PWR UNF. About one third of the core power is generated from the blanket and the reprocessing capacity per unit of electricity generated is half of that for the ARR. It is possible to discharge the PWR UNF from the blanket at an average burnup of ~120 MWd/kg whereas the average burnup from metallic thorium fueled blanket is ~70 MWd/kg. The higher discharge burnup is due to the softer neutron spectrum achieved by the oxide fuel. After accounting for the burnup at the first stage, this two-stage energy system can achieve an accumulated average burnup of ~190 MWd/kg and therefore improves the fuel utilization of natural uranium resource by a factor of three

while at the same time reducing the capacity of high level waste per unit of electricity generated. Compared with ARR, the S&B with PWR UNF fueled blanket has more positive feedback to coolant expansion in term of the sodium void worth because a larger amount of TRU driver fuel is required. A future study should focus on reducing the coolant density coefficient and comprehensive safety analysis.

Table 8-10 Performance Characteristics of the S&B Core with AIROX Processed PWR SNF Fueled Blanket

		PWR SNF by AIROX	ANL's ARR
Fuel form		Seed/Blanket U-TRU-10Zr/Oxide PWR SNF	U-TRU-10Zr
Target TRU CR of seed		CR=1.0	CR=1.0
Number of assemblies			
	Inner blanket	17	-
	Seed	101	151
	Outer blanket	153	-
Number of batches			
	Inner blanket	1	-
	Seed	3	3/3/4.5
	Outer blanket	9	-
P/D ratio		1.156/1.139	1.100
Permissible assembly power (MWth)		7.5/6.7	-
Fraction of max. permissible		0.96/0.98	-
Core power (MWth)		1000	1000
Core height (cm)		250	101.6
Core pressure drop (Mpa)		0.9	-
Cycle length (EFPD)		1215	370
Tot. residence time (EFPD)		3645/12150	1110/1110/1665
k_{eff} at BOEC		1.009±0.001	-
k_{eff} at EOEC		1.015±0.001	-
Burnup reactivity swing (%Δk/k)		0.56	-0.06
Burnup reactivity swing rate (%Δk/k /EFPY)		0.17	-0.06
Average blanket power fraction		31.3%	0.0%
Average discharge burnup (MWd/kg)		111.8/117.1	73.0
Peak radiation damage (DPA)		194/200	-[13]

[13] The peak radiation damage on the cladding of the ARR design is constrained by peak fast fluence of $4x10^{23}$ n(>0.1 MeV)/cm^2.

TRU/HM at BOEC (wt%)	15.3	14.6
Seed CR at BOEC	1.03	1.00
HM at BOEC (tons)	22.4/31.8	16.7
Specific power (MWt/tHM)	30.7/9.9	59.7
TRU feed rate (kg/EFPY)	0.1/0.0	-4.7
DU feed rate (kg/EFPY)	246.1/0.0	392.4
Reprocessing capacity (kg/GWt/Yr)	2243.7	5000.0
Safety Parameters at BOEC		
Sodium void worth ($)	10.82±0.06	6.29
Doppler coefficient (¢/°C)	-0.11±0.02	-0.11

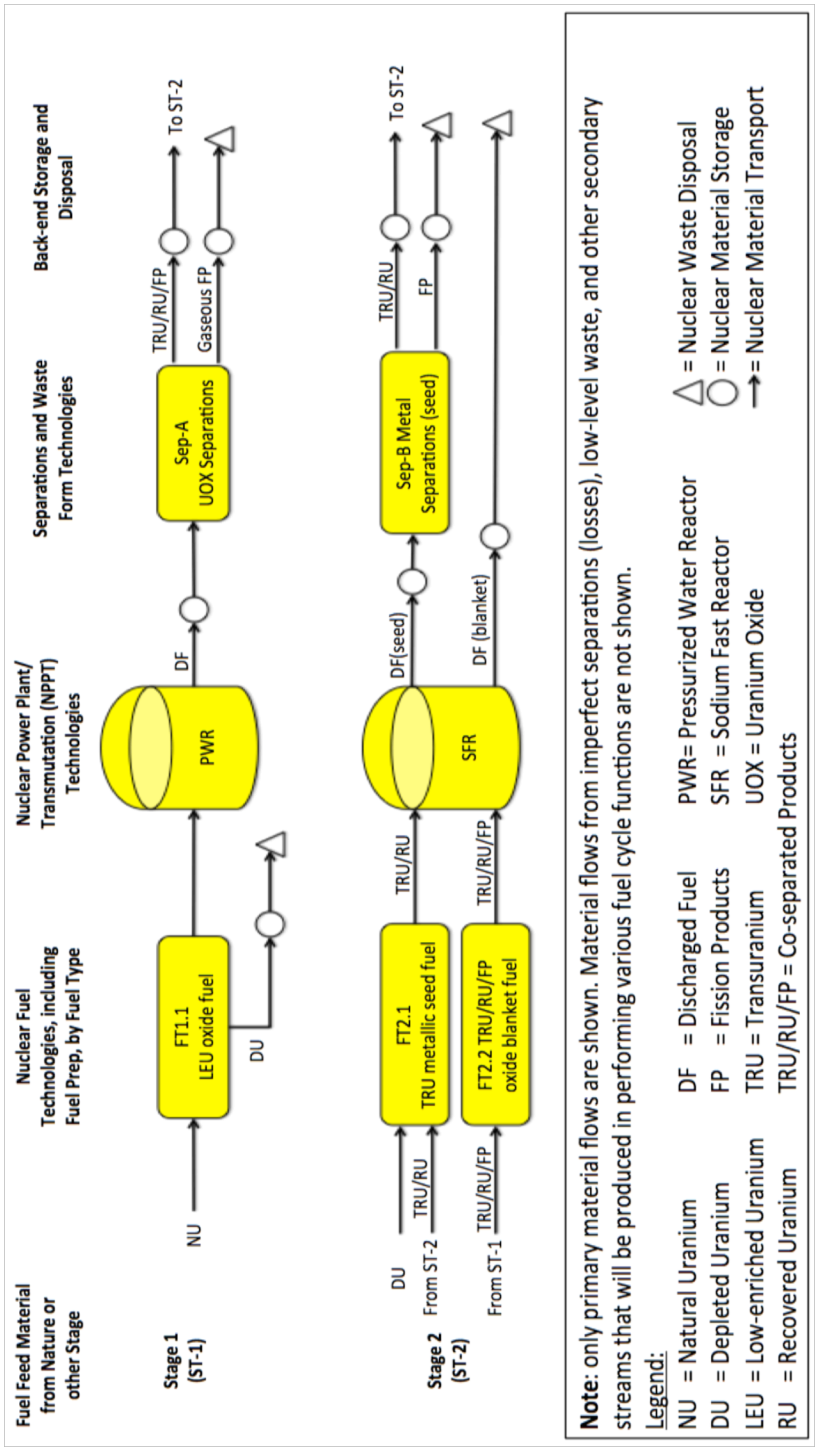

Figure 8-6 Fuel cycle scheme of PWR-S&B two-stage system using AIROX processed PWR SNF for the blanket

8.6. A three-stage PWR-S&B-PWR closed nuclear system

Instead of running the thorium blanket of the S&B reactor in a once-through mode and accumulating a large inventory of Trans-Th elements, the study[14] in this section assesses the feasibility of using the discharged Trans-Th to feed PWRs that operate on a closed fuel cycle that their fuel is recycled. This fuel cycle option provides a possible solution to the large amount of ^{233}U bred in the S&B core whose decay daughters are the major contributors to the radioactivity and radiotoxicity in the long-term (Section 7.5). The specific fuel cycle considered here is a three-stage energy system PWR(LEU)-S&B-PWR(Trans-Th) illustrated in Figure 8-7. Stage 1 are once-through low enriched uranium fueled LWRs, Stage-2 are S&B reactors having TRU transmuting seed and thorium blanket, while Stage-3 are LWRs that operate on a closed ^{233}U/Th fuel cycle. The recovered Trans-Thorium from Stage 2 are mixed with a certain amount of thorium as the makeup fuel of the Stage-3 PWR. All the discharged fuel is reprocessed and recycled except for the uranium recovered from Stage-1 discharged fuel and a fraction of the thorium discharged from Stage-2 blanket. The seed of Stage-2 S&B reactors is fed with TRU separated from Stage-1 PWR. This system may offer the fastest and, possibly, most cost effective way to get rid of the HLW from the nuclear industry. It also features a high PWR-SFR support-ratio of PWRs per SFR.

A typical Westinghouse 17×17 PWR fuel assembly design [113] is used for the burnup analysis of Stage-3 PWRs. Serpent 2 [114] with the ENDF/B-VII cross-section library is used for neutronics and burnup calculations. The equilibrium cycle with a three batch-shuffling scheme is searched by EDIS (developed by Dr. Staffan Qvist at University of California Berkeley [38]). The core average multiplication factor k_{core} is estimated from

$$k_{core} = \frac{1}{\sum_i f_i / k_i}$$

(Equation 8-3)

where

f_i = the fraction of core power generated by batch i;

k_i = the multiplication factor of batch i (axial leakage is included in the model).

This study assumes that the power is generated uniformly from the three batches and the radial leakage is 3%. The burnup of Stage-3 PWR is fixed at 50MWd/kg for the design

[14] This fuel cycle options is assessed by a visiting scholar -- Gang Wang from Tsinghua University.

variants and the amount of Trans-Th in the makeup fuel is determined to ensure the core criticality.

The Trans-Th discharged from the blanket of the S&B cores constrained by 100DPA, 200DPA, 300DPA, and 400DPA (Section 6.4) are charged to the Stage-3 PWR. The performance characteristics are summarized on Table 8-11. As the cladding material of the blanket is qualified for higher DPA value, the thorium blanket contributes a larger fraction of the core power for the S&B (Table 6-4). As a result, the TRU consumption rate of the seed decreases. When the blanket discharge burnup goes up, the trans-thorium generation rate of the blanket decreases. The support-ratio that is defined as the ratio between the electrical power fraction of PWR and SFR decreases correspondingly for the Stage-1 and Stage-3 PWRs. After combining the PWRs on both stages, one S&B core with radiation damage on cladding of 200 DPA enables supporting ~3.3 PWRs. This combined support-ratio will increase up to ~4.2 if the blanket is designed with radiation damage of 100DPA on the cladding. The support-ratio of conventional ABR is ~1.7 (Evaluation Group 32 [18]); a similar system, where Trans-Th bred from a thorium fueled SFR are burned by thorium fueled PWR on closed fuel cycle, has the support-ratio of only 0.17 (Evaluation Group 38 [18]). It is concluded that the S&B reactor in this three-stage energy system provides the substantial improvement of the combined support-ratio.

Table 8-11 Fuel Cycle Parameters of the PWR-S&B-PWR Systems

Property	Case1	Case2[15]	Case3	Case4
DPA for the blanket	100	200	300	400
Discharge burnup of the blanket in S&B, MWd/kg	35.1	70.2	121.3	171.6
Spent fuel discharged from S&B blanket, kg/GWt-EFPY	3785.2	3000.1	1751.3	1365.6
Discharge rate of Trans-thorium from S&B, kg/GWt-EFPY	239.5	223.3	148.7	120.4
^{233}U/HM loaded to $PWR_{stage-3}$ at BOEC, wt%	3.3	3.3	3.4	3.4
^{233}U/HM discharged from $PWR_{stage-3}$ at EOEC, wt%	2.0	2.0	2.1	2.1
Reprocessing capability for $PWR_{stage-3}$, kg/GWt-EFPY	7300	7300	7300	7300
Feed rate of Trans-Th $_{PWR(stage\ 3)}$, kg/GWt-EFPY	104.7	109.4	117.5	121.9
Support ratio of S&B-$PWR_{stage-1}$	2.3	1.6	1.5	1.3
Support ratio of S&B-$PWR_{stage-3}$	1.9	1.7	1.0	0.8
Combined support ratio of S&B-PWR	4.2	3.3	2.5	2.1

[15] Case 2 is the High-Transmutation case with TRU CR of 0.0 in Chapter 4

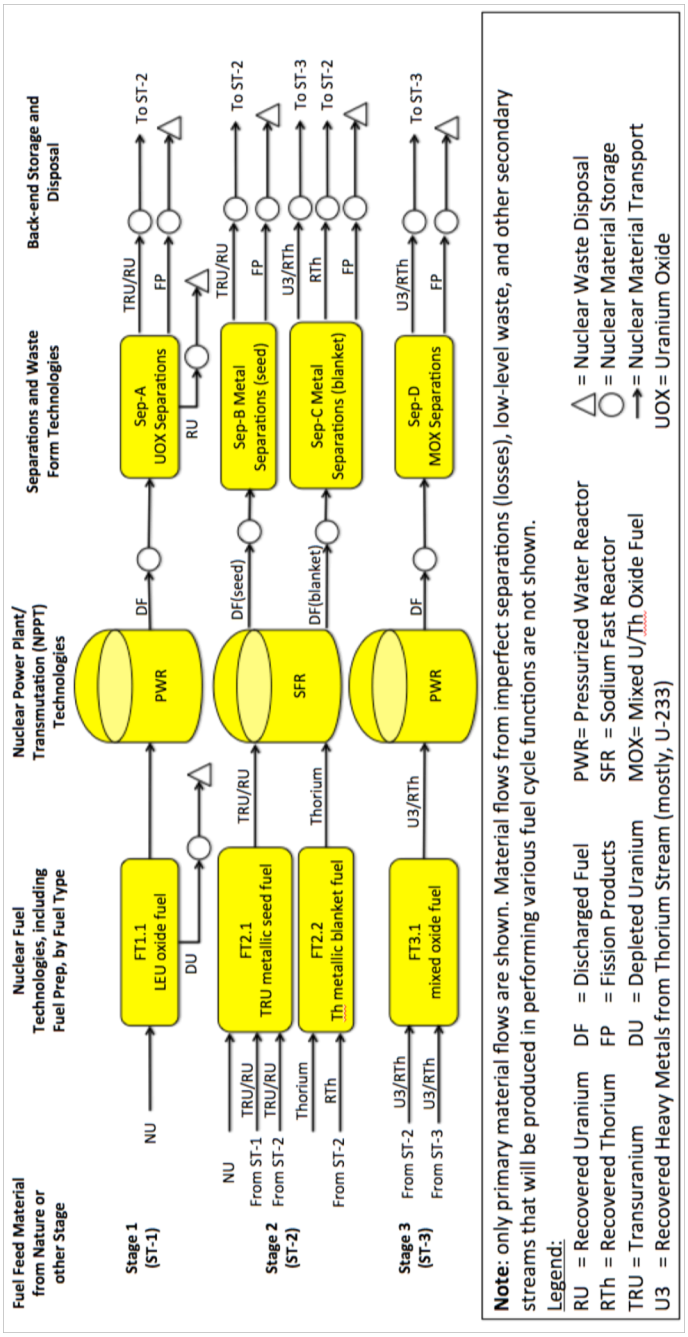

Figure 8-7 Fuel cycle scheme of a three-stage PWR(LEU)-S&B-PWR(Trans-Th) closed nuclear energy system

8.7. Application of discharged blanket fuel in Molten Salt Reactor

The thorium fueled Molten Salt Reactor was proposed and has been recognized as Generation IV reactor technology; Oak Ridge National Laboratory took the lead in researching the MSR through 1960s. The MSRs feature inherent safety, high outlet temperature yielding high efficiency to produce electricity and operates at a low pressure [115]. This section summarizes the neutronic feasibility studies of the utilization of the thorium discharged fuel from the blanket of the S&B core to MSRs. Instead of once-through mode for the thorium blanket, the accumulated Trans-Th elements are fed to MSRs for improved resource utilization. This fuel cycle option provides another possible solution to the large amount of ^{233}U bred in the S&B core whose decay daughters are the major contributors to the radioactivity and radiotoxicity in the long-term (Section 7.5).

This section summarizes the study[16] [116] focusing on the design of Molten Salt Reactor fed with the discharged fuel from the thorium blanket driven by CR=0.0 seed (Section 4.4). MocDown was extended with a script that enables Feed/Removal modeling and the online processing. The MSF was modeled by a single hexagonal pitch with a cylindrical flow channel in the center; the carbon to molten salt ratio is adjusted by changing the diameter of flow channel. FLiNaK is selected as the carrier salt due to its high solubility of heavy metals. The graphite reflectors are placed on the top and bottom; radial reflective boundary condition is applied and, therefore, the k_{inf} is required to be above 1.02 for the criticality. The model was validated with a modified version of Serpent2 [117].

The preliminary study shows that if the salt is fully reprocessed during operation, about 98% of the fed heavy metals can be converted into energy. If the once-though fuel cycle scheme is applied where only Uranium is recovered back to MSRs via fluorination method, the MSRs can achieve addition burnup of about 30% FIMA. Combined with the ~7% FIMA achieved by the blanket in the S&B core, this energy system can utilize up to 37% of the natural thorium. More detailed analysis is required to fully investigate this fuel cycle option.

8.8. Other possible fuel cycle options

The fuel cycle options listed in this section appear to be also of interest but have not been studied yet. Some of them represent a variant of Externally-Driven System (EDS) in which the excess neutrons from the seed rather than accelerator-driven spallation neutrons or fusion neutrons are the external neutrons used to drive the subcritical system.

[16] This fuel cycle option was assessed by a visiting scholar – Lucas David from INSTN

8.8.1. S&B core with Minor Actinides (MA) inert matrix blanket

This is a two-stage system using PWRs for Stage-1 and the S&B cores for Stage-2 as shown in Figure 8-8. The PWR is charged by LEU and has a discharge burnup of ~50 MWd/kg. The discharged fuel is reprocessed to recover Pu and MA for the S&B. Pu recovered from the PWRs and the Pu recovered from the seed of the S&B core are fed to the seed as a U-Pu-Zr ternary metallic fuel. The recovered MA from the PWRs together with that from both the seed and the blanket of the S&B core are used to make MA dispersion metallic fuel in Zr matrix (also called Inert Matrix Fuel or IMF). This IMF is charged to the subcritical blanket and driven by the neutrons that leak from the seed. A fraction of the MA is incinerated in the blanket and the discharged blanket fuel is reprocessed to recover the MA left. Only fission products and material losses from the fuel reprocessing and fabrication end up as nuclear waste and sent to the disposal. Natural thorium may also be used as part of the blanket fuel in order to minimize the net neutron leakage probability, reduce burnup reactivity swing and reduce the positive feedback to coolant voiding.

Another similar fuel cycle option is to operate the PWR on a closed Pu recycling. The seed on Stage-2 is designed to be fuel self-sustaining while the MA recovered from stage 1 and 2 is burned as IMF in the subcritical blanket with excess neutrons from the seed. This option is a design variant of Evaluation Group (EG) 36 in the Fuel Cycle Screening and Evaluation campaign [18]. The proposed fuel cycle option is based on critical reactor technology to achieve the same function as EG36; the critical reactor is expected for lower development risk, lower safety challenges, and lower overall costs as compared to external-driven systems [18].

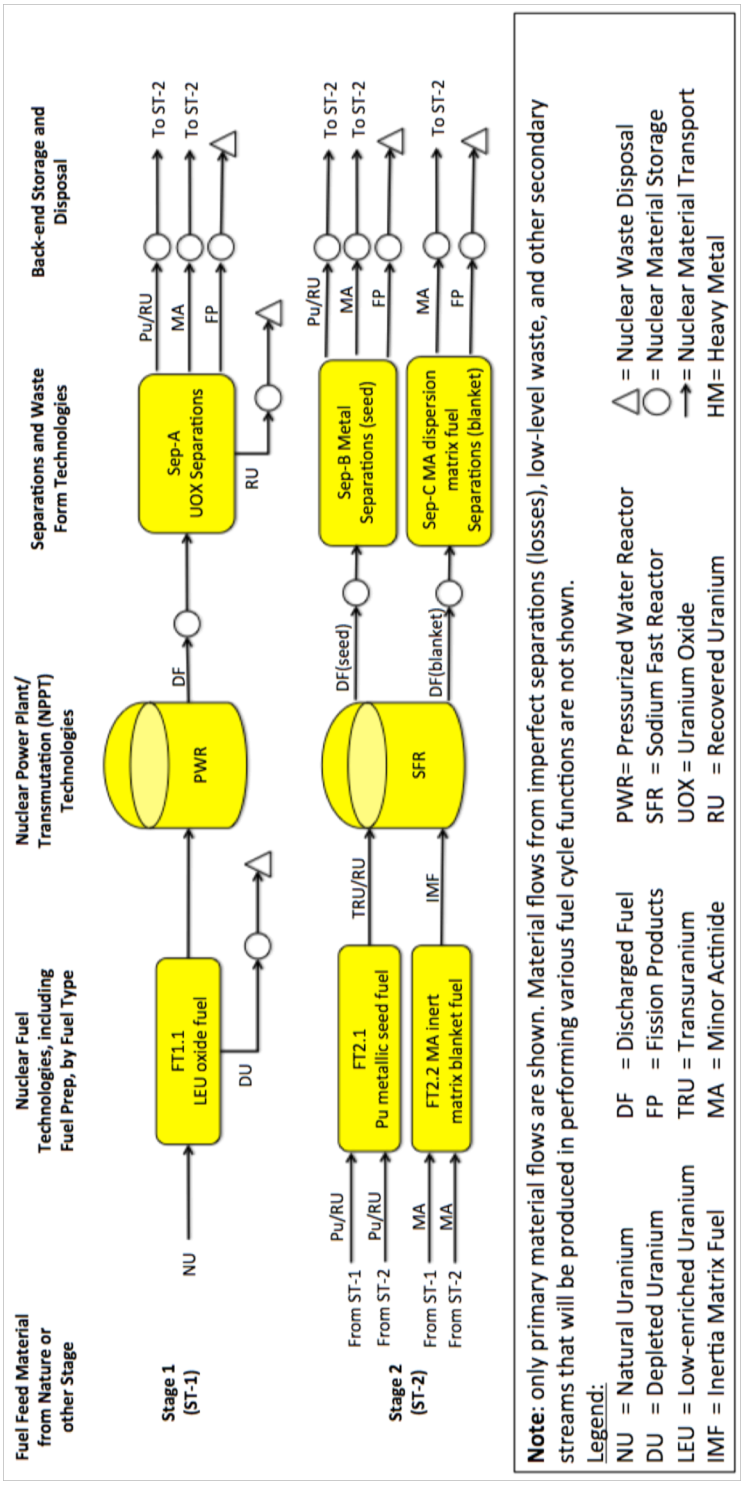

Figure 8-8 Fuel cycle scheme of the S&B core with minor actinide inert matrix blanket

8.8.2. S&B core with PWR as Pu burner

This two-stage S&B-PWR energy system is shown in Figure 8-9 where the SFR cores provide fissile material for the PWRs. The seed fuel is designed as fuel self-sustaining while the blanket is charged with depleted uranium. The feasibility of such energy system has been studied in [86] with TRU CR of 1.0 for the seed and about 40% of the core power is generated from the subcritical uranium blanket. The Pu bred in the blanket together with the Pu recovered from Stage-2 PWRs are used as Mixed Oxide (MOX) fuel which is charged to the PWRs. This is a design variant of EG29 in in the Fuel Cycle Screening and Evaluation campaign [18]. The PWRs operate on a closed fuel cycle and the Pu in the discharged fuel is recovered; both FP and MA from Stage-1 blanket and Stage-2 PWRs are sent to disposal. As a large fraction of core power is generated from Uranium fueled blanket, the Pu bred from the S&B can support a large number of PWRs. The preliminary study shows that the Pu production rate for Stage-1 S&B core is ~420 kg/GWe-yr; it can support about ~0.7 Stage-2 PWR in EG29 where the Pu destruction rate is ~606 kg/GWe-yr [18]. This option may be of interest for the scenario that economical uranium is nearly exhausted but the PWRs will still exist for decades.

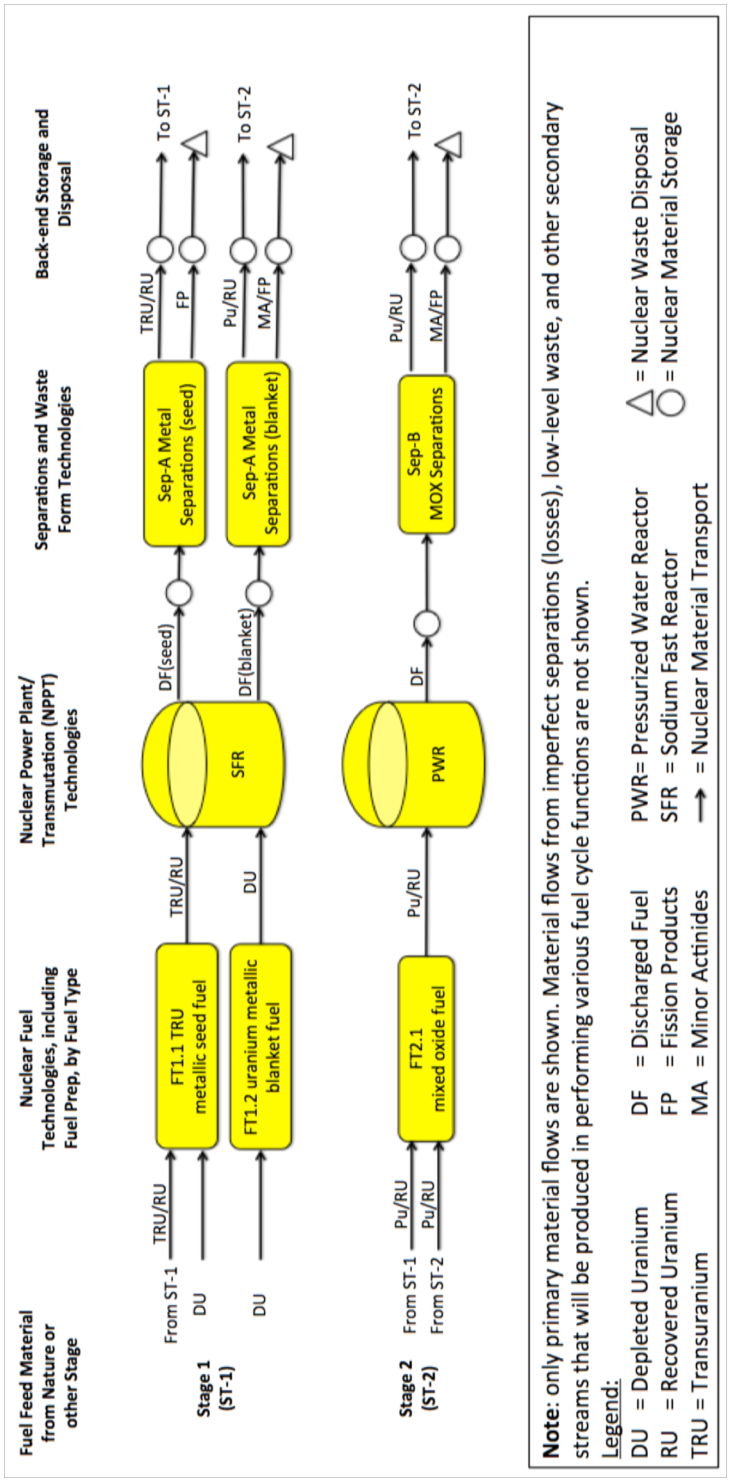

Figure 8-9 Fuel cycle scheme of S&B as Pu supplier to close-fuel cycle PWR

8.8.3. A self-sustaining S&B core configuration

A design variant of the fuel self-sustaining S&B core is shown in Figure 8-10; it is similar to the conventional SFR cores, like S-PRISM [44], ARR [43] and EG24 [18]. The TRU in the discharged fuel from the seed and blanket is recovered and sent back to the seed for next cycle; the recycled uranium is charged to the blanket. The seed region is charged with non-fertile (TRU-40Zr) fuel and discharges its fuel at an average burnup of ~370 MWd/kg (see Section 6.1). The subcritical blanket, driven by the excess neutrons from the seed, is fueled by natural/recycled uranium that achieves an average burnup of ~70 MWd/kg (Section 3.2.2) -- approximately same as a typical self-sustaining ARR [43]. Since the seed fuel with high fissile contents can achieve approximately five times the burnup of S-PRISM and ARR, the reprocessing capacity along with the fuel cycle cost per unit of electricity generated in the proposed S&B core is expected to be lower. This option is therefore possibly more economical as compared with conventional fuel self-sustaining SFRs.

Figure 8-10 Self-sustaining S&B cores

Chapter 9

9. Conclusions and Future Directions

9.1. Conclusions

9.1.1. Reactor design and the synergism

This study assessed the feasibility to design a Seed-and-Blanket Sodium-cooled Fast Reactor to generate a significant fraction of the core power from radial thorium fueled blanket that operates in breed-and-burn mode without reprocessing. The S&B cores are designed to fit within the vessel of S-PRISM and deliver the nominal power of S-PRISM at 1000 MWt. The designs discussed in this study meet major neutronic, thermal-hydraulic, and material constraints including criticality, burnup reactivity swing, fuel/cladding temperature, coolant pressure drop, and peak radiation damage of 200 DPA on the cladding of both seed and blanket fuel.

The neutron balance analysis (Section 3.2.1) concludes that a self-sustaining breed-and-burn mode of operation cannot be established by using metallic thorium as the feed fuel. Nevertheless, it is possible to operate a subcritical thorium blanket in the B&B mode with the help of excess neutrons that leak from the seed. Based on the neutron balance analysis it is expected that more external neutrons are required to drive a thorium rather than depleted-uranium fueled blanket to the same burnup.

The tradeoff study in Section 3.1 found that the seed fuel in S&B core can accommodate a wide range of TRU CR and there is a unique synergism (Section 4.6) between a low CR seed and a thorium blanket: a lower CR seed requires a higher loading of TRU which generates a larger fraction of excess neutrons. The higher TRU loading enables the seed to have a larger P/D ratio and, hence, higher seed power density and specific power. The larger fraction of excess neutrons available for driving the subcritical blanket increases the fraction of core power generated by the blanket. Since the blanket fuel requires no fuel reprocessing and remote fuel fabrication, its cost is orders of magnitude smaller than the seed fuel; the larger fraction of core power generated from the blanket reduces the fuel cycle cost of the reactor. As its fissile content builds up, the blanket reactivity increases over the cycle and partially compensates for the relatively large reactivity loss of a low CR seed. As the result, the core reactivity drop with burnup is significantly slower than in a conventional ABR designed to have identical CR. The relatively lower burnup reactivity swing combined with the higher HM loading of S&B cores enable very long cycle and, therefore, high reactor capacity factor. The high TRU content seed can achieve higher average discharge burnup due to the smaller magnitude of neutron flux at given fission rate, The high seed discharge burnup implies low capacity required for fuel

reprocessing per unit of S&B core power. As in the equilibrium core the blanket fuel adjacent to the seed has pretty high fissile contents -- the k_∞ is close to 1.0. The large inventory of fissile contents in the blankets at BOEC contributes to the relatively small fractional change in the blanket power density over the equilibrium cycle. Unlike most blankets in conventional SFR designs, the power shifting between the seed and the blanket over one cycle is easily manageable.

It further improves S&B performance by using an annular rather than a cylindrical seed and loading thorium assemblies at the radial center of core in addition to the periphery (Section 4.2): a larger fraction of power generated by the blanket; smaller burnup reactivity swing; longer cycles; smaller radial peaking factor; and less positive sodium void worth. Two high-performance cores were designed to benefit from the annular seed concept: (1) The ultra-long cycle core (Section 4.3) features a cycle length of 88 months or ~7 years — about 12 times longer than that of the reference ABR with a comparable TRU CR of 0.5; (2) The high TRU transmutation core (Section 4.4) features a CR of 0.0. The seed of this core transmutes TRU at a comparable rate as the reference ABR with CR=0.5, but requires only about one sixth of the reprocessing capacity per unit of core power. The thorium blanket can generate close to 60% of the core power. The annular S&B cores have a smaller sodium void worth than the reference compact ABR core despite of the low axial neutron leakage probability of the cores. This is due to the enhanced neutron leakage probability from the seed to the subcritical blanket upon coolant voiding. The application of thorium in the high transmutation S&B core assures that this core has a negative Doppler coefficient even though its seed is charged with non-fertile fuel.

9.1.2. Viability analysis for the S&B concept

Due to the unique synergism that exists between an annular TRU transmuting seed and the thorium B&B blanket, the proposed S&B cores were found to offer significant performance benefits. However, these S&B cores (Chapter 3 and 4) were designed to give an upper bound on the performance improvement that can be provided by this core concept. Some of the features in the reference S&B core introduce a number of design challenges. The core performances of the S&B design are sensitive to the design assumptions and constraints, including the active core height, pressure drop through the fuel bundle and radiation damage on cladding materials. Viable S&B cores can be designed without significant deviation from SFR core design practices. Among the design variants, the synergism claimed by the S&B concepts is generally preserved even if more strict assumptions are applied.

The TRU-10Zr fuel alloy assumed for the high transmutation S&B design (Section 4.4) has no sufficient fabrication and irradiation experience. As the TRU content of a metallic

transmutation fuel alloy increases, the fuel melting temperature decreases. Therefore, the seed fuel with TRU-10Zr fuel alloy was changed to the TRU-40Zr alloy because it can be supported by the existing irradiation data. A zirconium concentration of 40wt% provides acceptable melting temperature and, therefore, is used as the reference case (Section6.1) for the viability analysis in Chapter 6. Compared with the old case in Section 4.4, the fraction of power generated by the blanket decreases slightly to 50.7%.

Compared with the design practice of the conventional compact SFR cores, the large S&B core is expected to increase the SFR capital cost as it would require a longer reactor vessel and a more challenging seismic design. A parametric study (Section 6.2) was undertaken to quantify the effect of reducing the core height on the S&B core performance. The study shows that the S&B core with active height of 120cm will be comparable in volume, HM mass, and specific power with the S-PRISM core and could fit within the S-PRISM reactor vessel. 43.1% of this core power is generated by the once-through thorium blanket; the required capacity for reprocessing and remote fuel fabrication per unit of electricity generated will be approximately one fifth of that for a comparable ABR. The sodium void worth of this 120cm tall S&B core is significantly less positive than that of the reference ABR and the thermal expansion coefficients are more negative compared with those of large S&B cores. The promising performance characteristics of the S&B cores are derived from the unique synergism that exists between low conversion ratio TRU transmuting seed and B&B thorium blanket.

The pressure drop of the reference S&B core was initially designed for 0.9 MPa. This is higher than the pressure drop that conventional SFR cores are designed to have. Therefore, the sensitivity of the S&B core performance to the pressure drop (Section 6.3) was investigated for the reference 250cm tall S&B core. The pressure drop is reduced by a smaller fuel pin diameter – that is, increasing the coolant cross-section area. The outer diameter of all cores is not changed so the fuel inventory in the core decreases with the pressure drop. As the neutron economy of S&B cores deteriorates with a reduction in the fuel volume fraction, it is observed that the performance of the core will degrade with the reduction of the pressure drop. Nevertheless, as illustrated in Section 6.3, there is only a small degradation in the core performance over a pressure drop range from 0.9 down to 0.3 MPa. The fraction of core power generated by the blanket is reduced from 50.7% for 0.9 MPa to, 48.7%, 47.6% and 44.0% for a pressure drop of 0.7, 0.5 and 0.3 MPa, respectively. The effect of the pressure drop on the fuel reprocessing capacity is not significant.

The ongoing and future irradiation experiments and development of advanced cladding materials are expected to eventually enable to certify cladding materials to operate up to radiation damage level exceeding 200 DPA. Section 6.4 shows the effect of an increase in the permissible radiation damage level to the cladding of the blanket fuel on selected

S&B core characteristics. The seed fuel is discharged at the nominal radiation damage level since its burnup at 200 DPA has already been very high – between 300 and 400 MWd/kg. An increase in the permissible radiation damage level from 200 DPA to 400 DPA will result in an increase in the core power fraction that is generated by the thorium blanket from 50.7% to 64.2% and a corresponding decrease in the reprocessing capacity required to support the S&B core operation from 481.3 to 373.4 kg/GWt/Yr versus 2767.2 kg/GWt/Yr for the reference ABR core. The HM inventory in the seed slightly increases with DPA as the reduction in the seed power enables the seed to have a slightly tighter lattice pitch and, therefore higher fuel volume fraction. The sodium void reactivity worth slightly decreases as the blanket fuel is discharged at a higher DPA level.

The DPA calculation used in this project is verified and supported by literature related to the analysis of structural material samples irradiated in the FFTF. It is inconsistent with the fast fluence constraint of $4x10^{23}$ n(>0.1MeV)/cm^2 in the ANL's ABR design and the comparison of the performance characteristics between the S&B versus the ABR cores are biased in favor of the S&B cores. The sensitivity of the S&B core performance to the definition of radiation damage constraint was established by redesigning the reference S&B core to three different constraints: (1) 200 DPA assuming a displacement energy of 40eV – the reference case; (2) a peak fast fluence of $4x10^{23}$ n(>0.1MeV)/cm^2 – the one widely accepted by the fast reactor community; (3) 200 DPA assuming a displacement energy of 28eV. It is found that the application of the fast fluence constraint reduces the fraction of core power generated by the blanket from 50.7% to 41.9% and the achievable Seed/Blanket discharge burnup from 374.0/79.8 MWd/kg to 311.2/46.5 MWd/kg. As the result, the reprocessing capacity increases from 481.3 to 681.5 kg/GWth-Yr. It is still far lower – about one fourth, than that of CR=0.5 ABR -- 2767.2 kg/GWth-Yr. It is concluded that although the performance characteristics of the S&B cores are sensitive to the radiation damage constraint applied, the S&B cores offer very significant improvements relative to the conventional ABR core design by using identical constraint.

9.1.3. Fuel cycle analysis

The fuel cycle analysis (Chapter 7) found that the total fuel cycle cost of the PWR-S&B system is significantly lower than that of the PWR-ABR system (Section 7.4) due to (1) the large fraction of power generated from the low cost natural thorium fuel that operate in the breed-and-burn mode; (2) smaller fuel reprocessing capacity per unit of electricity generated. This cost is even below the level of current once-through PWRs. Moreover, due to the significantly longer fuel cycle, the capacity factor of the S&B reactor may be 10% higher than of the reference ABR thereby possibly offering ~10% lower O&M cost. As the S&B core can be designed with same active height as compact SFRs, the economic viability of such S&B reactors is expected to be superior to that of conventional SFRs.

Relative to the PWR-ABR system, the PWR-S&B system has comparable short-term radioactivity and radiotoxicity but much higher long-term values due to the disposal of ^{233}U from the thorium blanket. For the aspect of proliferation resistance, the seed fuel in S&B core has lower fissile Pu/Pu ratio, higher $^{238}Pu/Pu$ ratio, higher specific plutonium decay heat, higher spontaneous fission rate, and lower material attractiveness for weapon-use. The blanket discharges significant amount of ^{233}U. The high radiotoxicity of the discharged thorium fuel from the S&B could be minimized if the ^{233}U from the discharged thorium fuel is to fuel other reactors. If not separated from the thorium, the ^{233}U containing fuel discharged from the blanket of the S&B core is unattractive for weapons application.

Compared with PWR, the PWR-S&B system has significantly lower short-term radioactivity and radiotoxicity as the hazardous TRUs are recycled, but higher long-term values; higher proliferation resistance for the recovered plutonium; approximately 60% higher natural uranium utilization. With presently proven cladding materials the S&B cores can utilize 7% of thorium resource without need to develop irradiated thorium reprocessing capability. This is ~12 times the amount of energy LWRs generate per unit weight of natural uranium mined. As improved cladding materials become available or moderators are introduced to the blanket, the thorium utilization of S&B reactors will increase as well.

9.1.4. New fuel cycle options

The study explored a few new fuel cycle options established by the S&B concept (Chapter 8). Some of them represent the variants of Externally-Driven System (EDS) in which the excess neutrons from the seed rather than accelerator-driven spallation neutrons or fusion neutrons are the external neutrons used to drive the subcritical system. The major observations are summarized as below.

The neutronic analysis (Appendix A and Section 8.1) shows that it is feasible to design thorium-hydride fueled Sodium-cooled reactor for much less positive sodium void worth and several folds more negative Doppler coefficients than those of conventional SFRs. As the thorium-hydride fuel has H-to-Th ratio of 0.5, the spectrum prevailing in the SFR core is intermediate spectrum; the core fueled by such thorium hydride features a small DPA/FIMA ratio relative to conventional SFR core. Because of this, the fuel utilization could be significantly improved when thorium hydride is fed to the blanket driven by TRU burner. The full core analysis of the S&B design shows that the thorium hydride fueled blanket is able to discharge the fuel at the average burnup of 191.8 MWd/kg without violating the radiation damage constraint of 200 DPA. Without thorium fuel reprocessing, the resource utilization of natural thorium will be more than 30 times higher than that of natural uranium in current PWR plants.

A preliminary study (Section 8.2) also found that a thorium FCM fueled blanket can be driven by excess neutrons of a CR=0.5 seed up to burnup of at least 240 MWd/kg while generating about one third of the S&B core power if the FCM fuel is able to maintain its integrity and retain its fission products. The amount of energy that can be generated per unit of thorium in FCM fueled blanket without reprocessing can be from 40 to 80 times the energy generated by LWRs per unit of natural uranium. Even though the fabrication cost of the FCM fuel will be probably higher than that of metallic fuel, the overall economic advantage of the S&B core is likely to be preserved when using FCM fuel because the HM inventory in the FCM fueled blanket is one fifth of that for metallic thorium blanket and its burnup is much higher. However, it is necessary to determine the radiation damage limit of the FCM fuel under the condition prevailing in the blanket of the S&B core before the feasibility of the proposed reactor concept could be reliably assessed.

It is proposed (Section 8.5) that the blanket can be charged with the spent fuel from current PWRs after limited reprocessing. The limited reprocessing (AIROX) is applied to recycle the HM and fission products together and therefore features high proliferation resistance. Driven by the excess neutrons from fuel self-sustaining seed, the blanket can generate about one third of the core power and discharge its fuel at average burnup of ~120 MWd/kg. After combining the regular PWR and the once-through blanket, the fuel utilization of natural uranium resource is improved by a factor of three while the volume of HLW per unit of electricity generated is reduced correspondingly.

The S&B cores were considered to provide fissile contents to other reactors, like PWR (Section 8.6), Molten Salt Reactor (Section 8.7), and RBWR. A special case was investigated that the large amount of Trans-Th remaining in the discharge fuel of blanket are fed to PWR on closed fuel cycle. After accounting the PWRs supported by the seed, a typical S&B core can support 3.3 PWRs and this ratio will increase up to ~4.2 if the blanket discharges its fuel at the radiation damage on cladding material of 100 DPA.

The preliminary study suggests that the S&B concept can be designed for the function of several energy systems in the Evaluation Groups of the Fuel Cycle Evaluation and Screening campaign (like EG06, EG07, EG08 as Section 8.2; EG32 as typical S&B cores; EG38 as Section 8.6; EG36 as Section 8.8.1; EG29 as Section 8.8.2; EG24 as Section 8.8.3).

In conclusion, the SFR based on the S&B core configuration can be implemented using presently qualified cladding materials and start benefiting from the breed and burn mode of operation without extensive R&D efforts. It is expected to significantly improve the economics and resource utilization of Sodium-cooled Fast Reactor.

9.2. Future directions

Several challenges and limitations of this study need to be addressed with continuous R&D efforts before the advantages of S&B concept can be finally demonstrated. The research gaps are given below between the present state on knowledge of the S&B core design and the defendable S&B cores for licensing.

The future S&B active core height should be no longer than 150 cm so that it could fit within the S-PRISM reactor vessel (one of the GE designed cores is of this active height). Nevertheless, it is also recommended to design large S&B cores that will require some elongation of the S-PRISM reactor vessel because they may offer 2 to 3 years' cycles and, therefore, high capacity factors.

It is still preferred to apply DPA value for the radiation damage in future S&B core since it takes into account the specific energy dependence of neutron spectrum that may significantly vary across S&B cores. To resolve the inconsistency between the 200 DPA and the fast fluence of $4x10^{23}$ n/cm^2, it is necessary to re-evaluate past irradiation data along with more recent and ongoing irradiation experiments. The agreement upon methodology for calculating the radiation damage should be achieved such that the method adequately account for the specific energy dependence of the neutron spectra.

The Monte-Carlo based code, MocDown, is used throughout this project. Compared with most deterministic codes, it is computationally expensive and the core has to be modeled with coarse mesh. Rather than using R-Z geometry to represent the core, future S&B core designs need to be represented by Hexagonal-Z model and incorporate a right number of control and safety assemblies at discrete locations. The shutdown margin at cold zero power condition needs to be determined especially for the design with large negative Doppler coefficient. An explicit shuffling pattern will have to be used for each fuel assembly so that peak assembly power, peak burnup, peak fast fluence and peak DPA could be accurately determined.

The deterministic codes ARC (MCC-3/DIF3D/REBUS) are used as supplement in this study but only works for fast spectrum reactor. For several new cores where the neutron spectrum is much softer than conventional SFR, the ARC package may fail to capture the physics, like the double heterogeneity of the FCM fuel. The future research is suggested to use stochastic code to generate multi-group cross-sections for the full core calculation of DIF3D. The viability of the non-conventional SFR designs should be assessed with advanced modeling and simulating.

The design space of S&B core can still be explored and optimized further for better core performance. For example, the out-in fuel-shuffling scheme is applied to the S&B cases so far and stochastic methods such as the genetic algorithm or simulated annealing [118]

are available for the optimized fuel shuffling. A more recent study [39] found that 3-D fuel shuffling can reduce the DPA per unit of burnup. Without violating the radiation damage constraint of 200 DPA, a higher average discharge burnup is achievable by introducing 3-D shuffling scheme for the blanket fuel. In addition, the S&B cores feature low radial neutron leakage such that it is possible to replace or modify the reflector and shielding components by fuel assemblies for better economics.

A thorough safety analysis should be performed in order to identify the inherent safety of the S&B. Whereas the feasibility study performed so far only quantified and compared reactivity coefficients of the different designs, the detailed safety analysis is expected to simulate time-dependent transients and accidents using a suitable safety code package such as the ANL developed SAS4A/SASSYS-1 code system. As both axial and radial neutron leakage out of the S&B core are reduced to improve the neutron economics, transient analysis is necessary to understand the response to the Anticipated Transients Without Scram scenarios including ULOF, ULOHS, and UTOP.

A study needs to be undertaken to identify a promising strategy for transition from beginning-of-life (BOL) to equilibrium core composition in the most cost-effective way. At least a couple of approaches should be explored: (1) Enriching the first blanket fuel with TRU, Pu, or enriched uranium while using seed geometry and power density of the equilibrium core; (2) Starting with a larger volume but lower enrichment seed that will enable to safely operate the S&B at full power from beginning and gradually build up ^{233}U in thorium blanket assemblies. The safety of the S&B core will have to be analyzed for several core states during the transition to equilibrium period to assure passive safety.

The proposed S&B cores involve a few new fuel materials. It still lacks sufficient experience in the fabrication, irradiation, and reprocessing of TRU-40Zr inert matrix fuel. There is a need to develop fuel performance capability for inert-matrix fuel. Moreover, there may be some experience in the fabrication and irradiation of thorium dioxide fuel but not to the burnup level envisioned for the blanket fuel. The experience in the fabrication and irradiation of thorium hydride fuel as well as of FCM fuel with ThN kernels is much more scarce. It is necessary to develop fuel performance capability for different chemical forms in which the thorium fuel could be loaded to the blanket. For the applications that utilizing the ^{233}U (or Trans-Th elements) bred in the blanket it will be necessary to develop the reprocessing and fabrication technologies of the irradiated thorium fuel on commercial scale.

The fuel cycle options related to the S&B concept need to be evaluated thoroughly based on the criteria and metrics developed by the Fuel Cycle Evaluation and Screening campaign [18]. The conversion factors (for example LLW waste generation volume per ton of heavy metals) are given in the report for specific fuel cycle activities and the

consistent metrics should be applied to these new fuel cycle options in order to fully demonstrate the advantages of the S&B concept.

Reference

1. H. GRUENSPECHT, “International Energy Outlook 2011”, Center for Strategic and International Studies, U.S Energy Information Administration. September 19, 2011: Washington, DC (2011).
2. Department of Energy, Office of Nuclear Energy, “Light Water Reactor Sustainability (LWRS) Program”: http://www.energy.gov/ne/nuclear-reactor-technologies/light-water-reactor-sustainability-lwrs-program, accessed on October 7 2015.
3. J. LEDERMAN, “Climate Change: Obama Orders Steeper Cuts from Power Plants”, in Associated Press: http://bigstory.ap.org/article/3943010484c34715ae214c450308d8f5/obama-mandate-steeper-emissions-cuts-us-power-plants, accessed on October 7 2015.
4. World Nuclear Association, “Nuclear Power in the World Today”: http://www.world-nuclear.org/info/Current-and-Future-Generation/Nuclear-Power-in-the-World-Today, accessed on October 7 2015.
5. IAEA, “Power Reactor Information System – Home”: https://www.iaea.org/pris/, accessed on September 21 2015.
6. Wikipedia, “AP1000”: https://en.wikipedia.org/wiki/AP1000, accessed on October 7 2015.
7. U.S. Nuclear Regulatory Commission, “Final Safety Evaluation Report Related to Certification of the AP1000 Standard Design”, NUREG-1793 (2014).
8. E. GREENSPAN, “A Phased Development of Breed-and-Burn Reactors for Enhanced Nuclear Energy Sustainability”, Sustainability, 4(10): p. 2745-2764 (2012).
9. Z. XU, M.S. KAZIMI, M.J. DRISCOLL, “Impact of High Burnup on PWR Spent Fuel Characteristics”, Nuclear Science and Engineering, 151(3): p. 261-273 (2005).
10. B. PELLAUD, “Proliferation Aspects of Plutonium Recycling”, Journal of Nuclear Materials Management, 31(1): p. 30-38 (2002).
11. C.G. BATHKE, et. al., “The Attractiveness of Materials in Advanced Nuclear Fuel Cycles for Various Proliferation and Theft Scenarios”, Nuclear Technology, 179(1): p. 5-30 (2012).
12. Gen IV International Forum, “Technology Roadmap Update for Generation IV Nuclear Energy Systems”, OECD Nuclear Energy Agency (2014).
13. A.E. WALTAR, D.R. TODD, P.V. TSVETKOV, “Fast Spectrum Reactors”, Springer (2012).
14. C.E. TILL, Y.I. CHANG, “Plentifuel Energy - The Story of the Integral Fast Reactor” (2011).
15. IAEA, “Fast Reactor Database 2006 Update”, IAEA-TECDOC-1531, Vienna, Austria (2006).

16. A.L. NICHOLS, D.L. ALDAMA, M. VERPELLI, “Handbook of Nuclear Data for Safeguards Database Extensions”, IAEA-INDC(NDS)-0534, Vienna, Austria (2008).
17. G.S. STANFORD, “What Is the IFR?”: http://www.ne.anl.gov/About/reactors/integral-fast-reactor.shtml, accessed on October 7 2015.
18. R. WIGELAND, et. al., “Nuclear Fuel Cycle Evaluation and Screening – Final Report”, U. S. Department of Energy (2014).
19. H.V. DAM, “The Self-Stabilizing Criticality Wave Reactor”, In Proceedings of the Tenth International Conference on Emerging Nuclear Energy Systems (ICENES 2000), NRG, Petten, The Netherlands, p. 188 (2000).
20. G.I. TOSHINSKY, “LMFBR Operation in the Nuclear Cycle without Fuel Reprocessing”, In Proceedings of the International Topical Meeting on Advanced Reactors Safety (ARS'97), Orlando, Florida, USA, 1–5 June 1997; Volume 1, pp. 39–44 (1997).
21. E. TELLER, et. al., “Completely Automated Nuclear Power Reactors for Long-Term Operation II: Toward a Concept-Level Point Design of a High Temperature, Gas Cooled, Central Power Station System”, in Proceedings of the 8th ICENES, Obninsk, Russia (1996).
22. J.S. SLESAREV, et. al., “Problems of Development of Fast Reactors Self-fuel-provision without Fuel Reprocessing”, Atomkernenergie, Kerntechnik, 45(58-60) (1984).
23. G.J. FISCHER, R.J. CERBONE, “The Fast-Mixed Spectrum Reactor Interim Report Initial Feasibility Study”, Brookhaven National Laboratory (1979).
24. G.J. FISCHER, et. al., “A Fuel Management and Reactor Physics Study of the Fast Mixed-spectrum Reactor Concept”, Trans. Am. Nucl. Soc, 32: p. 792-794 (1979).
25. M.J. DRISCOLL, B. ATEFI, D.D. LANNING, “An Evaluation of the Breed/Burn Fast Reactor Concept”, MIT,Cambridge, MA, USA: MITNE-229 (1979).
26. S.M. FEINBERG, E.P. KUNEGIN, “Discussion Comments”, in Proceedings 2nd United Nations International Conference on Peaceful Uses of Atomic Energy, Geneva, Switzerland (1958).
27. H. SEKIMOTO, K. RYU, Y. YOSHIMURA, “CANDLE: The New Burnup Strategy”, Nuclear Science and Engineering, 139(3): p. 306-317 (2001).
28. E. GREENSPAN, F. HEIDET, “Energy Sustainability and Economic Stability with Breed and Burn Reactors”, Progress in Nuclear Energy, 53(7): p. 794-799 (2011).
29. J. GILLELAND, et. al., “Novel Reactor Designs to Burn Non-Fissile Fuels”, in Proceedings of ICAPP, Anaheim, CA, USA (2008).
30. C.B. AHLFELD, et. al., “Conceptual Design of a 500 MWe Traveling Wave Demonstration Reactor Plant”, in Proceedings of ICAPP, Nice, France (2011).

31. T.P. ELLIS, et. al., “Traveling-Wave Reactors: A Truly Sustainable and Full-Scale Resource for Global Energy Needs”, in Proceedings of ICAPP, San-Diego, CA, USA (2010).
32. F. HEIDET, E. GREENSPAN, “Superprism-sized Breed-and-Burn Sodium-cooled Core Performance”, Nuclear Technology, 181(2): p. 251-273 (2013).
33. F. HEIDET, E. GREENSPAN, “Performance of Large Breed-and-Burn Core”, Nuclear Technology, 181(3): p. 381-407 (2013).
34. F. HEIDET, E. GREENSPAN, “Neutron Balance Analysis for Sustainability of Breed-and-Burn Reactors”, Nuclear Science and Engineering, 171(1): p. 13-31 (2012).
35. F. HEIDET, E. GREENSPAN, “Breed and Burn Depleted Uranium in Fast Reactors without Actinides Separation”, in Proceedings of PHYSOR, Pennsylvania, USA (2010).
36. F. HEIDET, R. PETROSKI, E. GREENSPAN, “Minimum Burnup Required for Sustainable Operation of Fast Reactors without Recycling”, in Proceedings International Conference on Fast Reactors and Related Fuel Cycles: Challenges and Opportunities, Kyoto, Japan (2009).
37. E. GREENSPAN, F. HEIDET, “Fast Reactor for Maximum Fuel Utilization without Chemical Reprocessing”, in Proceedings of ICENES, Ericeira, Portugal (2009).
38. S.A. QVIST, “Safety and Core Design of Large Liquid-metal Cooled Fast Breeder Reactors”, in Nuclear Engineering Department, University of California, Berkeley (2013).
39. S.A. QVIST, J. HOU, E. GREENSPAN, “Design and Performance of 2D and 3D-Shuffled Breed-and-Burn Cores”, Annals of Nuclear Energy, 85: p. 93-114 (2015).
40. R.D. LEGGETT, L.C. WALTERS, “Status of LMR Fuel Development in the United States of America”, Journal of Nuclear Materials, 204: p. 23-32 (1993).
41. T.K. KIM, et. al., “Core Design Studies for a 1000 MWth Advanced Burner Reactor”, Annals of Nuclear Energy, 36(3): p. 331-336 (2009).
42. IAEA, “Thorium Fuel Cycle Potential Benefits and Challenge”, IAEA-TECDOC-1450 (2005).
43. E.A. HOFFMAN, et. al., “Preliminary Core Design Studies for the Advanced Burner Reactor over a Wide Range of Conversion Ratios”, ANL-AFCI-177, U. S. Department of Energy, Office of Nuclear Energy, Science and Technology (2006).
44. A.E. DUBBERLEY, et. al., “SuperPRISM Oxide and Metal Fuel Core Designs”, in Proceedings of ICONE 8: MD,USA (2000).
45. THE INDEPENDDENT, “New Life for Old Idea that Could Dissolve Our Nuclear Waste”, http://www.independent.co.uk/environment/green-living/new-

life-for-old-idea-that-could-dissolve-our-nuclear-waste-2376882.html, accessed on August 27 2015.
46. Institution of Mechanical Engineer, "UK Fast Reactor: A Roadmap for Development" (2013)
47. The Global Nuclear Energy Partnership (GNEP), US DOE: http://energy.gov/sites/prod/files/edg/news/archives/documents/GNEP/06-GA50035f_2-col.pdf (2006), accessed on October 7 2015.
48. T.K. KIM, private communication (2015).
49. G. ZHANG, A. CISNEROS, E. GREENSPAN, "Preliminary Study of SFR with Depleted Uranium Breed & Burn Blanket", Transactions of the American Nuclear Society, 108: p. 853-855 (2013).
50. S.L. HAYES, et. al., "Development of Metallic Fuels for Actinide Transmutation", in Proceedings of GLOBAL 2015, Paris, France (2015).
51. S. QVIST, E. GREENSPAN, "The ADOPT Code for Automated Fast Reactor Core Design", Annals of Nuclear Energy, 71(0): p. 23-36 (2014).
52. IAEA, "Comparative Assessment of Thermophysical and Thermohydraulic Characteristics of Lead, Lead-bismuth and Sodium Coolants for Fast Reactors", Vienna, Austria, (2002).
53. G.L. HOFMAN, L.C. WALTERS, T.H. BAUER, "Metallic Fast Reactor Fuels", Progress in Nuclear Energy, 31(1-2): p. 83-110 (1997).
54. W.S. YANG, "Fast Reactor Physics and Computational Methods", Nuclear Engineering and Technology, 44(2): p. 177-198 (2012).
55. R. MOORE, et. al., "MOCUP: MCNP-ORIGEN2 Coupled Utility Program", Idaho National Laboratory (1995).
56. H. TRELLUE, D. POSTON, "MONTEBURNS 2.0 | An Automated Multi-Step Monte Carlo Burnup Code System", Oak Ridge National Laboratory (2003).
57. F. HEIDET, "Maximum Fuel Utilization in Advanced Fast Reactors without Actinides Separation", in Nuclear Engineering Department, University of California, Berkeley (2010).
58. A. CISNEROS, "Pebble Bed Reactors Design Optimization Methods and Their Application to the Pebble Bed Fluoride Salt Cooled High Temperature Reactor (PB-FHR)", in Nuclear Engineering Department, University of California, Berkeley (2013).
59. Z. XU, P. HEJZLAR, M.S. KAZIMI, "MCODE, Version 2.2 - an MCNP-ORIGEN Depletion Program", MIT Center for Advanced Nuclear Energy Systems (2006).
60. J.T. GOORLEY, et. al., "Initial MCNP6 Release Overview - MCNP6 version 1.0", Los Alamos National Laboratory (2013).
61. A.G. CROFF, "A User's Manual For ORIGEN2 Computer Code", Oak Ridge National Laboratory (1980).

62. J.E. SEIFRIED, P.M. GORMAN, J.L. VUJIC, E. GREENSPAN, "Accelerated Equilibrium Core Composition Search Using a New MCNP-based Simulator", in Proceedings of Joint International Conference on Supercomputing in Nuclear Applications and Monte Carlo 2013 (SNA + MC 2013), Paris, France (2013).
63. M.B. CHADWICK, et. al., "ENDF/B-VII.0: Next Generation Evaluated Nuclear Data Library for Nuclear Science and Technology", Nuclear Data Sheets, 107: p. 2931—3060 (2006).
64. C.H. LEE, W.S. YANG, "MC2-3: Multigroup Cross Section Generation Code for Fast Reactor Analysis", Argonne National Laboratory (2011).
65. K.L. DERSTINE, "DIF3D: A Code to Solve One-, Two-, and Three-Dimensional Finite-Difference Diffusion Theory Problems", ANL-82-64, Argonne National Laboratory (1984).
66. B.J. TOPPEL, "A User's Guide to the REBUS-3 Fuel Cycle Analysis Capability", ANL-83-2, Argonne National Laboratory (1983).
67. G. ZHANG, E. GREENSPAN, A. JOLODOSKY, J. VUJIC, "Sodium Fast Reactors with Breed and Burn Blanket", in Proceedings of The 19th Pacific Basin Nuclear Conference: Vancouver, Canada (2014).
68. G.S. WAS, "Fundamentals of Radiation Materials Science": Springer Berlin Heidelberg (2007).
69. R.E. STOLLER, "Radiation Damage: Mechanisms and Modeling", Materials Science and Technology Division, ORNL. Joint EFRC Summer School, Knoxville, TN (2012).
70. ASTM Standards, "Standard Practice for Neutron Radiation Damage Simulation by Charged-Particle Irradiation", Journal of ASTM International, 1996 (Reapproved 2009). Volume: 12.02.
71. A.V. KARASIOV, L.R. GREENWOOD, "Neutron Flux Spectra and Radiation Damage Parameters for the Russian BOR-60 and SM-2 Reactors".
72. B.H. SENCER, et. al., "Microstructural Analysis of An HT9 Fuel Assembly Duct Irradiated in FFTF to 155 DPA at 443 °C", Journal of Nuclear Materials, 393(2): p. 235-241 (2009).
73. F. HEIDET, T.K. KIM, and T.A. TAIWO, "Thorium-fueled Breed-and-Burn Fuel Cycle", in Proceedings of PHYSOR 2014, Kyoto, Japan (2014).
74. T. TAK, D. LEE, T.K. KIM, "Design Of Ultralong-Cycle Fast Reactor Employing Breed-And-Burn Strategy", Nuclear Technology, 183 (2013).
75. F. HEIDET, private communication (2015).
76. L.R. GREENWOOD, L.S. KELLOGG, "Neutron Dosimetry for the MOTA-1G Experiment in FFTF", in Fusion Reactor Materials Semiannual Progress Report, p. 51-54 (1990).
77. L.R. GREENWOOD, R.K. SMITHER, "Neutron Damage Calculations for Materials Irradiation", ANL/FPP-TM-197 (1985).

78. L.R. GREENWOOD, “Dosimetry for the EBR-II-X287 Irradiation”, in Alloy Development for Irradiation Performance Semiannual Progress Report, p. 74-79 (1982).
79. S.K. CHENG, N.E. TODREAS, “Hydrodynamic Models and Correlations for Bare and Wire-Wrapped Hexagonal Rod Bundles - Bundle Friction Factors, Subchannel Friction Factors and Mixing Parameters”, Nuclear Engineering and Design, 92(2): p. 227-251 (1986).
80. Website of the Atomic KAERI. accessed on March 25, 2015.
81. R. PETROSKI, B. FORGET, C. FORSBERG, “Neutronic Evaluation of Breed-and-Burn Reactor Fuel Types Using an Infinite-Medium Depletion Approximation”, in Proceedings of PHYSOR, Pittsburgh, Pennsylvania (2010).
82. K. YU, M.J. DRISCOLL, P. HEJZLAR, “Neutronic Limits of Breed and Burn Fast Reactor Performance”, Transactions of the American Nuclear Society, 86: p. 335-336 (2002).
83. S.A. QVIST, E. GREENSPAN, “Inherent Safety of Minimum Burnup Breed-and-Burn Reactors”, in Proceedings of ICAPP, Chicago, IL (2012).
84. G. ZHANG, E. GREENSPAN, “Preliminary Study of Advanced Sodium-Cooled Burner Reactors with External and Internal Thorium Blankets”, in Transactions of the American Nuclear Society, 111: p293-298 (2014).
85. D.E. SHROPSHIRE, et. al., “Advanced Fuel Cycle Economic Analysis of Symbiotic Light-Water Reactor and Fast Burner Reactor Systems”, Idaho National Laboratory (2009).
86. G. ZHANG, E. GREENSPAN, A. JOLODOSKY, J. VUJIC, “SFR with Once-Through Depleted Uranium Breed & Burn Blanket”, Progress in Nuclear Energy, 82(0): p. 2-6 (2015).
87. T.R. ALLEN, et. al., “Characterization of Microstructure and Property Evolution in Advanced Cladding and Duct: Materials Exposed to High Dose and Elevated Temperature”, Journal of Materials Research, 30(9): p. 1246-1274 (2015).
88. K. ECKERMAN, et. al., “Compendium of Dose Coefficients Based on ICRP Publication 60”, in ICRP Publication 119, Ann. ICRP 41 (2012).
89. N. E. STAUFF, T.K. KIM, T.A. TAIWO, “Variations in Nuclear Waste Management Performance of Various Fuel-Cycle Options”, Journal of Nuclear Science and Technology, 52(7-8): p. 1058-1073 (2015).
90. D. GRENECHE, “The Thorium Cycle: An Assessment of Its Potentialities with A Focus on Non Proliferation Aspects”, in Transactions of the American Nuclear Society, Albuquerque, NM (2006).
91. J. KANG, F.N.V. HIPPEL, “U-232 and the Proliferation-Resistance of U-233 in Spent Fuel”, Science & Global Security, 9: p. 1-32 (2001).
92. IAEA, “The Physical Protection of Nuclear Material and Nuclear Facilities”, in INFCIRC/225/Rev.4 (1999).

93. C.G. BATHKE, et. al., “An Assessment of the Attractiveness of Material Associated with Thorium Fuel Cycles”, in Transactions of the American Nuclear Society: Anaheim, California (2014).
94. R.S. STONE, et. al., “Transient Behavior of TRIGA, A Zirconium-Hydride, Water-Moderated Reactor” Nuclear Science and Engineering, 6(4): p. 255-259 (1959).
95. M. SIMNAD, “Fuel-Elements for Pulsed TRIGA Research Reactors”, Transactions of the American Nuclear Society, 19: p. 128-129 (1974).
96. E. GREENSPAN, et. al., “Hydride Fuel for LWRs-Project Overview”, Nuclear Engineering and Design, 239(8): p. 1374-1405 (2009).
97. A.F. LILLIE, et. al., “Zirconium Hydride Fuel Element Performance Characteristics”, Atomics International/USAEC Rept. AI-AEC-13084 (1973).
98. M. SIMNAD, “Uranium Thorium Hydride Nuclear Fuel”, US Patent # 4493809 (1985).
99. N.E. STAUFF, et. al., “Analysis of Fuel Options for the Breakeven Core Configuration of the Advanced Recycling Reactor”, in Proceedings of GLOBAL 2013: Salt Lake City, Utah. p. 495-503 (2013).
100. K. KRAMER, “Fusion-Fission Blanket Options for the LIFE Engine”, Fusion Science and Technology, 61(3): p. 256-256 (2011).
101. E. MOSES, et. al., “A Sustainable Nuclear Fuel Cycle Based on Laser Inertial Fusion Energy”, Fusion Science and Technology, 56(2): p. 547-565 (2009).
102. J.J. POWERS, B.D. WIRTH, “A Review of TRISO Fuel Performance Models”, Journal of Nuclear Materials, 405(1): p. 74-82 (2010).
103. K.A. TERRANI, et. al., “Microencapsulated Fuel Technology for Commercial Light Water and Advanced Reactor Application”, Journal of Nuclear Materials, 427(1-3): p. 209-224 (2012).
104. K.A. TERRANI, et. al., “Fabrication and Characterization of Fully Ceramic Microencapsulated Fuels”, Journal of Nuclear Materials, 426(1-3): p. 268-276 (2012).
105. J.J. POWERS, “Fully Ceramic Microencapsulated Fuel in FHRs: A Preliminary Reactor Physics Assessment”, in Transactions of the American Nuclear Society: Anaheim, California (2014).
106. S. PETERSON, et. al., “Properties of Thorium, Its Alloys, and Its Compounds”, Oak Ridge National Laboratory (1965).
107. J. LEPPÄNEN, “Modeling of Nonuniform Density Distributions in the SERPENT 2 Monte Carlo Code”, Nuclear Science and Engineering, 174(3): p. 318-325 (2013).
108. R.J. MCCONN JR, et. al., “Compendium of Material Composition Data for Radiation Transport Modeling” , PNNL-15870 Rev. 1 (2011).
109. C.W. FORSBERG, C.M. Hopper, “Definition of Weapons-Usable Uranium-233”, ORNL/TM-13517 (1998).

110. D. MAJUMDAR, et. al., “Recycling of Nuclear Spent Fuel with AIROX Processing”, INIS, Editor, DOE/ID—10423, 24(20), p. 67 (1992).
111. J.S. LEE, et. al., “Research and Development Program of KAERI for DUPIC (Direct Use of Spent PWR Fuel in CANDU Reactors)”, in Proceedings of GLOBAL 1993, Sept. 12-17, Seattle, USA. (1993).
112. C.D. SANZO, private communication. 2014.
113. F. GANDA, E. GREENSPAN, “Neutronic Analysis of Hydride Fueled PWR Cores”, Nuclear Engineering and Design, 239(8): p. 1425-1441 (2009).
114. J. LEPPAENEN, A. ISOTALO, “Burnup Calculation Methodology in the SERPENT 2 Monte Carlo Code”, in Proceedings of PHYSOR, Knoxville, TN, USA (2012).
115. ORNL, Documents Related to Liquid-Halide (Fluoride and Chloride) Reactor Research and Development, http://www.energyfromthorium.com/pdf/, accessed on 10/2/2015.
116. L. DAVID, “Molten Salt Reactor Fueled with Thorium Blanket Discharged from SFR and Spent Nuclear Fuel from LWR”, Master thesis, Nuclear Engineering Department, in University of California Berkeley (2015).
117. M. AUFIERO, et. al., “An Extended Version of the SERPENT-2 Code to Investigate Fuel Burn-up and Core Material Evolution of the Molten Salt Fast Reactor”, Journal of Nuclear Materials, 441(1–3): p. 473-486 (2013).
118. S. KIRKPATRICK, et. al., “Optimization by Simulated Annealing”, Science, 220(4598): p. 671-680 (1983).
119. N. FRIEDMAN, “U.S. Submarines Since 1945: An Illustrated Design History”, Naval Institute Press, 1st edition (1994).
120. American Elements, Thorium Hydrde, http://www.americanelements.com/thhid.html, accessed on June 2 2014.
121. T. HINO, et. al., “Core Designs of RBWR (Resource-Renewable BWR) for Recycling and Transmutation of Transuranium Elements - an Overview”, in Proceedings of ICAPP 2014, Charlotte, USA, April 6-9 (2014).
122. J.E. SEIFRIED, et. al., “Self-Sustaining Thorium-Fueled Reduced Moderation BWR Feasibility Study”, Energy Procedia, 71(0): p. 69-77 (2015)
123. P.M. GORMAN, et. al., “The Fuel-Self-Sustaining RBWR-Th Core Concept and Parametric Studies”, in Proceedings of ICAPP 2014, Charlotte, USA (2014).
124. G. ZHANG, et. al., “Analysis of Local Void Reactivity Coefficients for the RBWR-Th”, Transactions of the American Nuclear Society, 108: p. 849-52 (2013).

Appendix

A. Self-sustaining Thorium Hydride Fueled Sodium-cooled Fast Reactor

A.1 Feasibility analysis of thorium hydride fuel in fast reactor

U-$ZrH_{1.6}$ fuel developed by Dr. Massoud Simnad has being successfully used for over 40 years in TRIGA type research reactors around the world with no safety problems [94-96]. Six hydride-fueled space reactors were built and operated, and one was placed in earth orbit for the Space Nuclear Auxiliary Power (SNAP) project [97]. It has been suggested that U-ThH_2 fuel is even more stable than U-$ZrH_{1.6}$ fuel and can operate at higher temperatures [98]. The Submarine Intermediate Reactor project investigated a metal-cooled reactor moderated by an array of solid beryllium in later 1950s and proved as a worthwhile alternative to Submarine Thermal Reactor [119]. The proposed thorium-hydride fueled reactor is, essentially, a Sodium-cooled Fast Reactor (SFR) with a relatively soft spectrum. The hydrogen-to-thorium atom ratio (H/Th) is a design variable to be determined by, primarily, neutronics optimization and safety analysis. The primary design objectives are (1) the performance characteristics of thorium hydride fueled SFR along with (2) inherent safety.

A large 3000 MWt sodium-cooled fast reactor [33] is used as the initial reference. It has an active core height of 200cm with 20 cm long axial blankets on both sides of the seed in order to improve neutron utilization. The fission gas plenum length is 250cm. The diameter of the active core is 400cm [33]. The hydride fuel is in the form of ThH_x where x is a design variable; it has a theoretical density of 9.5 g/cm^3 [120]. The assumed smear density is 90%. The ferritic martensitic steel HT-9 is used for the structural and cladding material.

A.2 Analysis method

This very preliminary assessment is based on a fuel unit cell analysis that accounts for axial but not for radial neutron leakage. The unit cell multiplication factor evolution with burnup k(BU) is processed to estimate the k_{eff} of a 5-batch core by taking the harmonic mean of k(BU) corresponding to the Beginning and End of Equilibrium Cycle (BOEC or EOEC) burnup of each of the 5 batches. The resulting k_{eff} does not account for radial leakage probability so our core keff design constraint is 1.010; a 3-D analysis of a representative thorium hydride fueled SFR having the reference core dimensions predicts a radial leakage probability of ~ 1.0 %.

The active core volume is divided into 50 axial burnup nodes. MCNP6 is used with ENDF/B-VII.0 cross-section libraries for neutronics calculations. ORIGEN2.2 is used for the burnup calculations with effective one group cross sections generated by MCNP6 for major actinides and fission products. MCNP6 and ORIGEN2.2 are coupled via a two-tiered solver – MocDown – that automates an efficient iterative search for the equilibrium composition of multi-fuel-batch cores depending on a prescribed fuel management scheme [62] (described on Section 2.5.1). The DPA value is calculated by a module built in MCNP6 assuming a collision efficiency of 80% (described on Section 2.7.2). All the actinides in the discharged seed and blanket are recycled back to the seed. Fresh hydride thorium is fed as the makeup fuel to seed and blanket.

A parametric study was first undertaken to determine the H-to-HM ratio that will provide a neutron spectrum comparable to that of a typical Reduced-moderation Boiling Water Reactor (RBWR) [121]. Table A-1 compares selected characteristics of the thorium hydride cores with H-to-HM ratio of 0.0, 0.5 and 1.0, and of the reference RBWR-Th core at discharge burnup of 2.5% FIMA [122]; the cycle length is determined to give an equilibrium cycle average burnup of 10% FIMA. All the cases included in Table A-1 are fuel-self-sustaining but the core with H-to-HM ratio of 0.5 and 1.0 are short of reactivity. The presented results are to indicate the trends only.

Two types of parameters are used to gauge the neutron spectrum – effective one-group cross-sections and fraction of fissions caused by neutrons in selected energy ranges. It is found that the thorium hydride core with H-to-HM ratio of 0.5 has the same neutron spectrum as that of the RBWR-Th core [122]. The higher the H-to-HM ratio is, the smaller becomes the ratio between radiation damage and burnup. The sodium void worth is also significantly reduced with addition of hydrogen but for the specific H/HM of 0.5 and 1.0 cores examined, the sodium void worth is still slightly positive at BOL. The reactivity worth of sodium absorption in these cores is larger than the total reactivity worth of sodium voiding. This implies that the combined spectral and leakage effects of sodium voiding is negative. Whereas the metallic thorium fueled SFR has large positive value ($8.11) and thorium dioxide fueled RBWR features large negative value (-$28.65), the absolute magnitude of the sodium void worth of the thorium hydride fueled SFR is significantly smaller.

Table A-1 Comparisons of Selected Characteristics of Three Sodium-cooled Cores and the RBWR-Th

Fuel forms (H-to-HM ratio)	Metallic (0)	Hydride (0.5)	Hydride (1)	RBWR-Th
Pitch-to-diameter ratio	1.15	1.15	1.15	1.13
H-to-Th of the seed at BOL	0.0	0.57	1.10	1.31
Capture cross sections (barns)				

Th232	0.232	0.456	0.575	0.461
U233	0.226	0.779	1.617	0.829
Fission cross sections (barns)				
Th232	0.009	0.016	0.019	0.018
U233	2.230	5.468	10.617	5.801
Fraction of fissions caused by neutrons in energy range				
<0.625 eV	0.00%	2.78%	13.32%	5.20%
0.625eV - 100keV	30.20%	69.25%	70.83%	67.02%
> 100 keV	69.80%	27.97%	15.85%	27.78%
k_{eff}				
BOEC	1.092	0.973	0.928	1.034
EOEC	1.083	0.945	0.904	1.025
Ave. BU of seed/full core, %				
FIMA	10.0	9.9	9.9	2.5
Peak DPA/BU (DPA/%FIMA)	12.7	7.6	6.2	-
Cycle length (EFPD)	576	560	560	356
Sodium void worth at BOL ($)	8.11±0.04	1.37±0.07	1.54±0.07	-28.64±0.07
Na absorption worth ($)	1.16	2.63	3.20	-

A.3 Comparison of thorium hydride vs. dioxide fueled cores

Table A-2 compares selected characteristics of the reference thorium hydride design with H-to-HM ratio of 0.5 and a thorium dioxide fueled SFR of identical dimensions. The core dimension was updated for this analysis: a seed length of 150 cm and axial blankets of 60cm each; the fission gas plenum length of 100 cm. The radial neutron leakage probability assumed is 1% for the hydride, and 3% for the oxide-fueled cores; the latter has a significantly harder spectrum. The fuel cycle scheme is similar to that of the RBWR-Th reference core [122]: fuel is recycled after a cooling period of 3 years. The fuel cycles were chosen to achieve criticality at EOEC, respectively.

The thorium dioxide fueled SFR core is used for this comparison since a recent study [99] found it possible to design metallic and oxide thorium fueled SFR cores containing a very short seed length – 60 cm, and long axial blankets – 80 cm, to have a negative sodium void worth. The thorium dioxide core features the softest neutron spectrum and the most negative sodium void worth out of a few combinations between fuel options and chemical forms [99].

Both thorium hydride and dioxide fueled core designs offer fuel sustainability. Relative to the thorium dioxide core, the thorium hydride core features a significantly softer spectrum, smaller k_{eff} – (Figure A-1), larger burnup reactivity swing per year and 30% smaller Trans-thorium concentration at BOL. The average discharge burnup of current thorium hydride fueled SFR design – 3.3% FIMA, is comparable with that of most intermediate spectrum reactors [122, 123] but lower than that of the ThO_2 fueled SFR – 11.8 %FIMA and of typical uranium fueled self-sustaining SFRs (7.3% FIMA for ANL's ARR [43] and 10.6 %FIMA for GE's S-PRISM [44]).

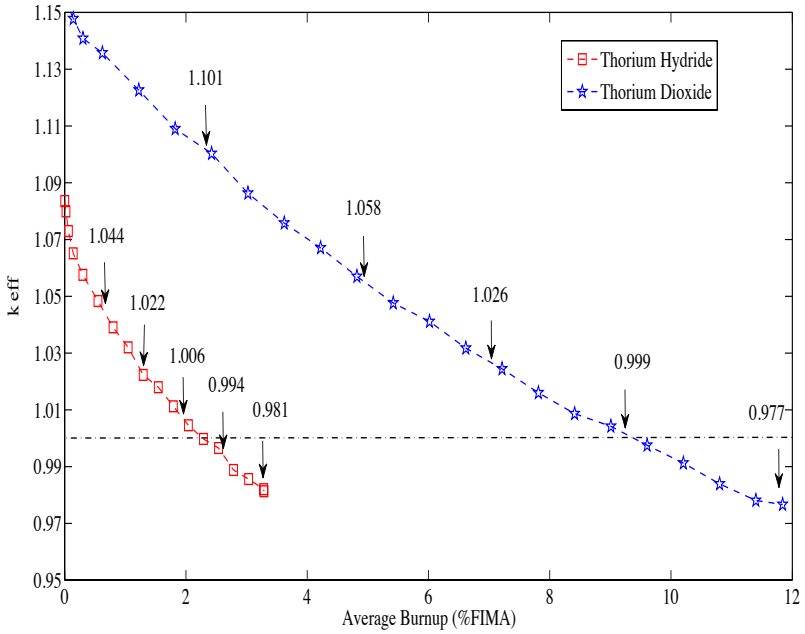

Figure A-1 Evolution of multiplication factor for thorium hydride and thorium dioxide fueled core on equilibrium cycle

Table A-2 Comparison of Selected Performance Characteristics of Reference Thorium Hydride and Dioxide SFR Cores

	Thorium Hydride	Thorium Dioxide
Fuel form	$ThH_{0.5}$	ThO_2
Pitch-to-diameter ratio	1.11	1.39
H-to-Th of the seed at BOL	0.575	-
Fraction of fissions caused by neutrons in energy range		
<0.625 eV	2.55%	0.00%
0.625eV - 100keV	68.81%	50.90%

> 100 keV	28.64%	49.10%
k_{eff} , BOEC/EOEC	1.029/1.009	1.066/1.030
Burnup reactivity swing, %Δk/k	1.92	3.22
Cycle length, EFPD	299.0	994.0
Ave. BU of seed/full core, % FIMA	5.8/3.3	20.2/11.8
Peak BU, % FIMA	7.5	24.4
Peak DPA	55	197
TransTh/HM of the seed, wt%	13.0%	19.3%
Safety Relevant Parameters		
Effective delayed neutron fraction	0.0034±0.0002	0.0035±0.0002
Sodium void worth at BOL/EOL, $	0.88/1.40±0.07	3.68/10.17±0.05
Sodium void worth at BOEC/EOEC, $	1.05/1.15	7.12/8.41
Δk/k due to 10% of hydrogen diffusing out of seed at BOL/EOL, $	-2.79/-1.70±0.08	-
Δk/k due to 100% of hydrogen diffusing out of seed at BOL/EOL, $	-13.80/3.54±0.07	-
Doppler coefficient at BOL/EOL (cents/K)	-1.25/-1.20±0.03	-0.24/-0.29±0.02

Figure A-2(a) shows that the neutron spectrum of the thorium hydride core is comparable to the RBWR-Th core spectrum and significantly softer than the thorium dioxide core spectrum. The latter is softer than that of the metallic uranium fueled SFR (ANL's ARR [43]). These spectra differences are exhibited more pronouncedly in the comparison of the energy dependent fission probability shown in Figure A-2(b) and can also be inferred from the fraction of fissions occurring in different energy ranges (Table A-2).

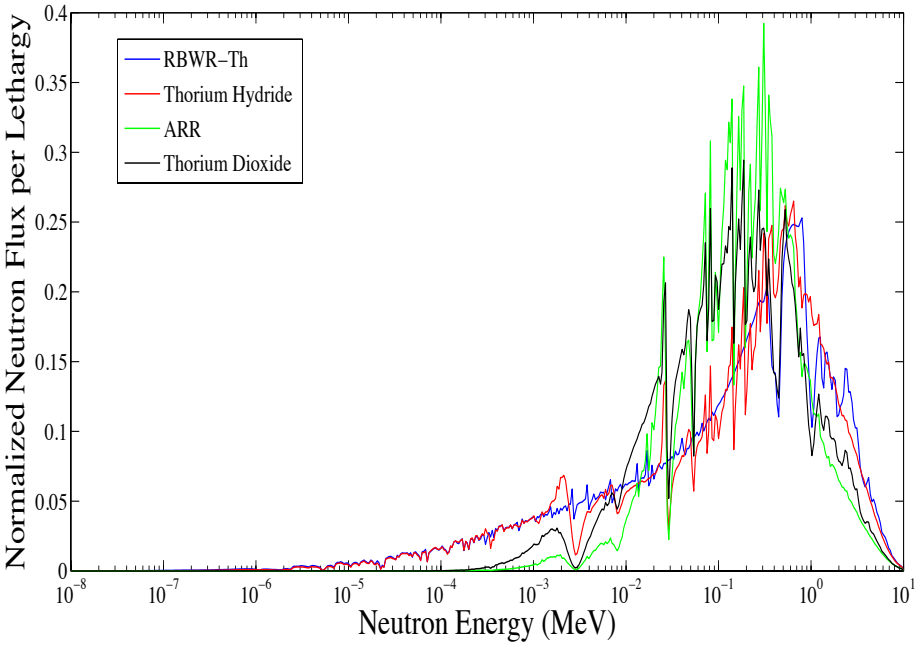
RBWR–Th
Thorium Hydride
ARR
Thorium Dioxide
Normalized Neutron Flux per Lethargy
Neutron Energy (MeV)

(a)

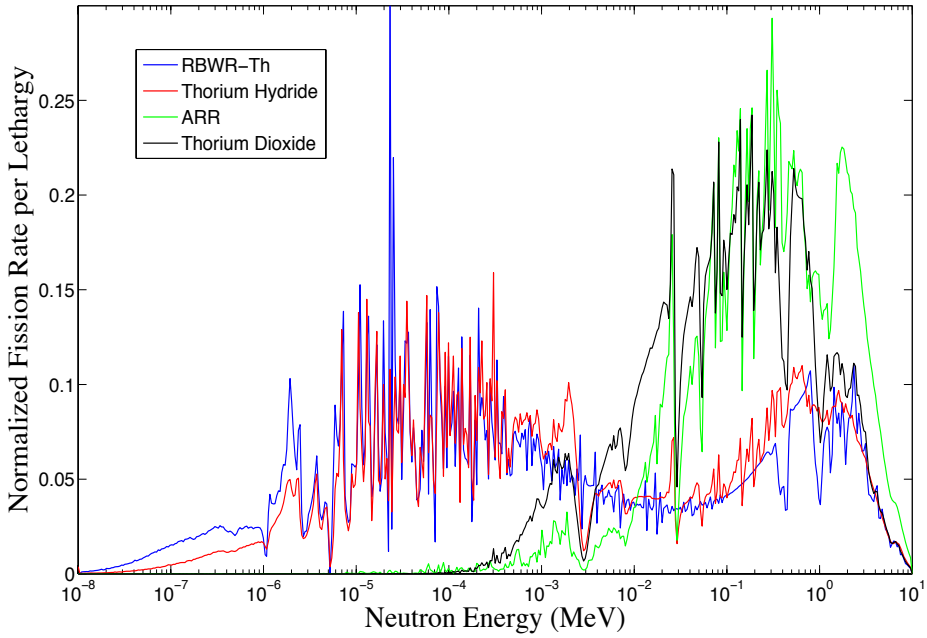
RBWR–Th
Thorium Hydride
ARR
Thorium Dioxide
Normalized Fission Rate per Lethargy
Neutron Energy (MeV)

(b)

Figure A-2 Normalized energy dependent neutron spectrum (a) and fission reaction rates (b) of RBWR-Th, Thorium Hydride (Reference), ANL ARR, and Thorium Dioxide (Reference)

Safety related characteristics are also compared in Table A-2. Most notable is the smaller sodium void reactivity worth of the thorium hydride core; the core average void reactivity worth is about $1 at both BOEC and EOEC. Detailed comparison of the sodium void worth components in several cores is given later.

A reactivity feedback mechanism that is unique to the hydride fuel is hydrogen dissociation and diffusion out from the fuel in the event of thorium hydride fuel temperature rise. Hydrogen migration from the seed into the gas plenum will cause spectrum hardening with positive reactivity feedback at BOL of up to $2.54 in the extreme hypothetical case of complete hydrogen loss. However, the resulting enhanced neutron leakage from the seed contributes -$15.42 negative feedback making the net effect -$13.80. At EOL initial migration of hydrogen out from the fuel will also have a negative reactivity effect but complete diffusion of hydrogen out from the fuel will have a positive reactivity of $3.54. However, the core average reactivity effect of even complete hydrogen diffusion out from the fuel is expected to be slightly negative by considering the absolute magnitudes. It ought to be realized that the hydrogen diffusion process out from the fuel is very slow and that complete loss of hydrogen is not practical. On the other hand, hydrogen uptake by the fuel with fuel temperature reduction is expected to result in reactivity gain that will have to be compensated by the control rods.

The Doppler coefficient of the reference case is 5-6 times more negative than that of the thorium dioxide reactor and much more negative than that of most SFRs [43, 54]. This is because of the significantly larger epithermal flux component of the hydride core that overlaps with the resonance region of most actinides. The large negative Doppler reactivity coefficient will also require the control rods to have large enough worth to provide adequate shutdown margin at cold zero power condition.

A.4 Reactivity coefficients of thorium hydride fuel in SFR

Detail analysis of the BOL sodium void worth is performed to understand the reactivity feedback from thorium hydride fuel with respect to RBWR-Th [122], ANL's 1000MWt Advanced Recycling Reactor (ARR) fueled by metallic U-TRU [43] and the thorium dioxide fueled SFR. The coolant is completely voided from the entire core, including blankets, and the leakage calculated is from the core to the reflectors. The results of this comparison are summarized in Table A-3. Figure A-2 compares the neutron spectrum and energy dependent fission rate of these cores. The similarity in the spectra of the thorium hydride and RBWR-Th cores is apparent. The metallic uranium fueled ARR has

the hardest spectrum while the thorium dioxide fueled core spectrum is much closer to the metallic uranium ARR than to the thorium hydride cores.

The spectral effect of the thorium hydride core is very small as compared to the other two SFR cores – thorium oxide and, in particular, metallic uranium fueled cores. These trends can be understood from the energy dependence of the fission reaction and of the η value rate of these cores displayed in, respectively, Figure A-2(b) and Figure A-3. While the fission rate of the thorium hydride core peaks between 10 and 100eV in which energy range η is declining with energy, the fission rate of the two SFR cores peak around 0.2 MeV (Figure A-2b) in which energy range η is steeply increasing with energy. The radial leakage probability, not accounted for in the present analysis, is expected to reduce the sodium void worth. The spectral effect of the RBWR-Th core is much more negative because its coolant-moderator voiding results in spectrum hardening on under-moderation condition [124]. Among the three sodium-cooled cores, the thorium hydride core features the least positive total coolant voiding reactivity effect at BOL.

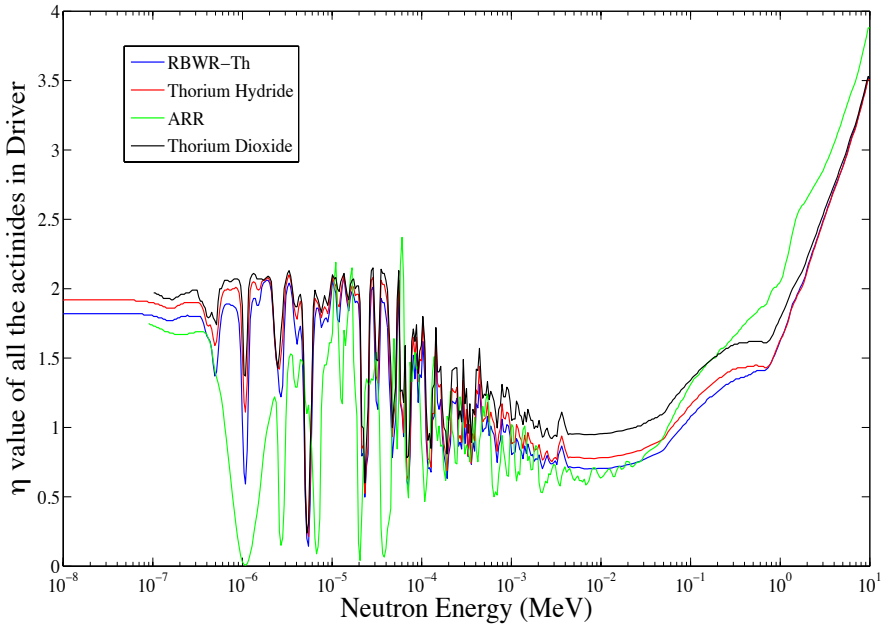

Figure A-3 Energy dependent eta of all the actinides in the seed

Table A-3 BOL Reactivity Change upon Coolant Voiding of Thorium Hydride (Reference), RBWR-Th, Thorium Dioxide (Reference) and ANL ARR

	Th Hydride		Thorium Dioxide	
	Reference	RBWR-Th	Reference	ANL ARR
Core power, MWt	3000	3000	3000	1000
Coolant type	Na	H_2O	Na	Na
Fuel form	$ThH_{0.5}$	ThO_2	ThO_2	U-10Zr-Pu
Spectral, $	0.41	-27.19	3.79	10.93
Seed, $	1.97	-	9.64	-
Blanket, $	-1.48	-	-5.79	-
Absorption, $	0.55	-0.42	1.85	-
Leakage out of active core, $				
upper	-0.07	-0.14	-0.86	-1.30[17]
lower	-0.08	-0.66	-1.10	-1.04
radial	-	-	-	-2.11
Total	0.81	-28.41	3.67	6.48

[17] The reactivity worth induced by the leakage out of ARR core is obtained by a R-Z model reproduced at UC Berkeley.